NASA/CR—2019-219983



Flow Quality Survey of the 9- by 15-Foot Low Speed Wind Tunnel (2015 and 2016 Tests) Prior to Acoustic Improvement Modifications

Aaron M. Johnson
Jacobs Technology, Cleveland, Ohio

April 2019

NASA STI Program . . . in Profile

Since its founding, NASA has been dedicated to the advancement of aeronautics and space science. The NASA Scientific and Technical Information (STI) Program plays a key part in helping NASA maintain this important role.

The NASA STI Program operates under the auspices of the Agency Chief Information Officer. It collects, organizes, provides for archiving, and disseminates NASA's STI. The NASA STI Program provides access to the NASA Technical Report Server—Registered (NTRS Reg) and NASA Technical Report Server—Public (NTRS) thus providing one of the largest collections of aeronautical and space science STI in the world. Results are published in both non-NASA channels and by NASA in the NASA STI Report Series, which includes the following report types:

- TECHNICAL PUBLICATION. Reports of completed research or a major significant phase of research that present the results of NASA programs and include extensive data or theoretical analysis. Includes compilations of significant scientific and technical data and information deemed to be of continuing reference value. NASA counter-part of peer-reviewed formal professional papers, but has less stringent limitations on manuscript length and extent of graphic presentations.

- TECHNICAL MEMORANDUM. Scientific and technical findings that are preliminary or of specialized interest, e.g., "quick-release" reports, working papers, and bibliographies that contain minimal annotation. Does not contain extensive analysis.

- CONTRACTOR REPORT. Scientific and technical findings by NASA-sponsored contractors and grantees.

- CONFERENCE PUBLICATION. Collected papers from scientific and technical conferences, symposia, seminars, or other meetings sponsored or co-sponsored by NASA.

- SPECIAL PUBLICATION. Scientific, technical, or historical information from NASA programs, projects, and missions, often concerned with subjects having substantial public interest.

- TECHNICAL TRANSLATION. English-language translations of foreign scientific and technical material pertinent to NASA's mission.

For more information about the NASA STI program, see the following:

- Access the NASA STI program home page at http://www.sti.nasa.gov

- E-mail your question to help@sti.nasa.gov

- Fax your question to the NASA STI Information Desk at 757-864-6500

- Telephone the NASA STI Information Desk at 757-864-9658

- Write to:
  NASA STI Program
  Mail Stop 148
  NASA Langley Research Center
  Hampton, VA 23681-2199

NASA/CR—2019-219983



Flow Quality Survey of the 9- by 15-Foot Low Speed Wind Tunnel (2015 and 2016 Tests) Prior to Acoustic Improvement Modifications

Aaron M. Johnson
Jacobs Technology, Cleveland, Ohio

Prepared under Contract NNC15BA02B

National Aeronautics and
Space Administration

Glenn Research Center
Cleveland, Ohio 44135

April 2019

This work was sponsored by the Advanced Air Vehicle Program
at the NASA Glenn Research Center

Trade names and trademarks are used in this report for identification only. Their usage does not constitute an official endorsement, either expressed or implied, by the National Aeronautics and Space Administration.

Level of Review: This material has been technically reviewed by expert reviewer(s).

Available from

NASA STI Program
Mail Stop 148
NASA Langley Research Center
Hampton, VA 23681-2199

National Technical Information Service
5285 Port Royal Road
Springfield, VA 22161
703-605-6000

This report is available in electronic form at http://www.sti.nasa.gov/ and http://ntrs.nasa.gov/

Flow Quality Survey of the 9- by 15-Foot Low Speed Wind Tunnel (2015 and 2016 Tests) Prior to Acoustic Improvement Modifications

Aaron M. Johnson
Jacobs Technology
Cleveland, Ohio 44135

Summary

A flow quality survey (FQS) was conducted in December 2015 and January 2016 to characterize the flow quality of the 9- by 15-Foot Low-Speed Wind Tunnel (9×15 LSWT) test section prior to the start of significant structural and acoustic modifications. The data from this FQS will be compared with data collected during a replicated FQS after completion of the acoustic improvement modifications. This document contains only the FQS data collected in December 2015 and January 2016 using the 15-ft survey rake and the 18-in. boundary layer rakes in the 9×15 LSWT. The spatial variation at one axial test section station (TSTA), nominally TSTA 198, and five vertical heights of the 15-ft survey rake was computed for Mach number, velocity, total and static pressure, total temperature, and flow angularity (pitch and yaw). Three hot-wire probes mounted to the 15-ft survey rake were used to measure turbulence intensity; however, data from a previous test entry were used as the mean turbulence intensity baseline value, as there were issues with the hot-wire performance. The boundary layer pressure profiles around the perimeter of the test section at TSTA 199 were also measured and the boundary layer heights computed. All calculated results are tabulated for each facility condition set point.

Introduction

The tests described in this report document the flow quality at a single test section station (TSTA) in the 9- by 15-Foot Low-Speed Wind Tunnel (9×15 LSWT) prior to acoustic and structural modifications to the test section, diffuser, and other portions of the tunnel loop. This entry is considered the fifth test section characterization entry (TSC5) in the 9×15 LSWT. The data from these tests will be compared with data collected following the completion of the acoustic improvement modifications to determine if Jacobs Technology has met the aerothermal flow quality acceptance criteria defined in the acoustic improvement modifications requirements. The following acceptance criteria were developed by Jacobs Technology, 9×15 LSWT facility engineers and manager, and the NASA Glenn Research Center wind tunnel calibration team:

- Ensure the 9×15 LSWT can reach Mach 0.22 with an empty test section (only 9×15 test section characterization hardware installed).
- Ensure pressure differential in corner 1 stays within the allowable structural range over the 9×15 LSWT operating range ($\Delta P_{S,c1} \leq 75.5$ psf).
- The following flow parameters will be assessed to ensure no degradation of said parameters occurred due to the acoustic improvement modifications:

  Flow uniformity $\quad \sigma\left(V/\overline{V}\right)_{post} \leq 110\% \bullet \sigma\left(V/\overline{V}\right)_{pre}$

  Flow angularity $\quad \mathrm{RMS}\left(\alpha,\beta\right)_{post} \leq 110\% \bullet \mathrm{RMS}\left(\alpha,\beta\right)_{pre}$

Temperature uniformity $\sigma\left(T/\bar{T}\right)_{post} \le 110\% \bullet \sigma\left(T/\bar{T}\right)_{pre}$

Turbulence intensity $avg\left(TI\right)_{post} \le 110\% \bullet avg\left(TI\right)_{pre}$

- Ensure the boundary layer height on the test section floor, ceiling, and walls has not increased significantly, thus maintaining the usable area in the test section.

The tests and data in this document pertain only to the FQS tests in December 2015 and January 2016. Where appropriate, descriptions and figures of the facility, hardware, instrumentation, etc., have been reproduced from the 1994 test entry calibration report (Ref. 1), as this FQS repeated many of the same tests with the same or similar hardware and instrumentation.

Nomenclature

Symbols

a	speed of sound
C	coefficient associated with flow-angle probe regression model
M	Mach number
n	number of values in a list (e.g., $n = 3$ if referring to the summation of all three hot-wire probe measurements)
P	pressure
P_1 to P_9	denotes pressure measured at 15-ft survey rake flow-angle probe pressure port locations 1 through 9
R	gas constant ($R = 1716$ ft-lbf/slug-R for air)
T	temperature
TI	turbulence intensity
V, u	velocity (u is typically used for turbulence intensity definitions)
w	weights used in the weighted analyses; weights are different for the pressure probes and temperature probes on the 15-ft survey rake due to differences in probe spacing
X	distance or position in the streamwise direction
Y	distance or position in the spanwise direction (e.g., distance from the north wall)
Y_1 to Y_8	denotes either vertical or lateral locations of boundary layer rakes 1 through 8 relative to test section floor or north wall, respectively
Z	distance or position in the direction of gravity (e.g., distance above the floor)
α	pitch flow angle
β	yaw flow angle
γ	ratio of specific heats (typically, $\gamma = 1.4$ for air)
δ	boundary layer height
σ	standard deviation

Subscripts

avg	denotes the mean value of a set of data
$c1$	refers to a measurement taken in corner 1 of the 8×6/9×15 wind tunnel facility
i	typically refers to the ith probe in an array of probes (e.g., on the 15-ft survey rake, $i = 1$ to 20 for the flow-angularity probes and $i = 1$ to 15 for the thermocouples)

S	static condition of a given parameter (e.g., P_S = static pressure)
T	stagnation condition of a given parameter (e.g., P_T = stagnation pressure)
w	refers to a weighted analysis, such as a weighted average
α	refers to pressure ratios associated with calculating the pitch flow angle
β	refers to pressure ratios associated with calculating the yaw flow angle

Description of Facility[1]

The 8- by 6-Foot Supersonic Wind Tunnel (8×6 SWT) and 9×15 LSWT complex, shown in Figure 1, is an atmospheric-pressure, continuous-flow wind tunnel. The airflow is driven through the facility by a seven-stage axial compressor (18-ft inlet diam.) powered by three 29,000-hp electric motors. The 8- by 6-ft test section is a porous-wall-type transonic test section with a Mach number range of 0.25 to 2.0. The 9- by 15-ft test section is located in the return leg of the 8×6 SWT loop and has a slotted-wall construction, resulting in an area that is 11 percent open. This test section has a Mach number range of 0.00 to 0.22. Conditions in the 9- by 15-ft test section are controlled by the large flow-control doors located upstream of the test section (Figure 1 and Figure 2). The test section is 28.6 ft long. The walls of the test section diverge 0.25°; the floor and ceiling do not diverge. The walls, floor, and ceiling of the 9- by 15-ft test section are equipped with removable acoustic panels. The acoustic treatment begins 4 in. downstream of the test section inlet (TSTA 4) and extends for 27.5 ft. The acoustic panels reduce the inside height and width of the test section by about 4 in. A more detailed description of the facility can be found in Reference 2, and Reference 1 contains details of the previous facility calibration.

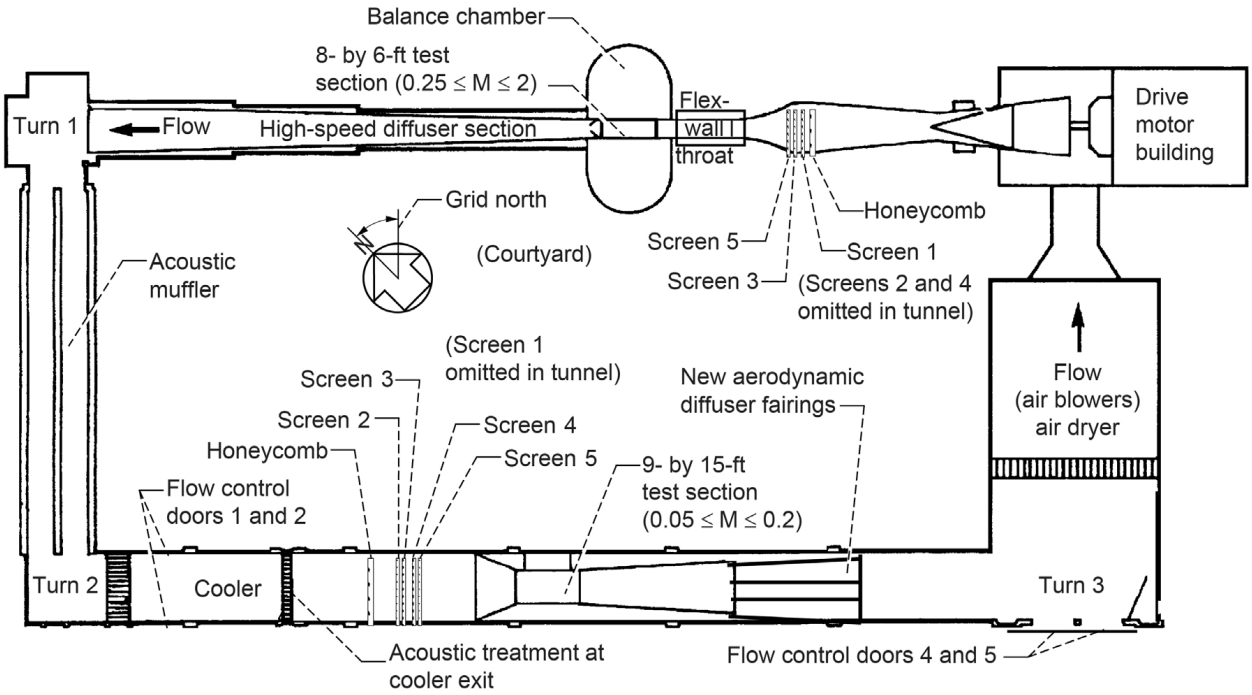

Figure 1.—Plan view of 8- by 6-Foot Supersonic and 9- by 15-Foot Low-Speed Wind Tunnel facility.

[1]Adapted from Reference 1.

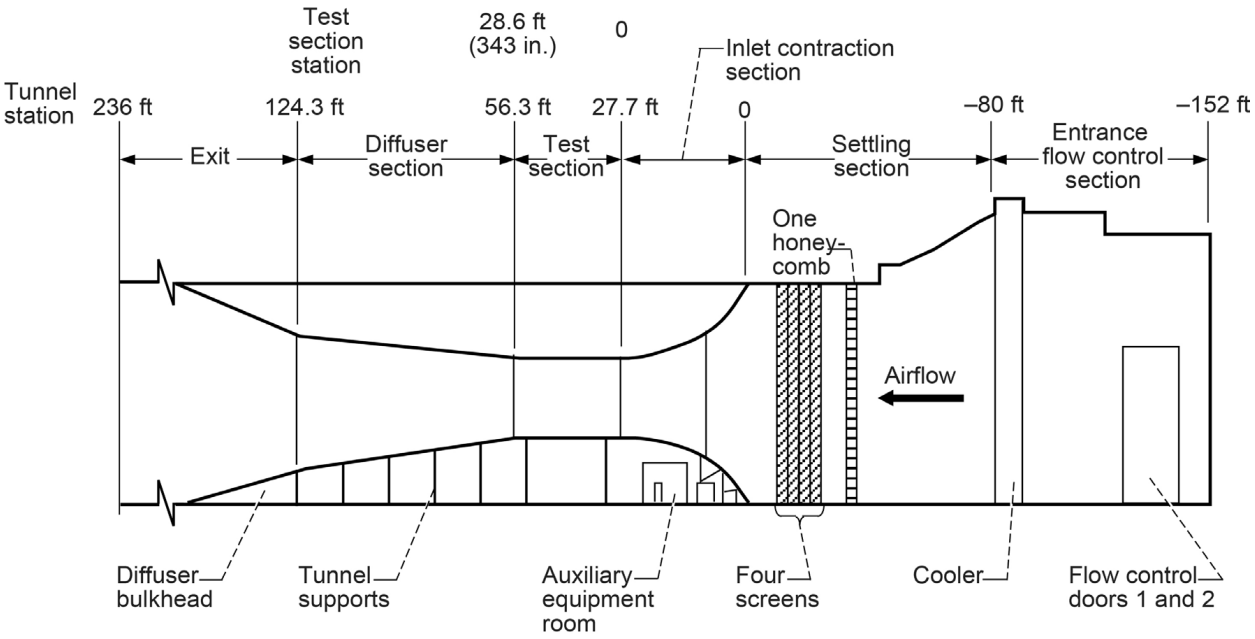

Figure 2.—Elevation view of 9- by 15-Foot Low Speed-Wind Tunnel facility.

Instrumentation and Test Hardware[2]

Several different types of flow-sensing probes were used in the FQS, including pitot-static probes, five-hole hemispherical-head flow-angularity probes, thermocouples, and hot-wire probes. Each of the probe types, their associated support systems, and their locations are described below.

15-ft Survey Rake

A typical installation of the 15-ft survey rake is shown in Figure 3. The main body of the rake is in the form of a box comprising four 1-in. channel sections (2024-T3511 aluminum) riveted together in pairs to form two I-beams; these beams are then connected by aluminum cover plates, which form the upper and lower surfaces of the rake body. Leading- and trailing-edge fairings (6061–T6 aluminum) are added to the main structure to provide the aerodynamic contours. The rake was constructed in three sections of approximately 5 ft each to better control the overall straightness of the rake, then assembled prior to installation of the instrumentation. The overall length of the rake is 176 in. (14 ft, 8 in.). The survey rake is supported at both ends by bolting the rake to wall-mounted support plates. These support plates are 106 in. high, and the bolts are arranged such that the rake can be positioned vertically every 6 in. above or below the test section centerline. The rake is also supported at the centerline by a section of streamline tubing that spans from floor to ceiling. This streamline tubing support replaces the cable supports used during previous calibration entries and duplicates the calibration setup used successfully in the Glenn Icing Research Tunnel (IRT).

The 15-ft survey rake instrumentation layout is shown in Figure 4. The instrumentation mounted on the rake includes 20 flow-angularity probes, 15 thermocouples, and three hot-wire probes (single-wire probes were used in the 2015/2016 FQS). The flow-angularity probe spacing on the rake is not centered about the rake centerline. This was done to provide a more detailed mapping of the flow field at the location in the test section where research test articles are often positioned (the test articles are offset from

[2]Adapted from Reference 1.

the test section centerline to allow more room for the article to be tested at high incidence angles). During the FQS, the 15-ft survey rake was inverted (flipped end for end) so that the more tightly spaced probes were positioned on the south side of the test section to provide detailed flow-field data in the area where the fan drive rig had recently been installed.

The flow-angle probes are five-hole, hemispherical-head probes, which allows resolution of two flow-angle components (pitch and yaw). Figure 5 shows details of the flow-angle probes. The flow-angle probes were calibrated for the Mach number range of 0.05 to 0.20 (the Mach number range of the 9- by 15-ft test section is 0.00 to 0.20). The probe calibration was conducted by General Dynamics, Convair Division, in San Diego, California; details of the probe calibration and data reduction techniques are contained in Reference 3. Total pressure is sensed by a port at the center of the probe tip. Four independent static pressure measurements are made using taps on the probe body; these four measurements are then averaged to indicate the static pressure at each probe. These probes extend 20.7 in. ahead of the leading edge of the rake.

Aspirated thermocouples with chromel-alumel (type K) sensing elements are used. The thermocouples are mounted to the bottom surface of the survey rake, with the heads of the thermocouples about even with the rake's leading edge. With the rake body in its inverted orientation during the FQS, the thermocouples protrude from the top surface of the rake body.

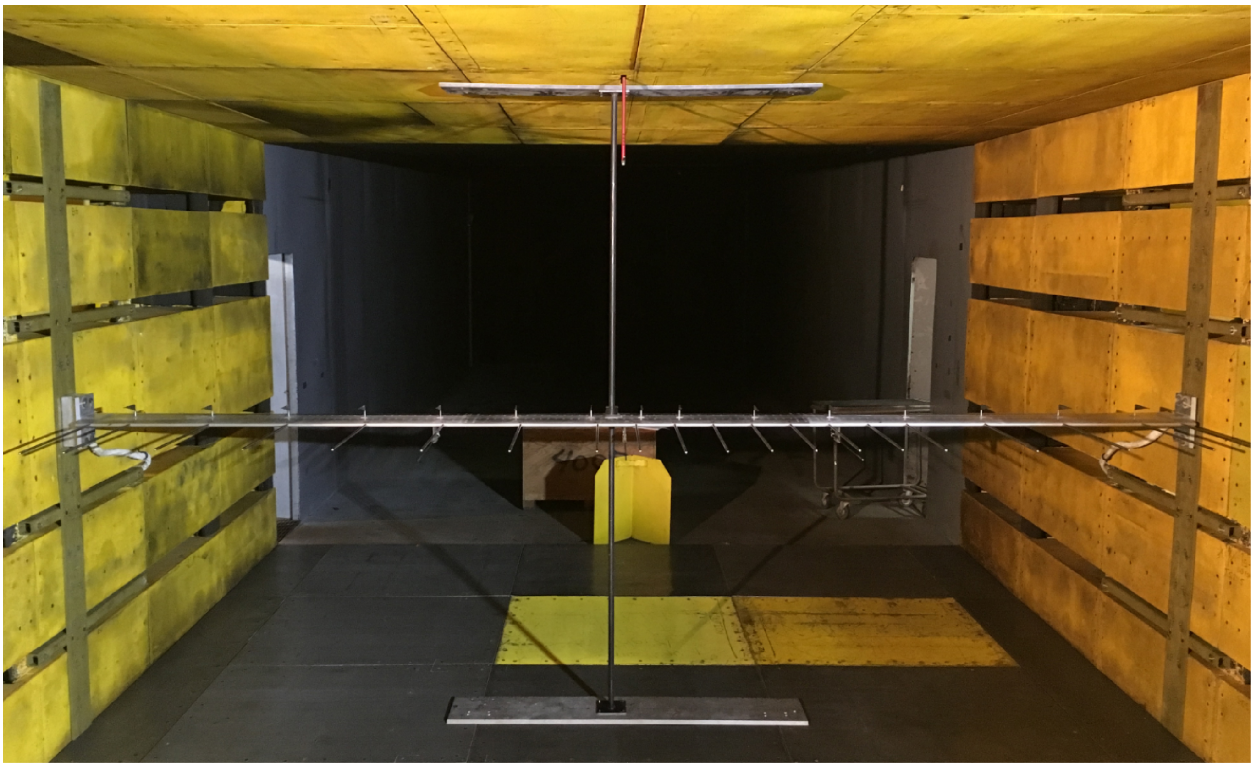

Figure 3.—Installation of 15-ft survey rake at centerline rake height and test section station 198 in inverted configuration during 2015/2016 flow quality survey.

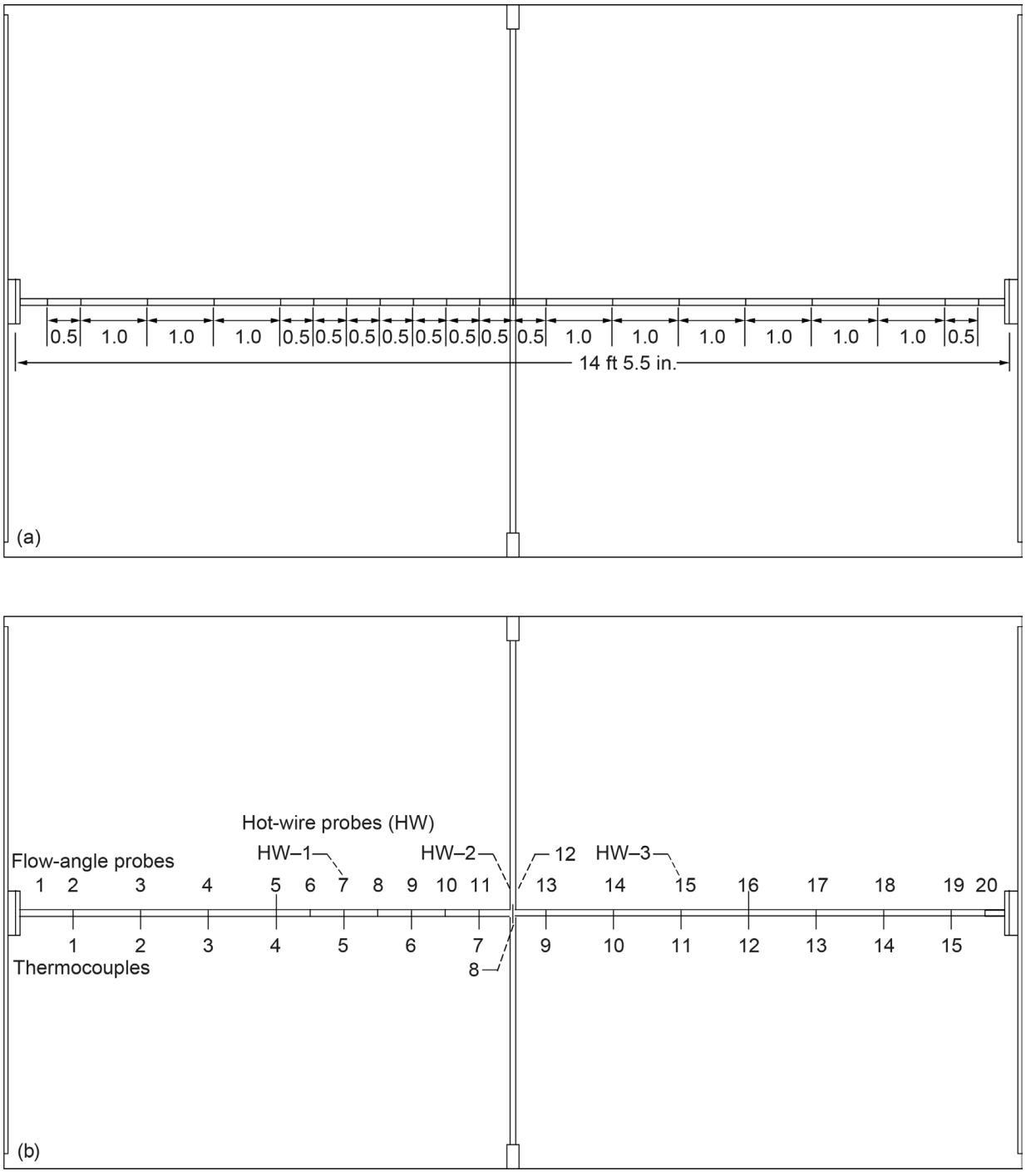

Figure 4.—Instrumentation layout of 15-ft survey rake with rake in normal configuration (upstream looking aft). Location and numbering scheme of all probes is reversed when survey rake is in inverted configuration, as in 2015/2016 flow quality survey. Dimensions are in feet unless otherwise noted. (a) Layout showing spacing between flow-angle probes. (b) Layout showing flow-angle probes, thermocouples, and hot-wire (HW) probe locations.

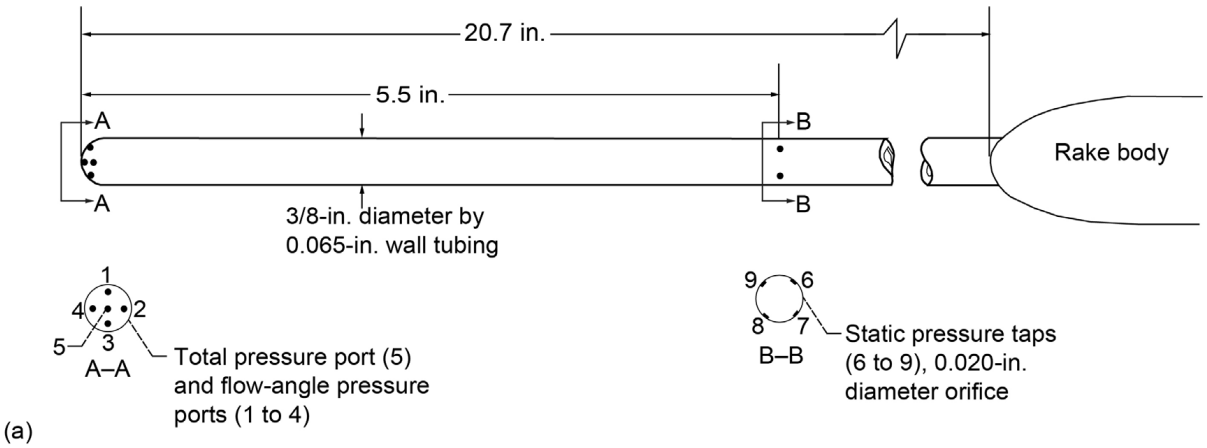

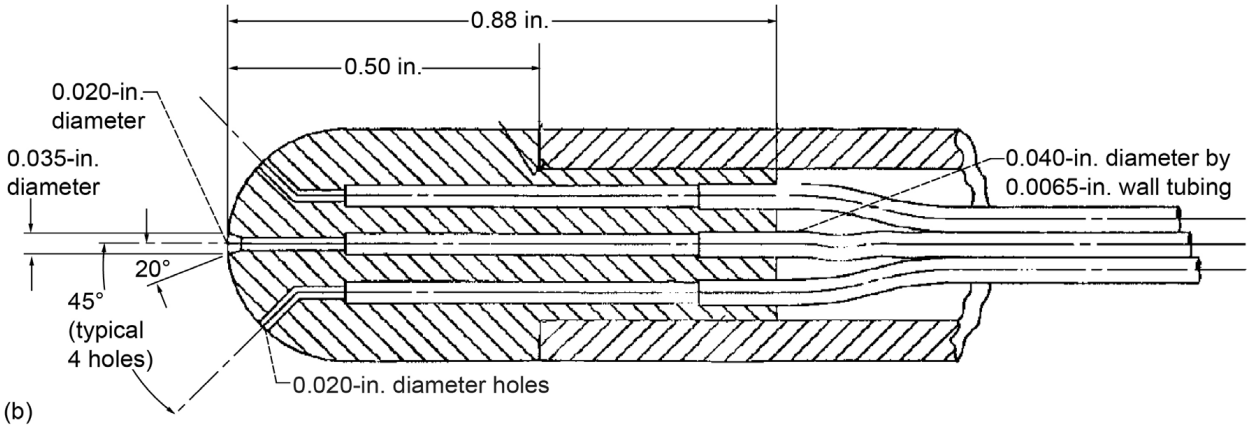

Figure 5.—Details of five-hole, hemispherical-head flow-angle probes (linear dimensions in inches). Probe port locations are valid when survey rake is in its normal configuration; numbering scheme rotates by 180° when survey rake is in inverted configuration, as in 2015/2016 flow quality survey. (a) General dimensions and port locations. (b) Probe tip internal detail.

Probe no.	Distance from tunnel surface, Z, in.
1 (Base)	0.250
2	0.500
3	0.750
4	1.000
5	1.250
6	1.500
7	2.000
8	2.250
9	3.000
10	3.500
11	4.000
12	4.500
13	5.500

Probe no.	Distance from tunnel surface, Z, in.
14	6.500
15	7.500
16	8.500
17	9.500
18	10.500
19	11.500
20	12.500
21	13.500
22	14.500
23	15.500
24	16.500
25 (Tip)	17.500

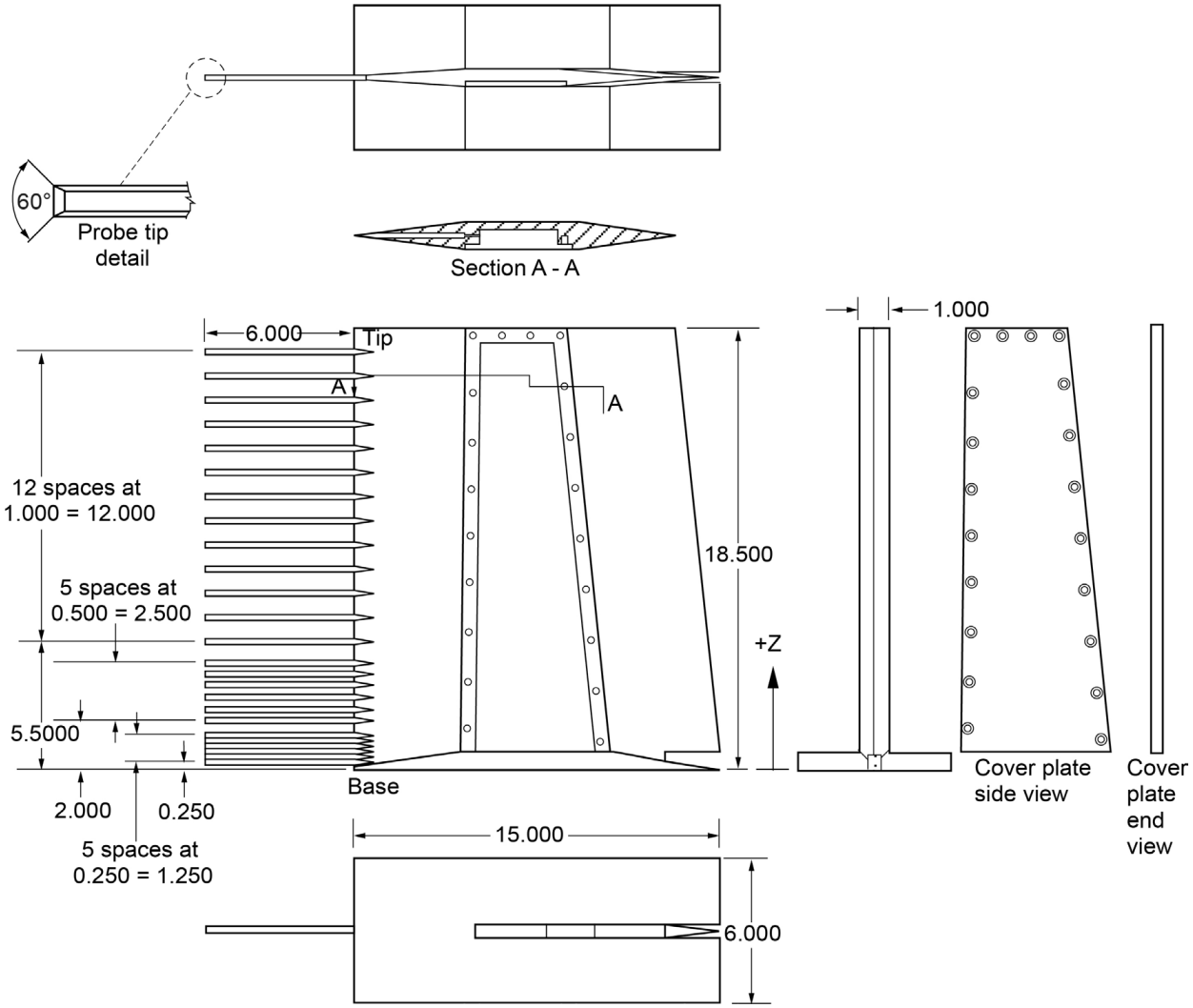

Figure 6.—Diagram of boundary layer rakes and spacing of rakes' pitot tubes. All dimensions are in inches.

Boundary Layer Rakes

Boundary layer surveys in the 9- by 15-ft test section were carried out using six boundary layer rakes. A schematic of the boundary layer rakes used in these surveys is shown in Figure 6. The test configuration for the FQS is shown in Figure 7. Also included are the rake numbering scheme and location information (Figure 8 and Table I).

Each rake had 25 total pressure probes spaced so that a dense pressure distribution could be obtained near the test section surface. Six 10–24 countersunk socket head cap screws were used to fasten each boundary layer rake base plate to a 3/16-in.-thick aluminum plate. The same fasteners used to mount the acoustic boxes to the tunnel structure were used to mount the boundary layer rake and plate assemblies. Each 3/16-in.-thick aluminum plate had a 30° leading-edge bevel.

Tunnel Rakes

Two ceiling-mounted rakes were used to measure the test section operating conditions. These tunnel rakes provide the reference measurements needed to calculate calibrated freestream test section conditions and are also used during customer testing, not just test section characterization entries. Each rake was composed of one pitot-static probe and four thermocouples (type E). The pitot-static probe extended 12.25 in. from the test section ceiling. Figure 9 gives the axial locations of these rakes in the test section. The upstream test section rake, referred to as the “bellmouth rake,” was 2.5 ft off test section centerline toward the north test section wall, and the downstream test section rake, referred to as the “aft rake,” was 0.09 ft off centerline toward the north wall. The total pressures were sensed using the electronically scanned pressure (ESP) system 15-psid rack-mounted modules with an accuracy of ±0.0075 psia; the difference between the total and static pressure was measured by delta pressure transducers with an accuracy of ±0.005 psid.

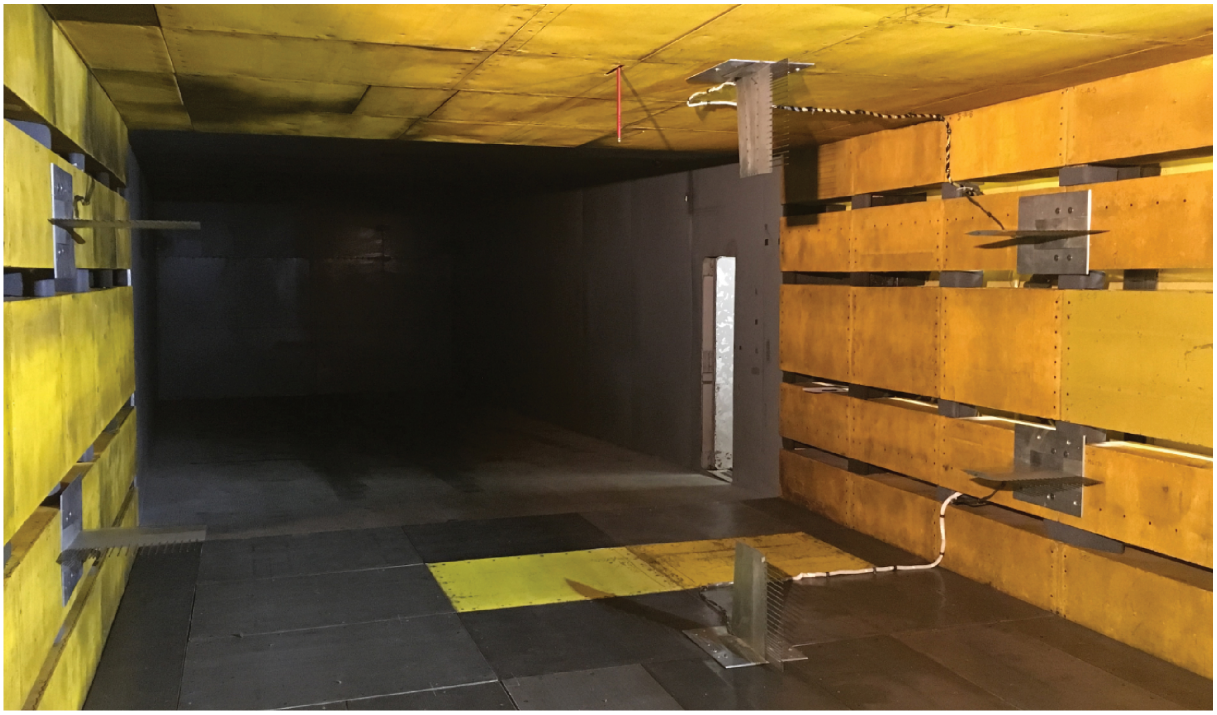

Figure 7.—Installation of six boundary layer rakes at test section station 199 in 9- by 15-Foot Low-Speed Wind Tunnel test section during 2015/2016 flow quality survey.

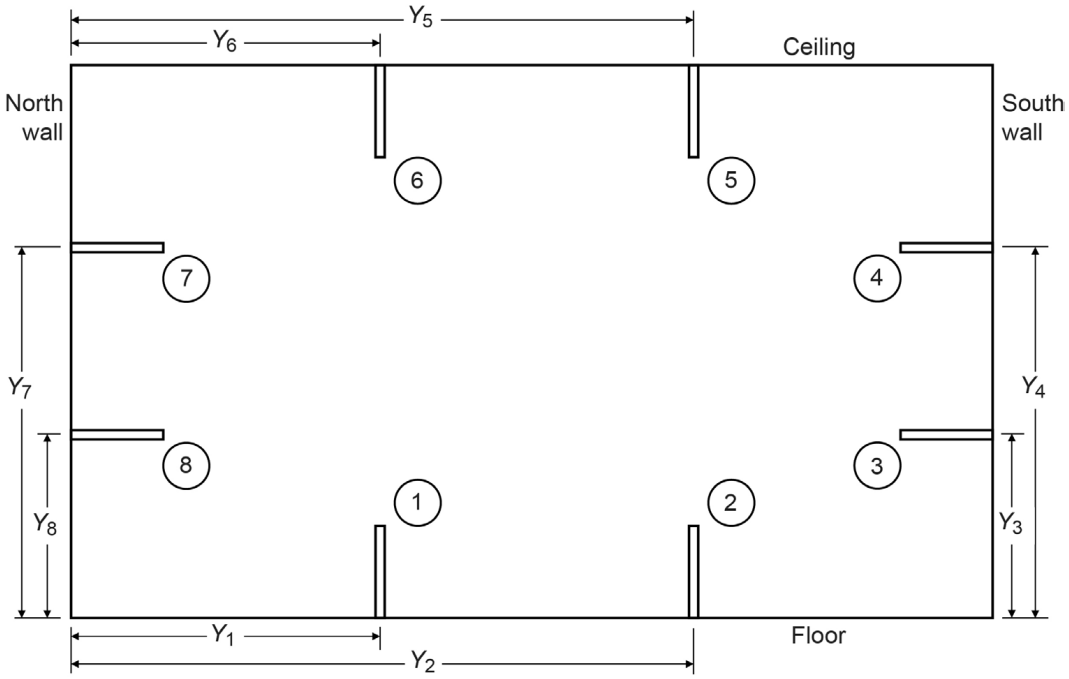

Figure 8.—Numbering schematic and relative location of six 18-in. boundary layer rakes in 9- by 15-Foot Low-Speed Wind Tunnel test section during 2015/2016 flow quality survey (FQS) (upstream looking aft). See Table I for location details. Note that rakes 1 and 6 were not used during this FQS; their appearance in this figure is simply as a placeholder.

TABLE I.—LOCATIONS OF 18-in. BOUNDARY LAYER RAKES IN 9- BY 15-FOOT LOW SPEED WIND TUNNEL TEST SECTION (FIGURE 8)

Rake	X,[a] in.	Y,[b] in.	ΔZ,[c] in.
[d]1	---------	---------	--------
2	199.250	110.625	0.1875
3	199.375	28.800	0.1880
4	199.375	75.200	0.1875
5	199.250	111.125	0.1875
[d]6	---------	---------	--------
7	199.000	75.950	0.1875
8	199.000	28.800	0.1880

[a]Streamwise distance from tunnel zero station to rake base plate leading edge.

[b]Spanwise distance from tunnel north wall to rake trailing edge for floor and ceiling mounted rakes; vertical distance from tunnel floor to rake trailing edge for wall mounted rakes.

[c]Distance between rake base plate and tunnel walls, ceiling, or floor (typically 3/16 in. due to mounting plates).

[d]Rakes 1 and 6 were not used during this flow quality survey.

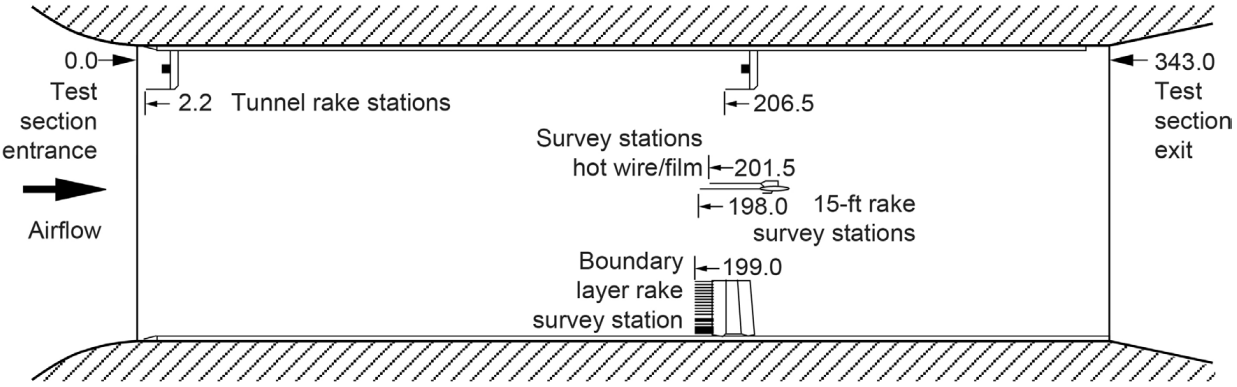

Figure 9.—Test section stations of tunnel rakes, flow-angle probes, hot-wire probes, and boundary layer rake pitot tubes in 9- by 15-Foot Low-Speed Wind Tunnel during 2015/2016 flow quality survey.

Data Systems

The standard tunnel data system was used for the aerodynamic calibration test. Steady-state pressure data for the aerodynamic calibration were acquired with an ESP system. The ESP system uses plug-in modules, each containing 32 individual transducers that can be addressed and scanned at a rate of 10,000 ports/sec. On-line calibration of all ESP transducers is typically performed automatically every 2 hr or at the discretion of the test engineer. Calibration is carried out by the operation of a pneumatic valve in each module that allows three pressures measured with precision digital quartz transducers to be applied. For these tests, 15-psid modules were used.

Real-time data acquisition and display was provided by Escort D+. This system accommodates the ESP inputs as well as all steady-state analog and digital signals used, including survey rake and tunnel facility thermocouples and pertinent tunnel control parameters such as compressor speed. The Escort D+ facility microcomputer acquires these data, converts them to engineering units, executes calculations, checks limits on selected channels, and displays the information in alphanumeric and graphical form with a 1-sec update rate. For this test, each collected data reading was 100 scans (100 sec) of data.

A research engineer familiar with hot-wire measurements assisted in the measurement and data reduction of the hot-wire signals. Three single-wire TSI (TSI Inc.) hot wires were used during the FQS with three anemometers (1 anemometer per sensor).

Test Setup and Procedures

15-ft Survey Rake

The 15-ft survey rake was installed at one flow-field axial survey station, TSTA 198; past flow quality surveys have used as many as five flow-field axial survey stations. The survey station is defined as the distance from the test section inlet (TSTA 0) to the tip of the flow-angularity probes. Data were collected with the 15-ft rake at five vertical positions: centerline, ±12, and ±24 in. from the centerline. For the entirety of this flow quality survey, the 15-ft rake was in the inverted configuration to concentrate measurement near the south side of the test section. The instrumentation numbering scheme is also reversed in the inverted configuration: probe 1 is nearest the south wall of the test section, with probe numbers increasing monotonically toward the north wall of the test section. At each position, data were taken at Mach numbers of 0.22, 0.20, 0.15, and 0.10 in three-motor operation and 0.15, 0.10, and 0.05 in one-motor operation. In addition, for the rake at the vertical centerline, the maximum test section Mach number of 0.23 was achieved.

The first test run was at station 198, with the rake at the vertical centerline. Prior to the first run, the flow-angularity probe alignment offsets were measured using a FaroArm® (FARO Technologies, Inc.) portable coordinate measuring machine, and the baseline rake body pitch and yaw angles were measured using a digital inclinometer and tape measure, respectively. For each rake height change, the rake body pitch and yaw angles were measured and compared with the baseline values. The differences from the baseline values were used to correct the measured flow angles for rake body misalignment induced by the model change.

Three TSI model 1210 single-element hot-wire probes were mounted on the 15-ft rake. Coaxial cables were used to connect the hot-wire probe supports to TSI IFA-100 anemometers located in the facility's auxiliary control room. The probe supports were rigidly mounted to the 15-ft rake structure via aluminum mounting blocks. The angularity of the hot-wire mounting blocks was not taken into account because only single-wire hot wires were used. The hot-wire sensors were removed between test runs and during 15-ft survey rake position changes to prevent accidental breakage. None of the hot wires failed during the test entry; however, during the first two runs (with the rake at centerline and 12 in. below centerline) it was found that the cable connecting the hot wire closest to the north wall was faulty and was introducing excessive noise into the signal. This cable had been routed within the rake body trailing edge. Prior to the next run (with the rake at 24 in. above centerline), this cable was disconnected and a 25-ft cable was used to connect the hot-wire sensor to the longer coaxial cable. The 25-ft extension cable was secured along the trailing edge of the rake body, down the central vertical support, and along the test section floor using aluminum tape.

Boundary Layer Rakes

Six boundary layer rakes were used at TSTA 199. Two rakes were mounted on each test section wall and one rake was mounted to the floor and ceiling near the south test section wall, as shown in Figure 7. Data were taken at Mach numbers of 0.23, 0.22, 0.20, 0.15, and 0.10 in three-motor operation and 0.15, 0.10, and 0.05 in one-motor operation.

Data Reduction

15-ft Survey Rake

The 15-ft survey rake measured the following freestream flow parameters during the FQS: total pressure, static pressure, total temperature, flow angularity, and turbulence intensity. The following equations were used to calculate flow-field parameters.

Mach number, M, at each of the 20 flow-angularity probes was determined using a ratio of the probe static pressure, P_S, to total pressure, P_T, and the isentropic relation (Equation 44 from Ref. 4, using ratio of specific heats $\gamma = 1.4$) where P_S is the average of P_6, P_7, P_8, and P_9:

$$M = \sqrt{\frac{2}{\gamma - 1}\left(\left(P_S / P_T \right)^{\frac{-(\gamma-1)}{\gamma}} - 1 \right)} \tag{1}$$

Total temperature, T_T, is sensed by each of the 15 thermocouple probes on the 15-ft survey rake. Velocity is determined using the definition of Mach number, M = V/a, where a is the speed of sound ($a = \sqrt{\gamma R T_S}$). The static temperature, T_S, is calculated using the following relation (Equation 43 from Ref. 4):

$$T_S = \frac{T_T}{1 + \frac{\gamma - 1}{2} M^2} \tag{2}$$

The local velocity is then determined using

$$V = M * a = M * \sqrt{\gamma R T_S} \tag{3}$$

In calculations where pressure and temperature are used together, allowances were made for the different number and position of flow-angle probes and thermocouples; the 20 flow-angularity probes and 15 thermocouples are not typically collocated laterally along the length of the rake (refer to Figure 4). The Mach number associated with the flow-angle probe closest to each thermocouple was used to compute the static temperature. In the velocity calculation, either 1) a flow-angle probe and the adjacent thermocouple probe or 2) the average of the measurements made by the two thermocouples on either side of a flow-angle probe were used, as appropriate (depending on local probe locations).

Two components of flow angle were measured by the five-hole hemispherical-head flow-angularity probes on the survey rake. As the name implies, the head of each probe has five pressure orifices, as shown in Figure 5. The center port (port 5) senses the total pressure, P_T. Ports 1 and 3 are used in determining the pitch flow angle, α, and ports 2 and 4 are used for the yaw flow angle, β. The difference in pressure measured by a pair of opposing ports on a given flow-angularity probe is related to the flow angle through an extensive probe calibration and resulting regression curve. The probe calibration is based on the relationship between the probe attitude (flow angle) and two pressure ratios, P_α and P_β. The pressure ratios are defined as:

$$P_\alpha = \frac{P_3 - P_1}{P_T - P_{avg}} \tag{4}$$

$$P_\beta = \frac{P_4 - P_2}{P_T - P_{avg}} \tag{5}$$

where $P_{avg} = (P_1 + P_2 + P_3 + P_4)/4$. The flow angle is related to these pressure ratios through a calibration equation using coefficients C_0 to C_9; for the pitch flow angle, α, the relationship is:

$$\alpha = C_0 + C_1 P_\alpha + C_2 P_\beta + C_3 P_\alpha^2 + C_4 P_\beta^2 + C_5 P_\alpha P_\beta + C_6 P_\alpha^3 + C_7 P_\beta^3 + C_8 P_\alpha^2 P_\beta + C_9 P_\alpha P_\beta^2 \tag{6}$$

A similar equation is used for the yaw flow angle, β. A positive angle in the pitch direction is defined as the flow pointing up toward the ceiling of the test section, and a positive angle in the yaw direction is defined as the flow pointing toward the south wall of the test section. Details of the probe calibration are not included in this report but may be found in Reference 3. Details on correcting the flow-angle data for rake and probe misalignment are described in Reference 5.

The single-element hot wires were calibrated in situ using the local velocity at the nearest five-hole flow-angularity probe. The mean velocity in the streamwise direction is the mean of the calibrated velocity data from each hot wire. This assumes that the flow angularity is negligible and that the vast majority of the velocity sensed by the probe is purely in the streamwise direction. The standard deviation of the sensed velocity data about the mean velocity was calculated; this feeds into the turbulence intensity (*TI*) calculation. These quantities are defined below, where u is the velocity measured at the hot-wire probe:

$$\bar{u} = \frac{1}{n}\sum_{i=1}^{n} u_i \tag{7}$$

$$\sigma(u) = \sqrt{\frac{1}{n}\sum_{1}^{n}(u_i - \bar{u})} \tag{8}$$

$$TI = \frac{\sigma(u)}{\bar{u}} * 100\% \tag{9}$$

For the FQS, the area of concern in the survey plane was the "core" area of the test section: between ±60 in. from the test section centerline in the spanwise direction and ±30 in. from the centerline in the vertical direction. Calculated data points for every probe, even those outside the area of interest, are presented in the figures to follow. In the figures, flow-field data measured by the 15-ft survey rake were normalized by the corresponding variables measured at the aft test section rake (e.g., total temperature measured by the survey rake is normalized by total temperature measured by the aft rake). This normalization removes run-to-run variations in atmospheric conditions so that the data are more readily comparable.

As part of the acceptance criteria for the 9×15 LSWT acoustic improvement modifications, several values were calculated to assess the flow quality at each nominal Mach number setting in the test section. The weighted standard deviations of the freestream velocity and total temperature sensed by the 15-ft survey rake in the core of the test section were calculated. The weighted standard deviations of the total pressure, static pressure, and Mach number were also calculated and included in the results. Weighted analyses were required as the 15-ft survey rake's probe spacing (both pressure and temperature probes) is irregular. The core probes were chosen based on the desire to only assess the flow quality using measurements free from boundary layer influence. The core for variables that include parameters sensed by five-hole flow-angle probes consists of probe numbers 4 through 17, and the core for the total temperature measurements consists of thermocouple probes 3 through 13.[3] To assess the variation of the core flow, the local measurements on the survey rake were normalized by the weighted average of that parameter across the core of the rake during each run; the weighted average value of a measured parameter across the core of the rake during each run is denoted by a bar over the variable, such as $\bar{V}$. Weighted values are denoted by a subscript *w*. To remove run-to-run variation in the measured parameters caused by facility set-point errors, the ratios of local velocity to the aft rake velocity during that specific run were multiplied by the average aft rake velocity across all runs at that test section Mach number setting. This new local velocity value is considered normalized. These ratios, which have run-to-run variation removed, are gathered from each rake height for a given nominal Mach number, and the weighted standard deviations are calculated using the following equation:

$$\sigma_w\left(V/\bar{V}\right) = \sqrt{\frac{n\sum_{i=1}^{n} w_i\left(\frac{V_i}{\bar{V}} - \overline{\left(\frac{V}{\bar{V}}\right)}\right)^2}{(n-1)\sum_{i=1}^{n} w_i}} \tag{10}$$

[3]A small number of data points from the total temperature data set were omitted from the pool of points used in the weighted standard deviations at select Mach numbers. The data points were suspect due to an observed, unusually slow response and the possibility of an unreliable electrical connection.

The calculations for the total temperature, total pressure, static pressure, and Mach number weighted standard deviations are similar to this equation (total temperature standard deviation will have a smaller value of n). The root-mean-square (RMS) values for the calculated pitch and yaw flow angles are calculated as shown below using the core five-hole flow-angularity probe measurements. The RMS values are calculated for each nominal Mach number setting.

$$\mathrm{RMS}_w(\alpha) = \sqrt{\frac{\sum_{i=1}^{n} w_i \alpha_i^2}{\sum_{i=1}^{n} w_i}} \tag{11}$$

$$\mathrm{RMS}_w(\beta) = \sqrt{\frac{\sum_{i=1}^{n} w_i \beta_i^2}{\sum_{i=1}^{n} w_i}} \tag{12}$$

The mean turbulence intensity in the test section must also be assessed as part of the acceptance process for the acoustic improvement modifications. The average of the turbulence intensity measured by the three probes at the five rake heights was to be used as a measure of the mean turbulence intensity at a given Mach number set point.[4] As will be discussed in the results section, however, the 15-ft survey rake hot-wire measurements were deemed invalid. Consequently, freestream turbulence measurements from a 2008 fan test entry were used as a measure of the turbulence levels prior to the acoustic improvement modifications (see Appendix for details).

Boundary Layer Rakes

The boundary layer rakes measured total pressure profiles in the boundary layer. To calculate the Mach number profiles, the static pressure measured at the aft-tunnel rake was assumed to be constant for all boundary layer rakes. This was assumed regardless of rake position. To compute the boundary layer velocity profile, a constant speed of sound was assumed for all rakes regardless of the rake position. The speed of sound used was that computed using the static temperature at the aft-tunnel rake. For each rake, the velocity profiles were then normalized by the boundary layer rake tip velocity. This forced the velocity ratio at the boundary layer rake tip to be 1.0. Moving away from the tunnel surface, the first two experimental velocity ratio data points that bound the value 0.990 were used to find the boundary layer height, δ. The distances of those two probes from the tunnel surface, Z, and their computed velocity ratio were used in a linear interpolation routine. In equation form, the boundary layer height can be written as:

$$\delta = Z\big|_{V/V_\infty = 0.990} \tag{13}$$

[4]The turbulence intensity measurements at the hot-wire probe nearest the north wall were later excluded from the data set for rake heights at centerline and –12 in. from centerline due to a faulty cable that induced noise into the signal.

Discussion of Results

Flow-Field Surveys

Figure 10 to Figure 16 show the velocity profile across the test section at five rake heights. Figure 17 to Figure 23 show the total temperature profile across the test section at five rake heights. The spanwise profiles of the total pressure, static pressure, and Mach number in the test section are also included in Figure 24 to Figure 44. The figures displaying the velocity, total pressure, and Mach number distributions have values at the outermost flow-angularity probe locations, which fall outside the y-axis limits. These data points were not included on the figures to allow for details of the core profiles to be observable. Figure 45 to Figure 51 and Figure 52 to Figure 58show the pitch and yaw flow-angle distributions, respectively, for the five rake heights. All standard deviation and RMS values for the above parameters are tabulated in Table II.

The pressure differential in corner 1 of the facility was recorded by facility instrumentation and the tunnel control system. The delta pressure in corner 1, $P_{S,c1}$, is shown in Table II in pounds per square foot (psf). Across all conditions, the corner 1 delta pressure readings were below the facility structural limit of 75.5 psf. Not shown in Table II, the highest pressure differential was observed during the test entry while at a test section Mach number of 0.23. The pressure differential was 13.9 in. of water (72.3 psf) at this test section condition, which is still below the 75.5 psf structural limit in corner 1 of the facility.

During postprocessing of the hot-wire data, it was discovered that the anemometers were not properly tuned for frequency response, making the turbulence intensity measurements taken during the FQS invalid. Consequently, values for test section turbulence intensity prior to the acoustic improvement modifications were taken from a fan test conducted in 2008. The 2008 test utilized three hot-wire stands, each at a different lateral and axial position in the test section, with TSI model 1246 cross-wire probes located vertically near the test section centerline. For more details on the test setup and data analysis methods from the 2008 fan test entry, see Appendix A. The turbulence intensity measurements from the three hot-wire probes were averaged for Mach 0.2 and Mach 0.1 (three-motor operation) and are included in Table II along with the other acceptance criteria data.

TABLE II.—TABULATED FLOW-FIELD SURVEY VALUES OF INTEREST FROM 2015/2016 FLOW QUALITY SURVEY IN 9×15 LOW-SPEED WIND TUNNEL USING 15-ft SURVEY RAKE.

Mach no. / Values of interest	Three-motor operation				One-motor operation		
	0.22	0.20	0.15	0.10	0.15	0.10	0.05
$\sigma\left(V/\bar{V}\right)$	1.45×10^{-3}	1.38×10^{-3}	1.32×10^{-3}	1.53×10^{-3}	1.18×10^{-3}	1.64×10^{-3}	3.45×10^{-3}
$\sigma\left(T_T/\bar{T}_T\right)$	3.08×10^{-3}	2.99×10^{-3}	2.24×10^{-3}	1.43×10^{-3}	1.23×10^{-3}	5.35×10^{-4}	3.89×10^{-4}
$\sigma\left(P_T/\bar{P}_T\right)$	1.45×10^{-5}	1.32×10^{-5}	1.35×10^{-5}	1.16×10^{-5}	1.19×10^{-5}	1.11×10^{-5}	1.05×10^{-5}
$\sigma\left(P_S/\bar{P}_S\right)$	7.07×10^{-5}	5.84×10^{-5}	3.20×10^{-5}	1.84×10^{-5}	3.05×10^{-5}	2.42×10^{-5}	7.08×10^{-6}
$\sigma\left(M/\bar{M}\right)$	9.55×10^{-4}	9.75×10^{-4}	1.00×10^{-3}	1.34×10^{-3}	9.48×10^{-4}	1.56×10^{-3}	3.45×10^{-3}
RMS(α), deg	2.11×10^{-1}	2.08×10^{-1}	2.22×10^{-1}	2.54×10^{-1}	2.23×10^{-1}	2.63×10^{-1}	6.11×10^{-1}
RMS(β), deg	2.67×10^{-1}	2.62×10^{-1}	2.55×10^{-1}	2.28×10^{-1}	2.53×10^{-1}	2.33×10^{-1}	4.90×10^{-1}
Mean (TI), %	----------	0.11	----------	0.11	----------	----------	----------
$\Delta P_{S,c1}$, psf	67.6	56.1	33.3	18.2	32.2	15.6	4.7

TABLE III.—BOUNDARY LAYER HEIGHTS AS CALCULATED FROM BOUNDARY LAYER RAKES INSTALLED IN 2015/2016 FLOW QUALITY SURVEY

[All boundary layer heights are in inches.]

Mach no. / Rake no.	Three-motor operation					One-motor operation		
	0.23	0.22	0.20	0.15	0.10	0.15	0.10	0.05
[a]1	-------	-------	-------	-------	-------	-------	-------	-------
2	5.69	5.68	5.65	5.62	5.65	5.56	5.43	5.84
3	11.15	11.12	11.32	11.03	10.47	11.26	11.21	10.57
4	12.61	12.61	11.95	11.50	12.80	11.63	12.68	14.05
5	4.72	4.71	4.88	4.85	4.87	4.61	4.60	4.46
[a]6	-------	-------	-------	-------	-------	-------	-------	-------
7	12.93	13.00	13.26	13.64	14.16	12.99	13.28	13.70
8	10.91	10.70	10.87	10.61	10.52	11.51	12.28	12.68

[a] Rakes 1 and 6 were not used during this flow quality survey.

Boundary Layer

Figure 59 to Figure 66 show the total pressure profiles measured by the boundary layer rakes as a function of the distance from the test section flow surface at a given nominal Mach number set point. The distance from the flow surface, Z, is on the y-axis to assist in visualization of the boundary layer profile. Figure 67 to Figure 74 show the calculated velocity profiles as a function of the distance from the test section flow surfaces at a given nominal Mach number set point. The velocity profile plots also show the $V/V_\infty = 0.990$ line; the point at which the velocity profile curves first cross $V/V_\infty = 0.990$ (when approaching from the tunnel surface) is defined as the boundary layer height, δ. Figure 75 to Figure 82 show a bar chart for the boundary layer height, δ, at each boundary layer rake at a given nominal Mach number set point. Refer to Figure 8 and Table I for the position of the boundary layer rakes in the test section. Table III shows a summary of the boundary layer rake heights for each nominal Mach number set point.

Concluding Remarks

The flow quality survey (FQS) of the 9- by 15-Foot Low-Speed Wind Tunnel (9×15 LSWT) was completed in a single test entry in late 2015 and early 2016. This entry was necessary to capture the state of the flow quality in the 9×15 LSWT test section prior to the start of the acoustic improvement modifications.

The data acquired during the FQS were used to quantitatively evaluate the test section flow quality at a single axial station, including uniformity of several test section flow parameters, flow angularity, and turbulence intensity. Because the turbulence intensity data from this entry were invalid, turbulence measurements from a 2008 fan test entry were chosen to represent the turbulence levels in the test section prior to the acoustic improvement modifications. Boundary layer height data were also acquired across the operating range of the facility. Additionally, the data from this entry are evidence of the 9×15 LSWT capability to operate over its full operating range and reach Mach 0.23 while the corner 1 static pressure differential remained below structural limits. The flow quality data from this entry will be compared with FQS data collected following completion of the 9×15 LSWT acoustic improvement modifications.

Appendix—Turbulence Intensity from 2008 Fan Test Entry in 9- by 15-Foot Low-Speed Wind Tunnel

During a fan test entry in 2008 in the 9- by 15-Foot Low-Speed Wind Tunnel (9×15 LSWT), hot-wire data were acquired with probes mounted on supports at three locations in the test section (see Figure 83). The probe closest to the model was referred to as the "downstream probe," the next closest probe to the model was farther upstream and was referred to as the "middle probe," and the most upstream probe from the model was referred to as the "upstream probe." The downstream probe was positioned 30 in. south of the test section centerline and at test section station (TSTA) 168.8. The middle probe was positioned along the test section centerline and at TSTA 99.4. The upstream probe was positioned 60 in. south of the test section centerline and at TSTA 30.0. All three probes were located at the elevation of the model centerline, which was approximately equal to the test section centerline. Figure 84 shows a profile view of one of the hot-wire probe stands mounted in the wind tunnel, while Figure 83 shows all three stands installed in the 9×15 LSWT during the 2008 fan test. TSI (TSI Inc.) model 1246 cross-wire probes were used during this test entry.

Data were acquired by the three hot-wire probes at Mach 0.2 and Mach 0.1, and at each freestream condition, data were acquired at three model fan speeds: 5,425 RPMC,[5] 7,525 RPMC, and 8,750 RPMC. Data were acquired at a sampling rate of 200 kHz for 3 sec. Initial postprocessing of the data indicated that low-frequency oscillations of the "mean" flow contributed significantly to the measured root-mean-square (RMS) of the velocity measured at each hot wire. The influence of the model fan blades could also be seen in the hot-wire signals. These two effects were removed during subsequent postprocessing. The effect of the fan blades was removed by ensemble averaging the data from the different fan revolutions and subtracting the ensemble average from the time trace on a revolution-by-revolution basis. The effect of the low-frequency oscillations was negated by considering only a short time segment of the signal during which the mean remained relatively constant (i.e., there was little low-frequency drift in the signal). The short time segment considered was equivalent to one revolution of the fan.

The results in Table IV under each probe's pseudonym are an average of the measurements made at the three locations in the wind tunnel. For the flow quality survey prior to the acoustic improvement modifications, the mean turbulence intensity values of the freestream flow for Mach 0.20 and Mach 0.10 (three-motor operation) are considered to be the average of the measurements made at the three locations in the wind tunnel. This is shown in the "Average" column of Table IV. These results are similar to the turbulence intensity measurements from the 1994 calibration test's results, where axial turbulence intensity levels are quoted at between 0.05 and 0.20 percent at axial station 202 for nearly all vertical heights of the 15-ft survey rake (Ref. 1).

TABLE IV.—TURBULENCE INTENSITY VALUES FROM THREE HOT-WIRE STANDS USED IN 2008 FAN TEST ENTRY IN 9- BY 15-FOOT LOW-SPEED WIND TUNNEL AND THEIR AVERAGES AT MACH 0.20 AND 0.10

Mach number, M (three-motor operation)	Turbulence intensity, percent			
	Hot-wire stand			Average
	Upstream	Middle	Downstream	
0.20	0.10	0.13	0.10	0.11
0.10	0.11	0.11	0.12	0.11

[5]RPMC stands for revolutions per minute corrected, a parameter commonly calculated for 9×15 LSWT fan test models.

References

1. Arrington, E. Allen: Calibration of the NASA Lewis Research Center 9- by 15-Foot Low Speed Wind Tunnel (1994 Test). NASA CR–195438, 1997. http://ntrs.nasa.gov
2. Soeder, Ronald H.: NASA Lewis 9- by 15-Foot Low-Speed Wind Tunnel User Manual. NASA TM–106247, 1993. http://ntrs.nasa.gov
3. Healy, Laura J.: Low-Speed Calibration of NASA Lewis Research Center Flow Angularity Probes. NASA Report No. GDC6660–91–1–001, Contract NAS3–26191, 1991.
4. Ames Aeronautical Laboratory Research Staff: Equations, Tables, and Charts for Compressible Flow. NACA Report 1135, 1953. http://ntrs.nasa.gov
5. Arrington, E. Allen; Pickett, Mark T.; and Soeder, Ronald H.: Calibration of the NASA Lewis Research Center 9- by 15-Foot Low Speed Wind Tunnel (1992 Test). NASA TM–106860, 1995. http://ntrs.nasa.gov

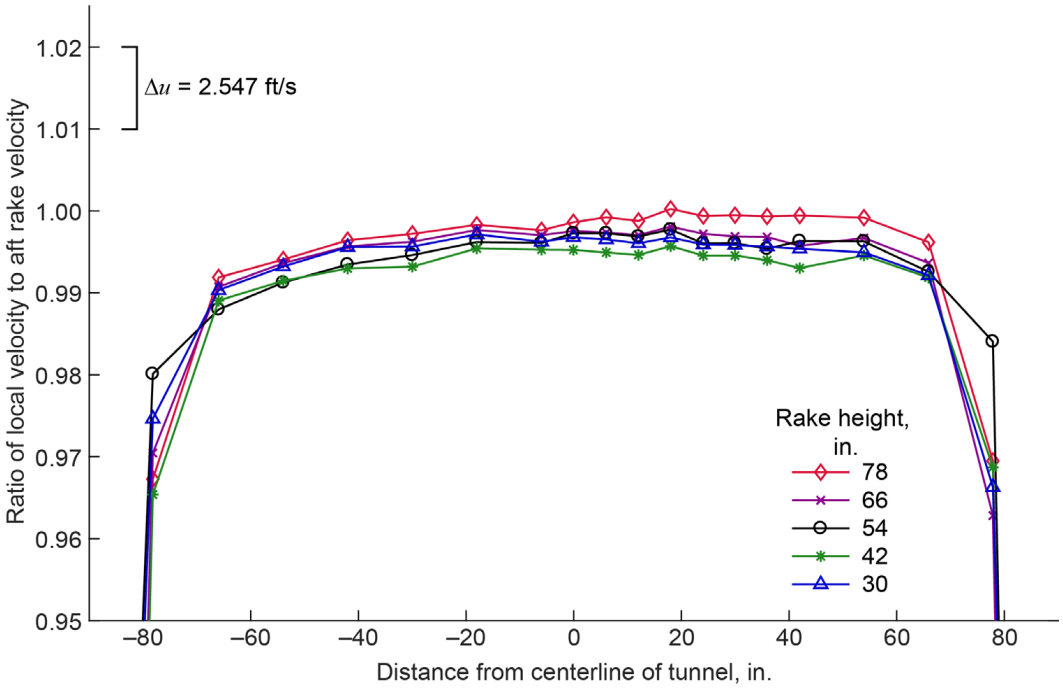

Figure 10.—Test section velocity (V) distribution at test section station 198 during 2015/2016 flow quality survey in 9- by 15-Foot Low-Speed Wind Tunnel (upstream looking aft) at Mach 0.22 (three-motor operating mode).

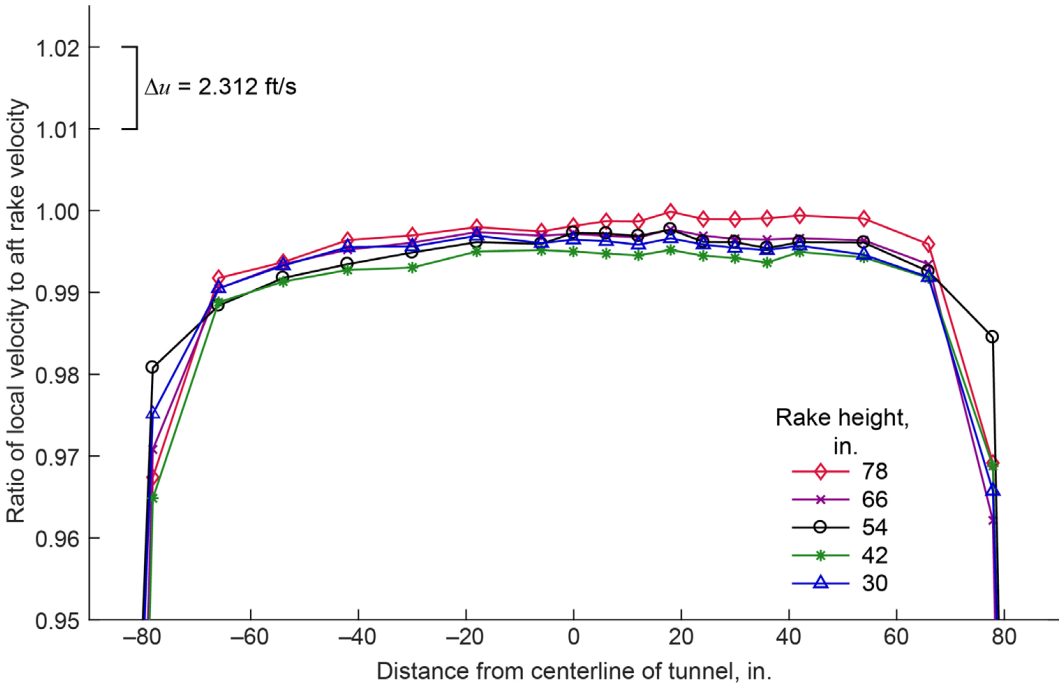

Figure 11.—Test section velocity (V) distribution at test section station 198 during 2015/2016 flow quality survey in 9- by 15-Foot Low-Speed Wind Tunnel (upstream looking aft) at Mach 0.20 (three-motor operating mode).

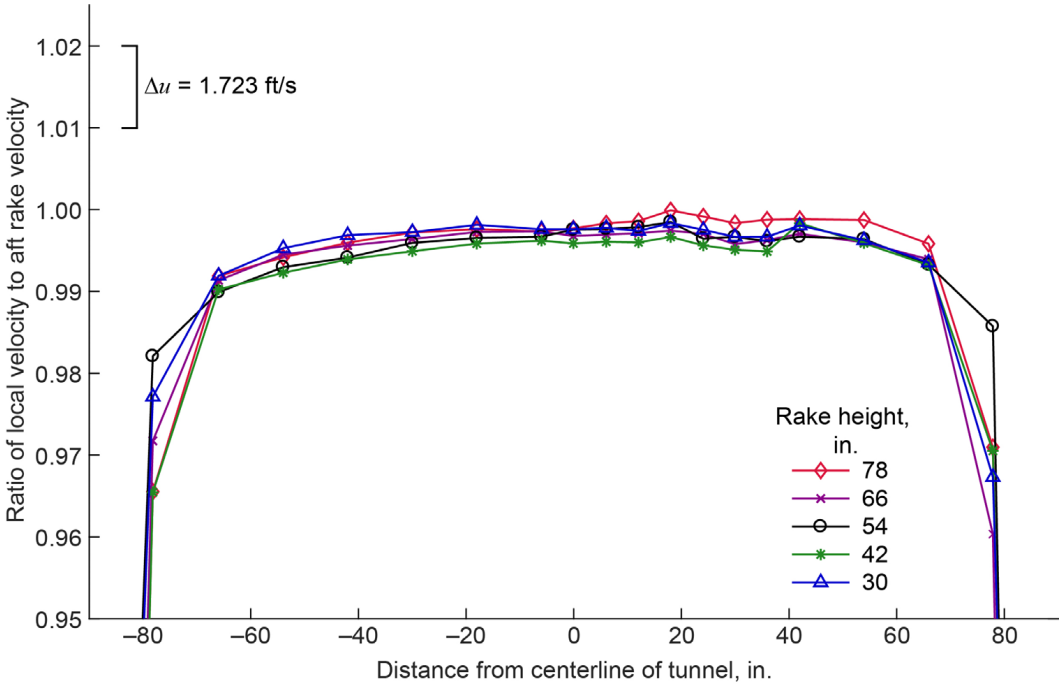

Figure 12.—Test section velocity (V) distribution at test section station 198 during 2015/2016 flow quality survey in 9- by 15-Foot Low-Speed Wind Tunnel (upstream looking aft) at Mach 0.15 (three-motor operating mode).

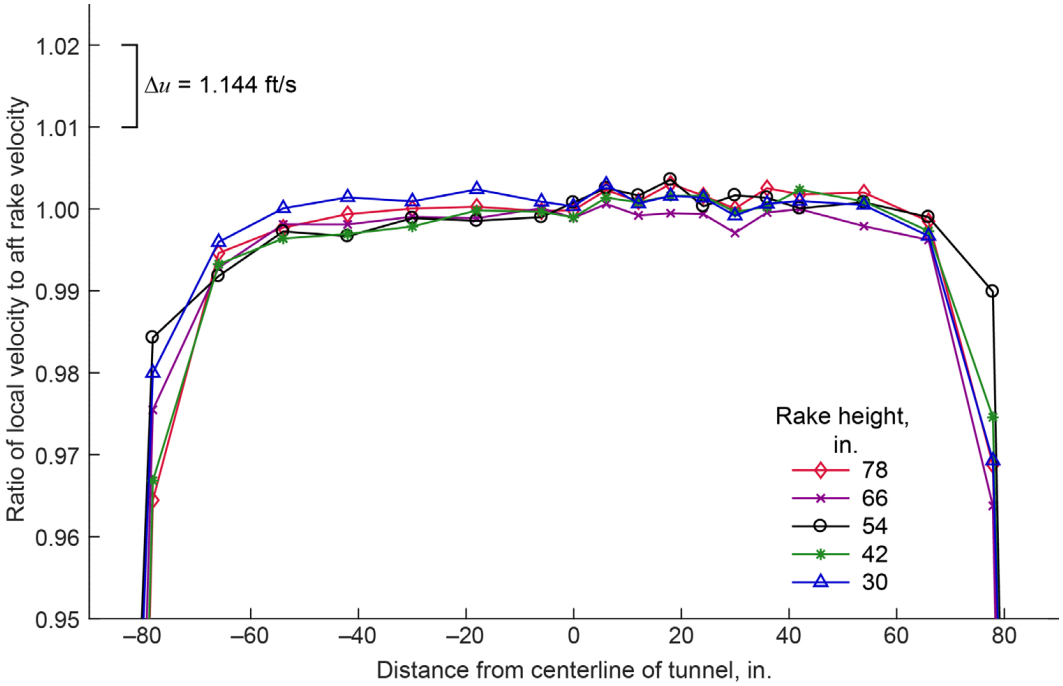

Figure 13.—Test section velocity (V) distribution at test section station 198 during 2015/2016 flow quality survey in 9- by 15-Foot Low-Speed Wind Tunnel (upstream looking aft) at Mach 0.10 (three-motor operating mode).

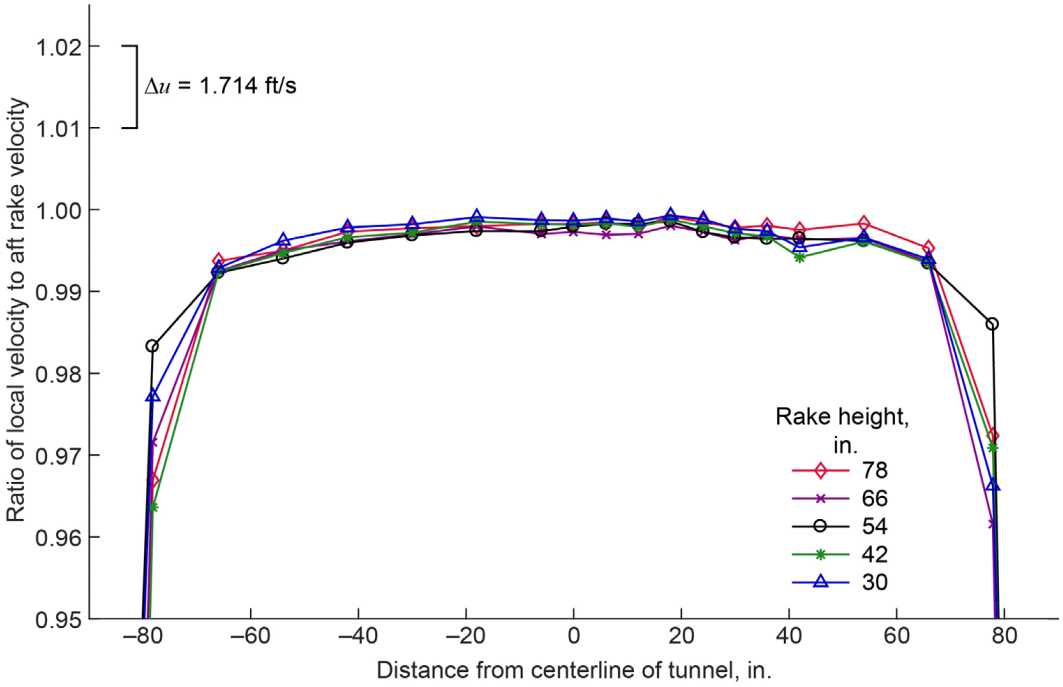

Figure 14.—Test section velocity (V) distribution at test section station 198 during 2015/2016 flow quality survey in 9- by 15-Foot Low-Speed Wind Tunnel (upstream looking aft) at Mach 0.15 (one-motor operating mode).

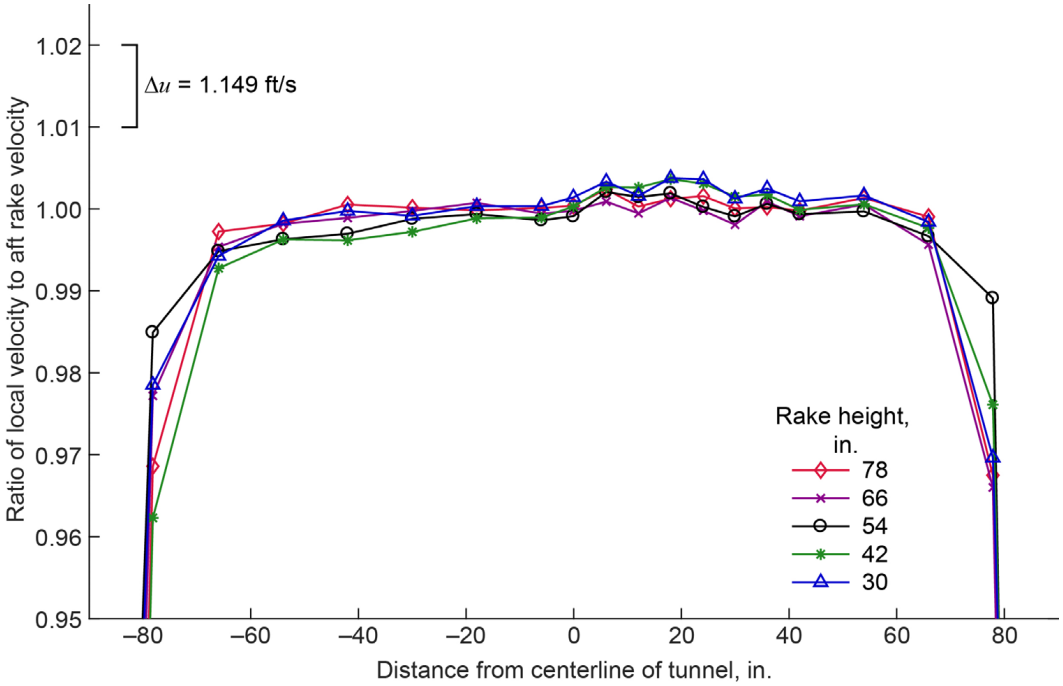

Figure 15.—Test section velocity (V) distribution at test section station 198 during 2015/2016 flow quality survey in 9- by 15-Foot Low-Speed Wind Tunnel (upstream looking aft) at Mach 0.10 (one-motor operating mode).

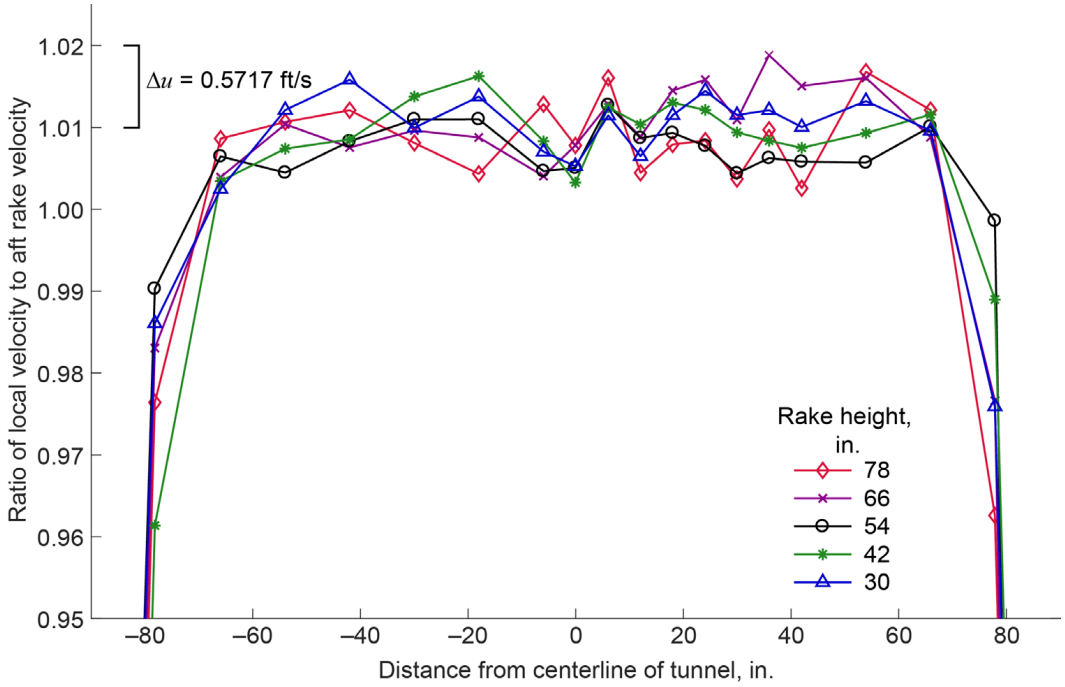

Figure 16.—Test section velocity (V) distribution at test section station 198 during 2015/2016 flow quality survey in 9- by 15-Foot Low-Speed Wind Tunnel (upstream looking aft) at Mach 0.05 (one-motor operating mode).

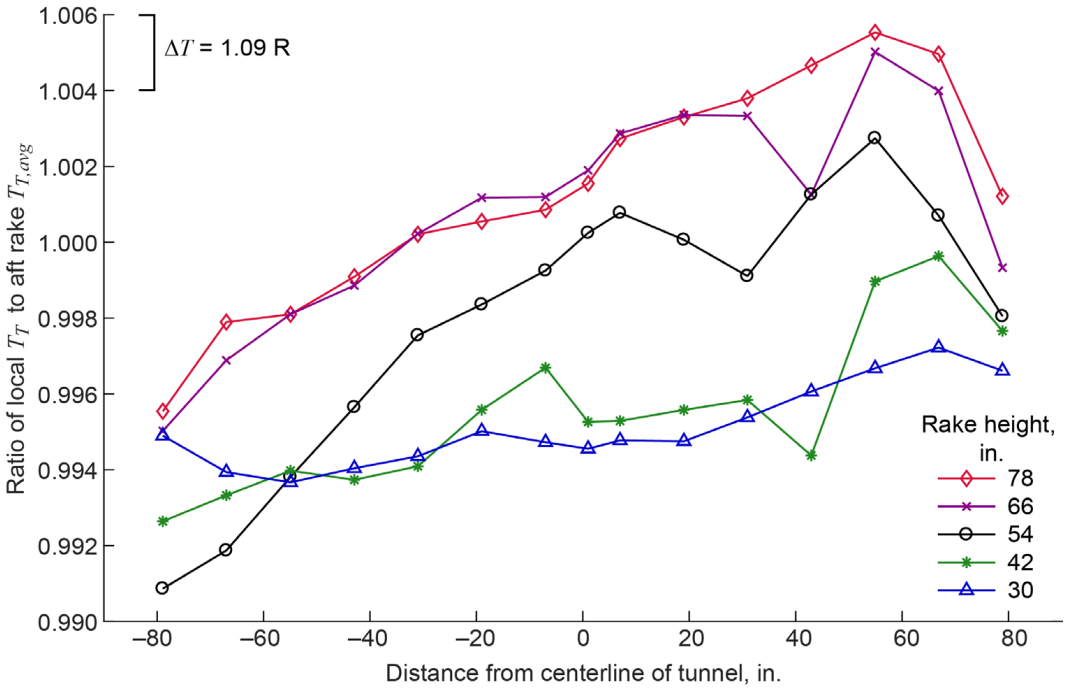

Figure 17.—Test section total temperature (T_T) distribution at test section station 198 during 2015/2016 flow quality survey in 9- by 15-Foot Low-Speed Wind Tunnel (upstream looking aft) at Mach 0.22 (three-motor operating mode).

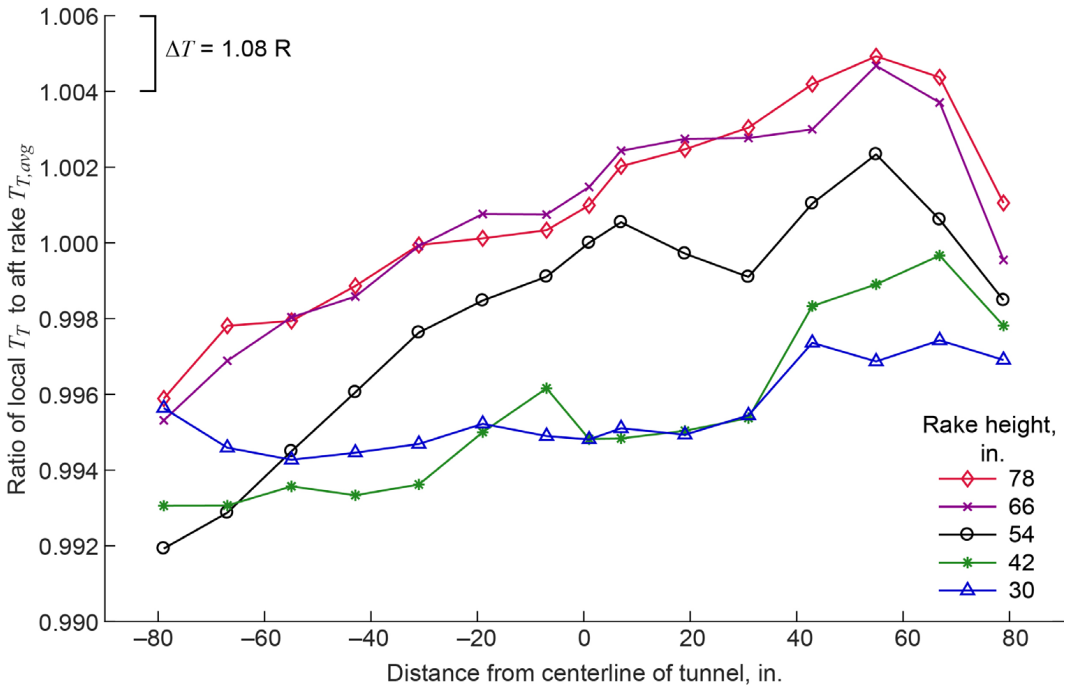

Figure 18.—Test section total temperature (T_T) distribution at test section station 198 during 2015/2016 flow quality survey in 9- by 15-Foot Low-Speed Wind Tunnel (upstream looking aft) at Mach 0.20 (three-motor operating mode).

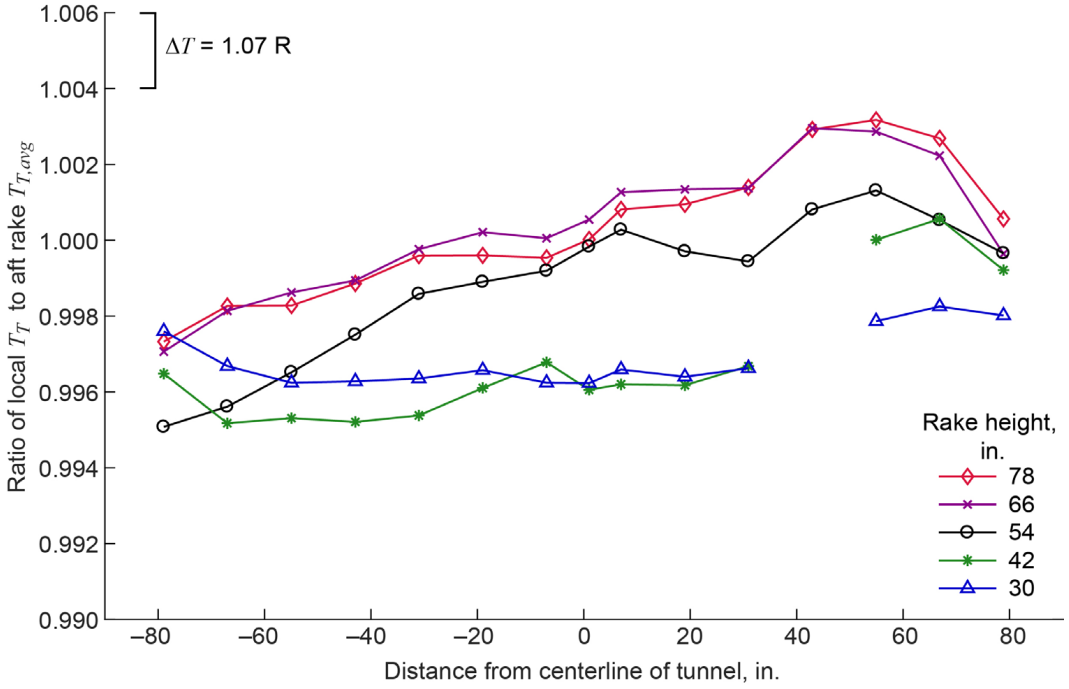

Figure 19.—Test section total temperature (T_T) distribution at test section station 198 during 2015/2016 flow quality survey in 9- by 15-Foot Low-Speed Wind Tunnel (upstream looking aft) at Mach 0.15 (three-motor operating mode).

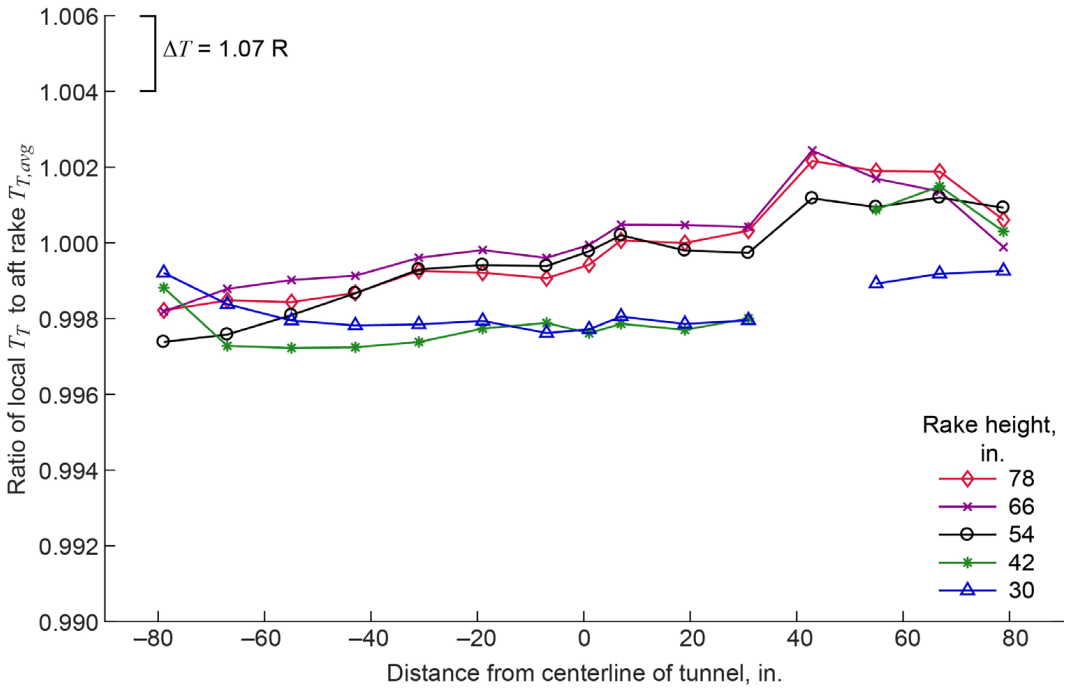

Figure 20.—Test section total temperature (T_T) distribution at test section station 198 during 2015/2016 flow quality survey in 9- by 15-Foot Low-Speed Wind Tunnel (upstream looking aft) at Mach 0.10 (three-motor operating mode).

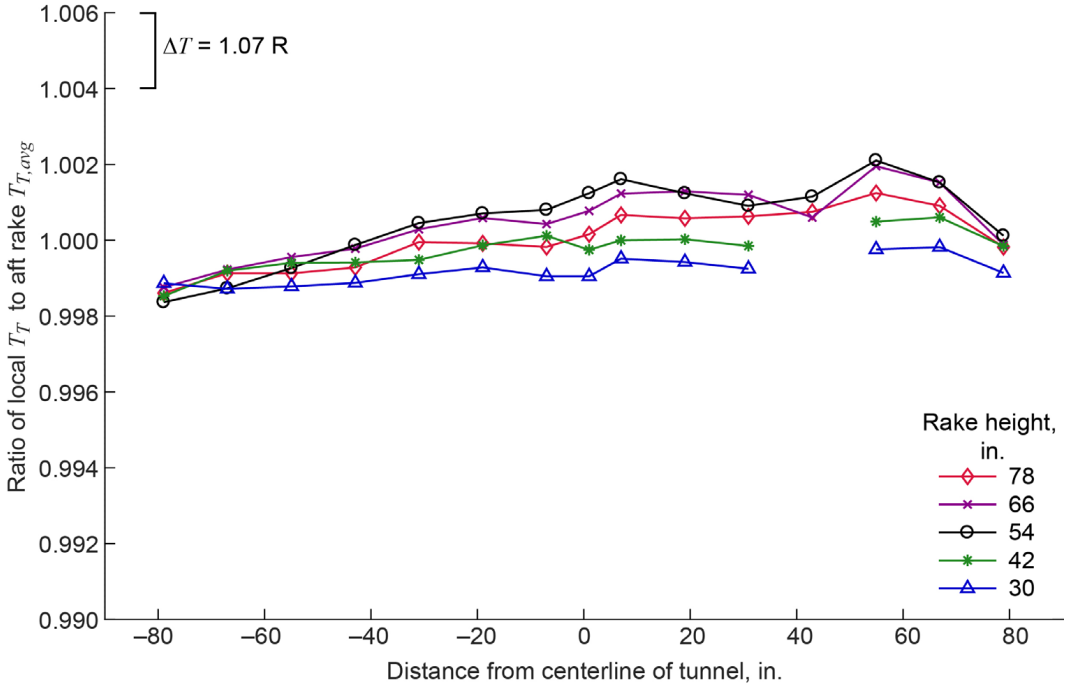

Figure 21.—Test section total temperature (T_T) distribution at test section station 198 during 2015/2016 flow quality survey in 9- by 15-Foot Low-Speed Wind Tunnel (upstream looking aft) at Mach 0.15 (one-motor operating mode).

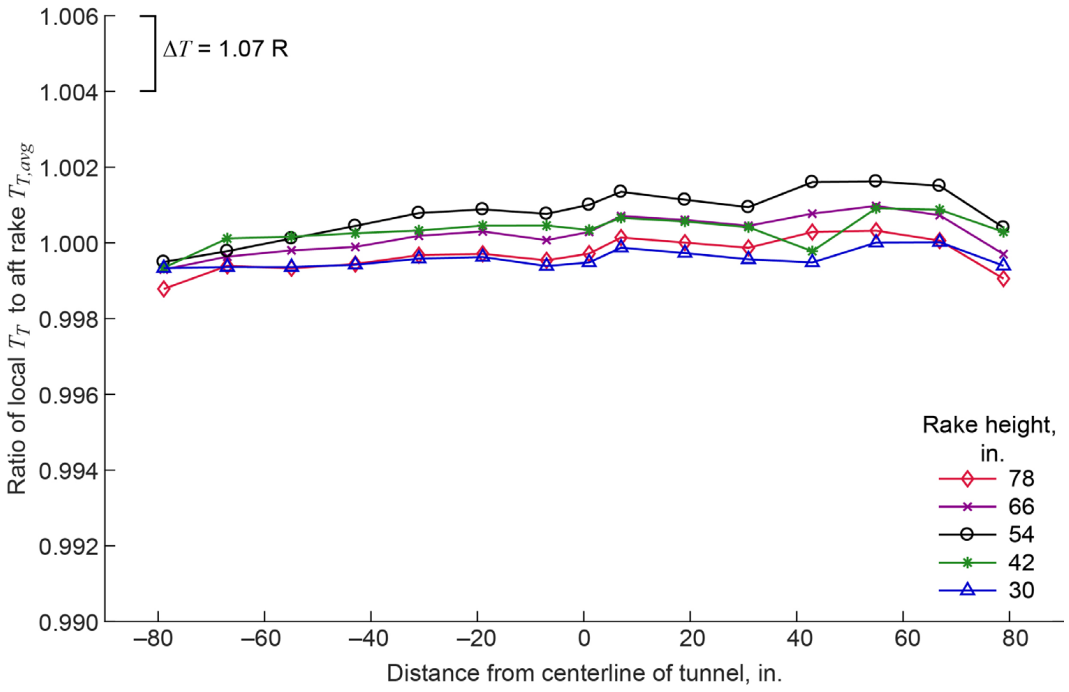

Figure 22.—Test section total temperature (T_T) distribution at test section station 198 during 2015/2016 flow quality survey in 9- by 15-Foot Low-Speed Wind Tunnel (upstream looking aft) at Mach 0.10 (one-motor operating mode).

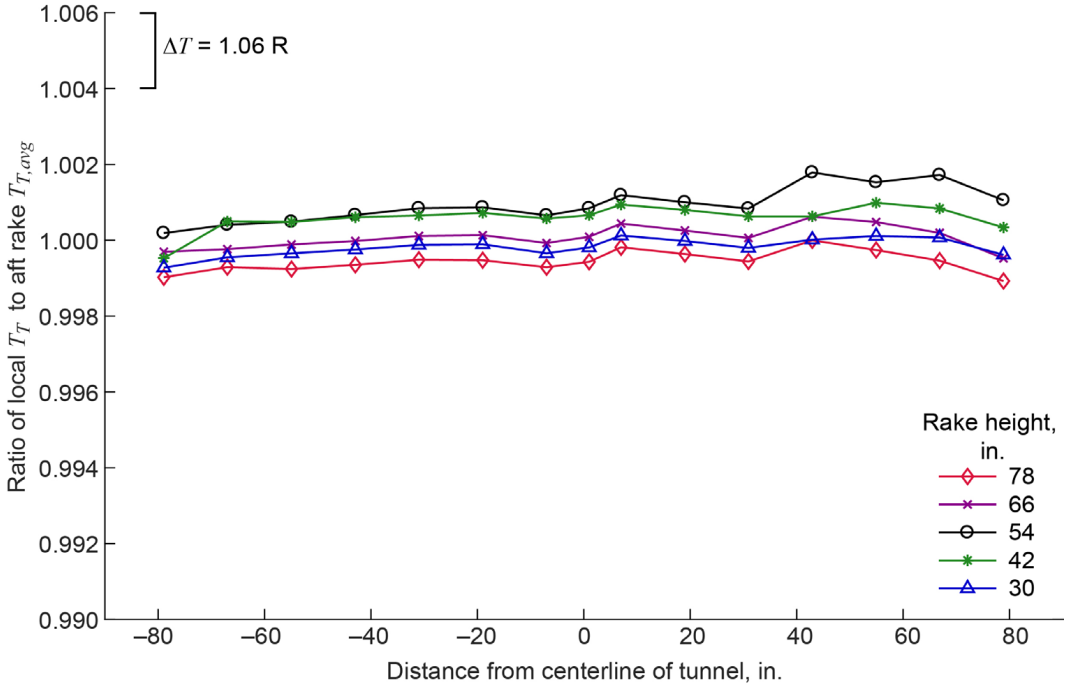

Figure 23.—Test section total temperature (T_T) distribution at test section station 198 during 2015/2016 flow quality survey in 9- by 15-Foot Low-Speed Wind Tunnel (upstream looking aft) at Mach 0.05 (one-motor operating mode).

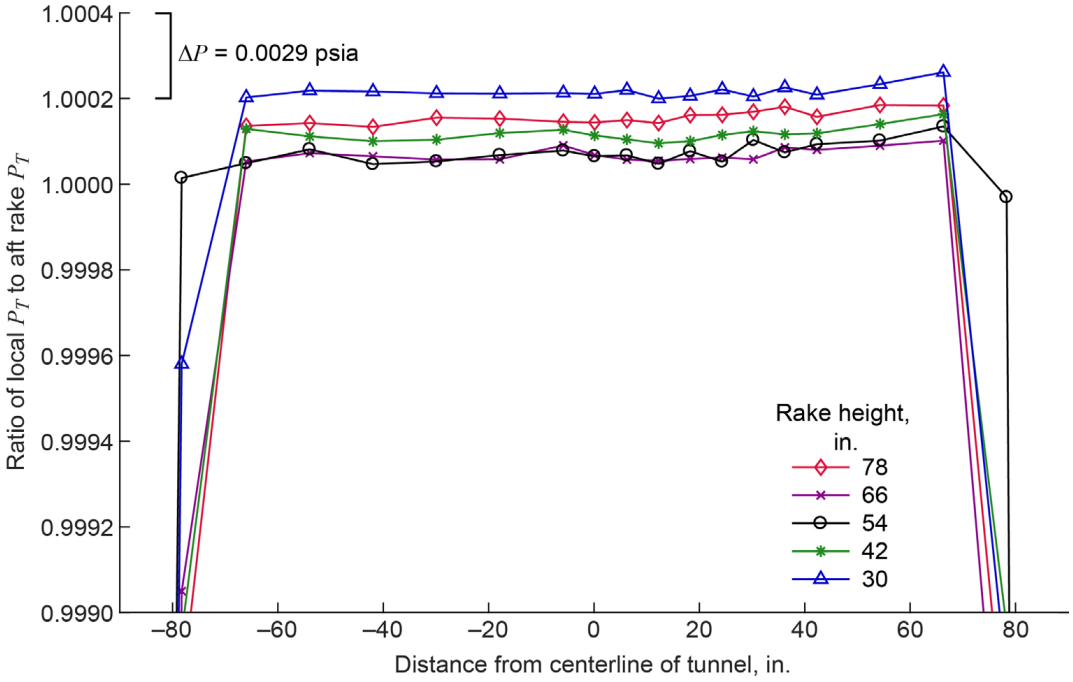

Figure 24.—Test section total pressure (P_T) distribution at test section station 198 during 2015/2016 flow quality survey in 9- by 15-Foot Low-Speed Wind Tunnel (upstream looking aft) at Mach 0.22 (three-motor operating mode).

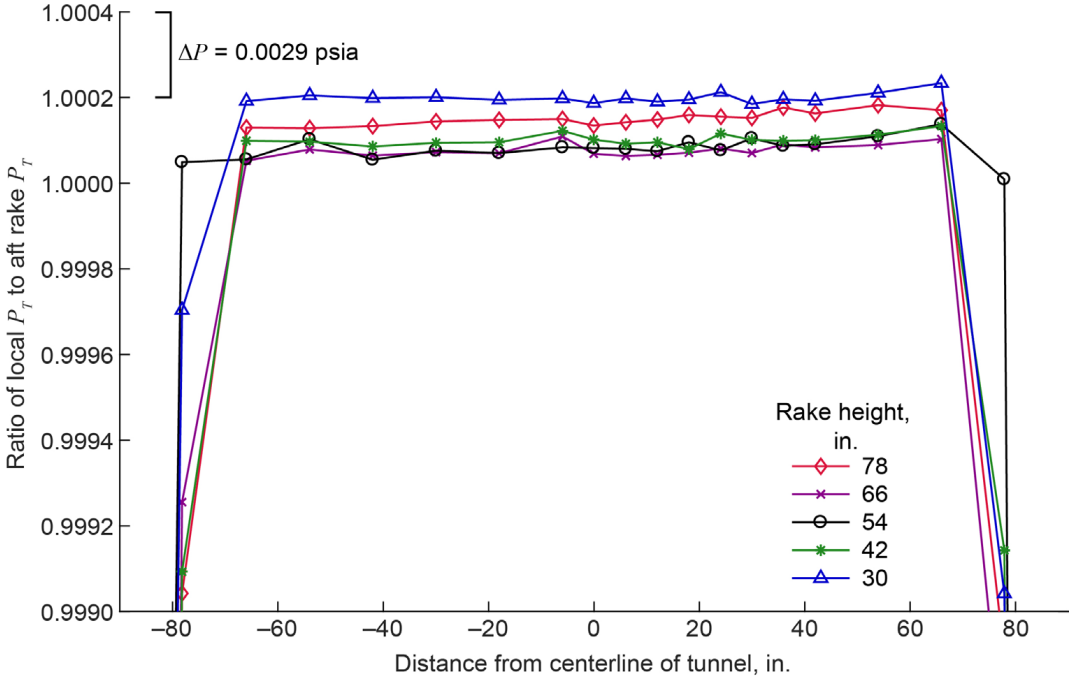

Figure 25.—Test section total pressure (P_T) distribution at test section station 198 during 2015/2016 flow quality survey in 9- by 15-Foot Low-Speed Wind Tunnel (upstream looking aft) at Mach 0.20 (three-motor operating mode).

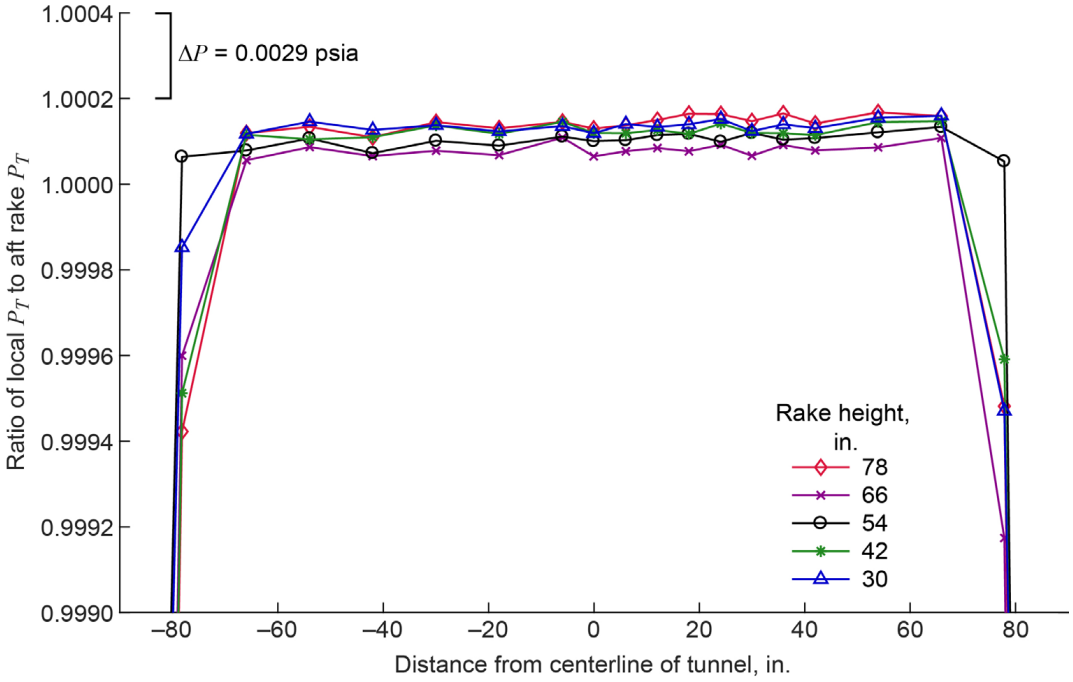

Figure 26.—Test section total pressure (P_T) distribution at test section station 198 during 2015/2016 flow quality survey in 9- by 15-Foot Low-Speed Wind Tunnel (upstream looking aft) at Mach 0.15 (three-motor operating mode).

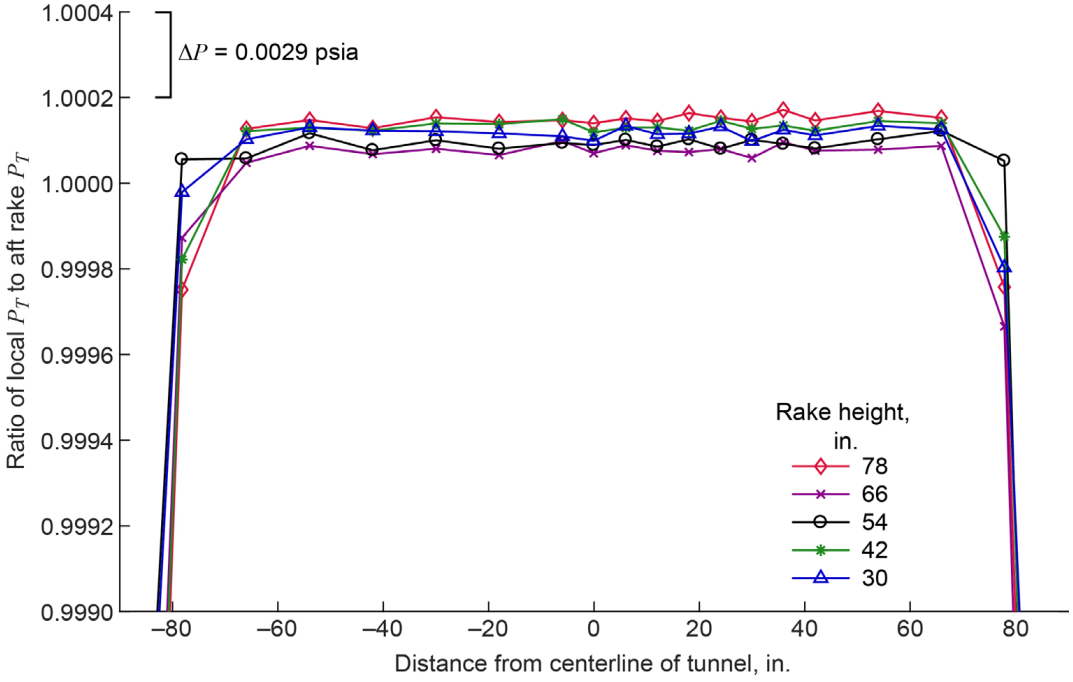

Figure 27.—Test section total pressure (P_T) distribution at test section station 198 during 2015/2016 flow quality survey in 9- by 15-Foot Low-Speed Wind Tunnel (upstream looking aft) at Mach 0.10 (three-motor operating mode).

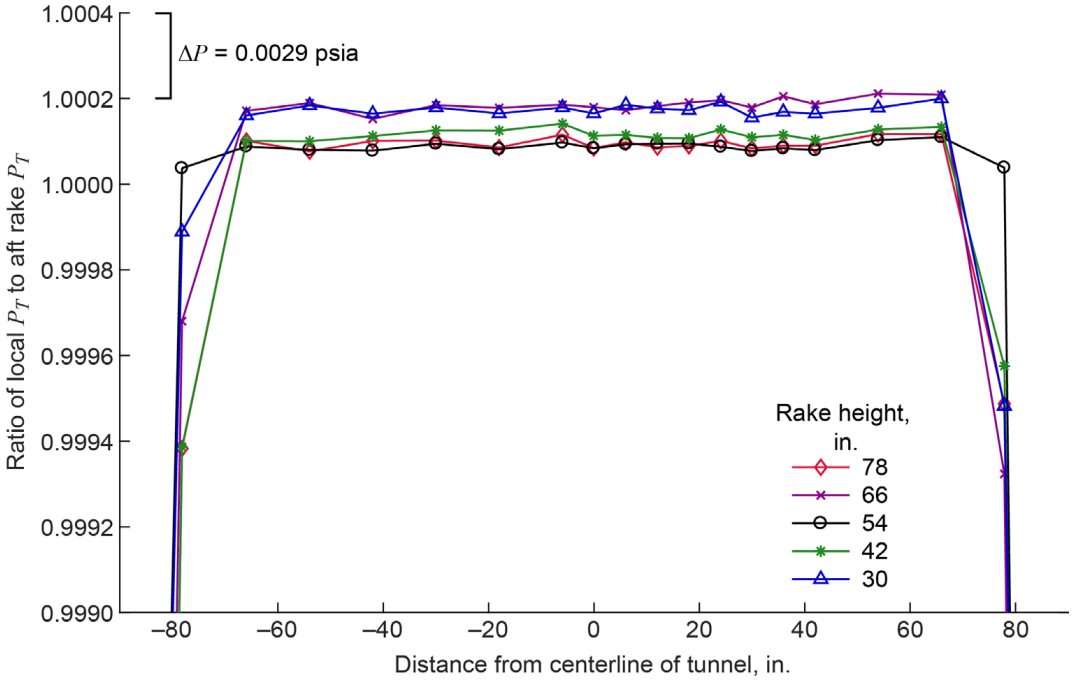

Figure 28.—Test section total pressure (P_T) distribution at test section station 198 during 2015/2016 flow quality survey in 9- by 15-Foot Low-Speed Wind Tunnel (upstream looking aft) at Mach 0.15 (one-motor operating mode).

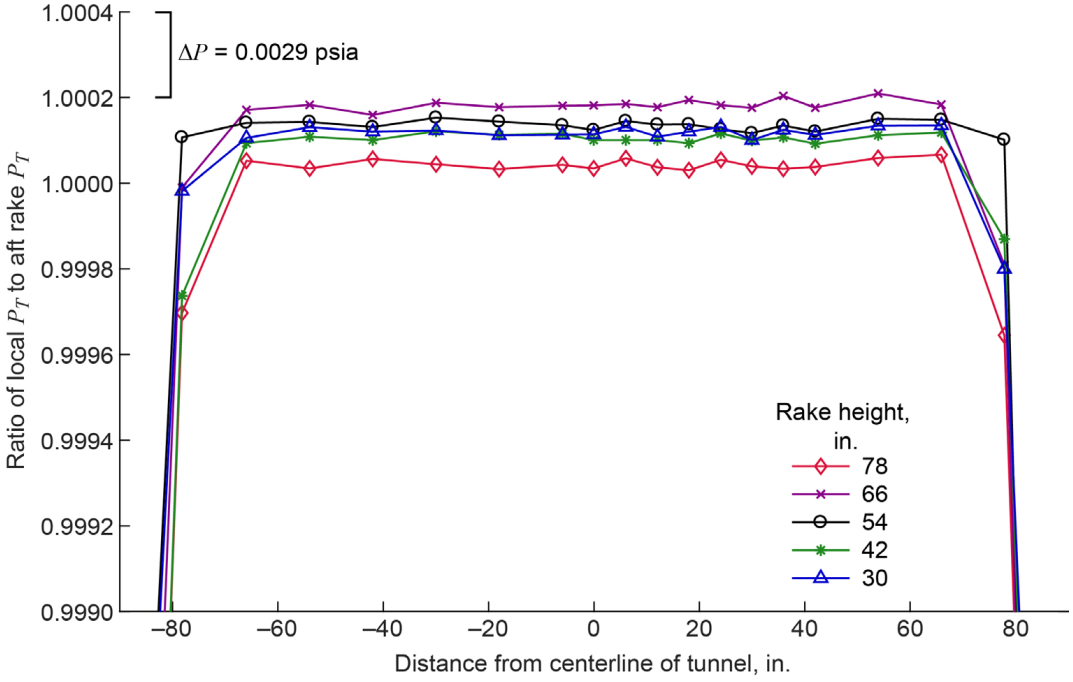

Figure 29.—Test section total pressure (P_T) distribution at test section station 198 during 2015/2016 flow quality survey in 9- by 15-Foot Low-Speed Wind Tunnel (upstream looking aft) at Mach 0.10 (one-motor operating mode).

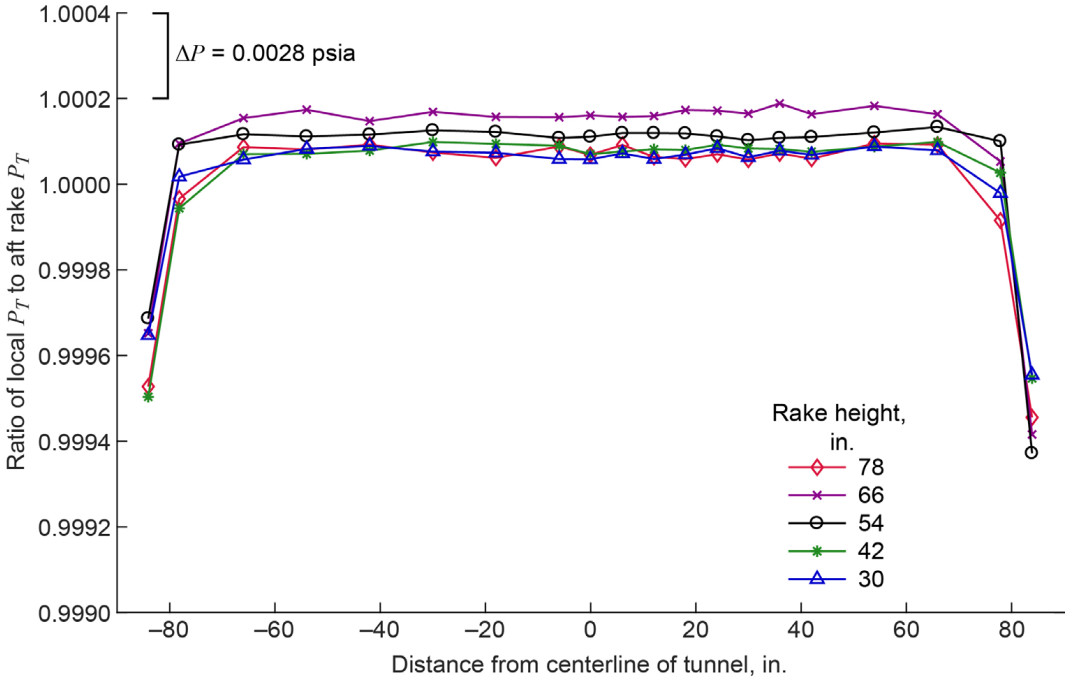

Figure 30.—Test section total pressure (P_T) distribution at test section station 198 during 2015/2016 flow quality survey in 9- by 15-Foot Low-Speed Wind Tunnel (upstream looking aft) at Mach 0.05 (one-motor operating mode).

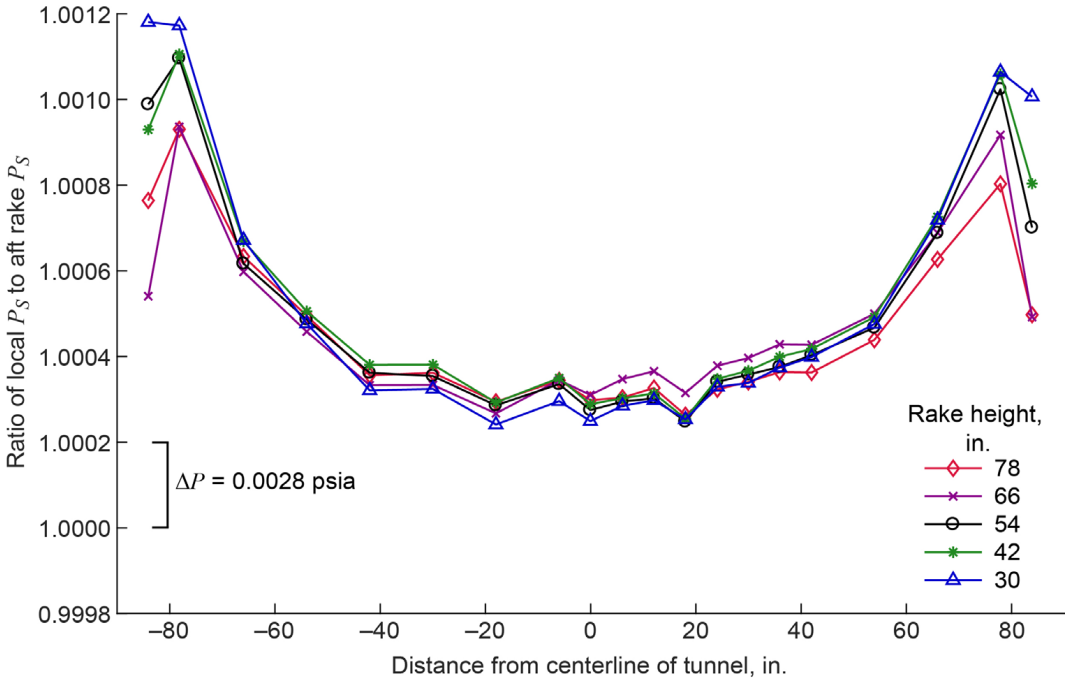

Figure 31.—Test section static pressure (P_S) distribution at test section station 198 during 2015/2016 flow quality survey in 9- by 15-Foot Low-Speed Wind Tunnel (upstream looking aft) at Mach 0.22 (three-motor operating mode).

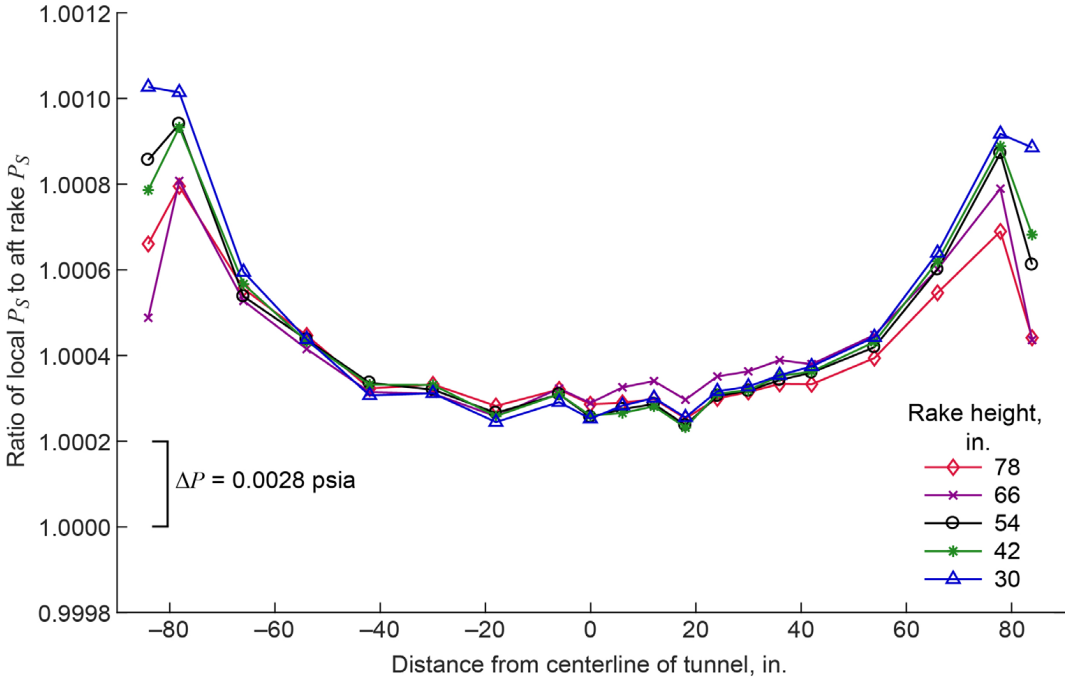

Figure 32.—Test section static pressure (P_S) distribution at test section station 198 during 2015/2016 flow quality survey in 9- by 15-Foot Low-Speed Wind Tunnel (upstream looking aft) at Mach 0.20 (three-motor operating mode).

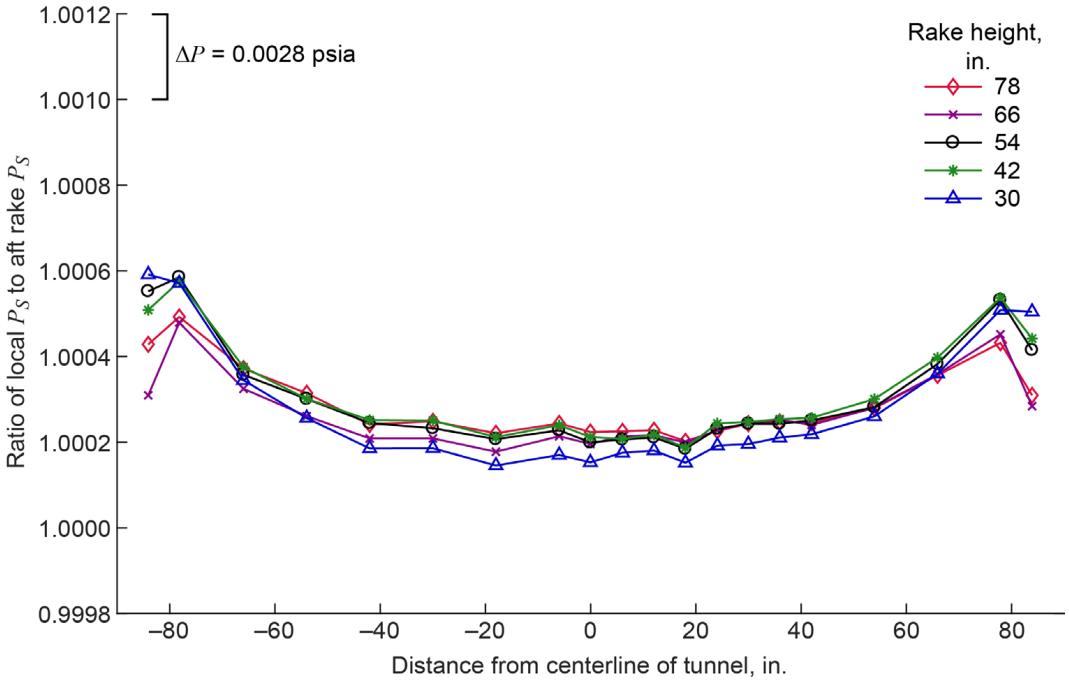

Figure 33.—Test section static pressure (P_S) distribution at test section station 198 during 2015/2016 flow quality survey in 9- by 15-Foot Low-Speed Wind Tunnel (upstream looking aft) at Mach 0.15 (three-motor operating mode).

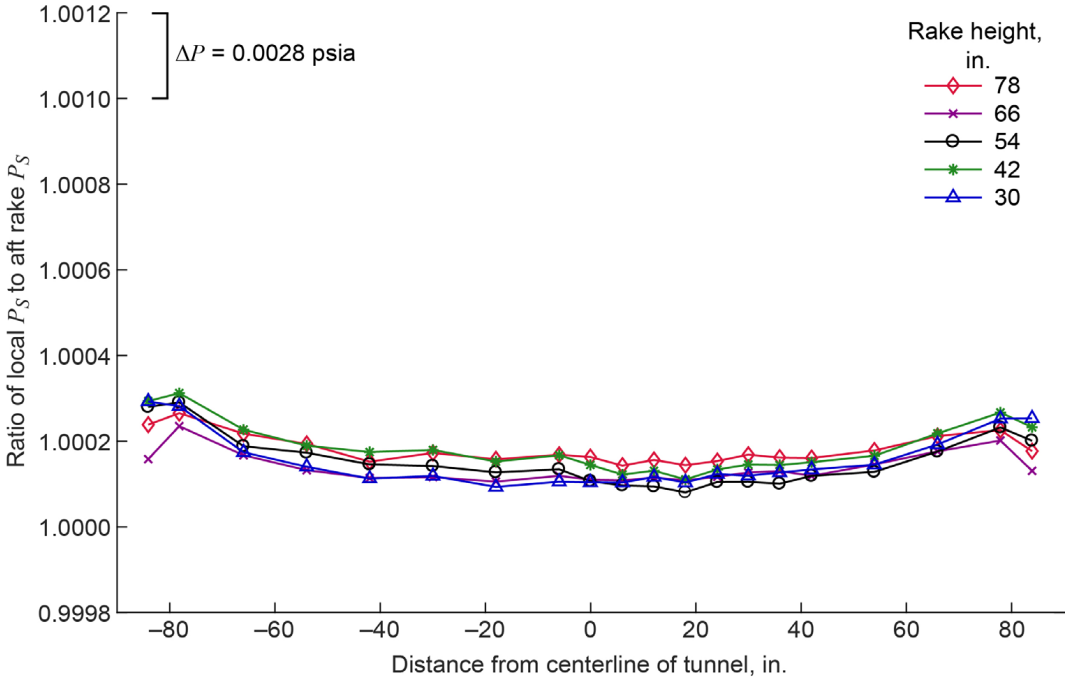

Figure 34.—Test section static pressure (P_S) distribution at test section station 198 during 2015/2016 flow quality survey in 9- by 15-Foot Low-Speed Wind Tunnel (upstream looking aft) at Mach 0.10 (three-motor operating mode).

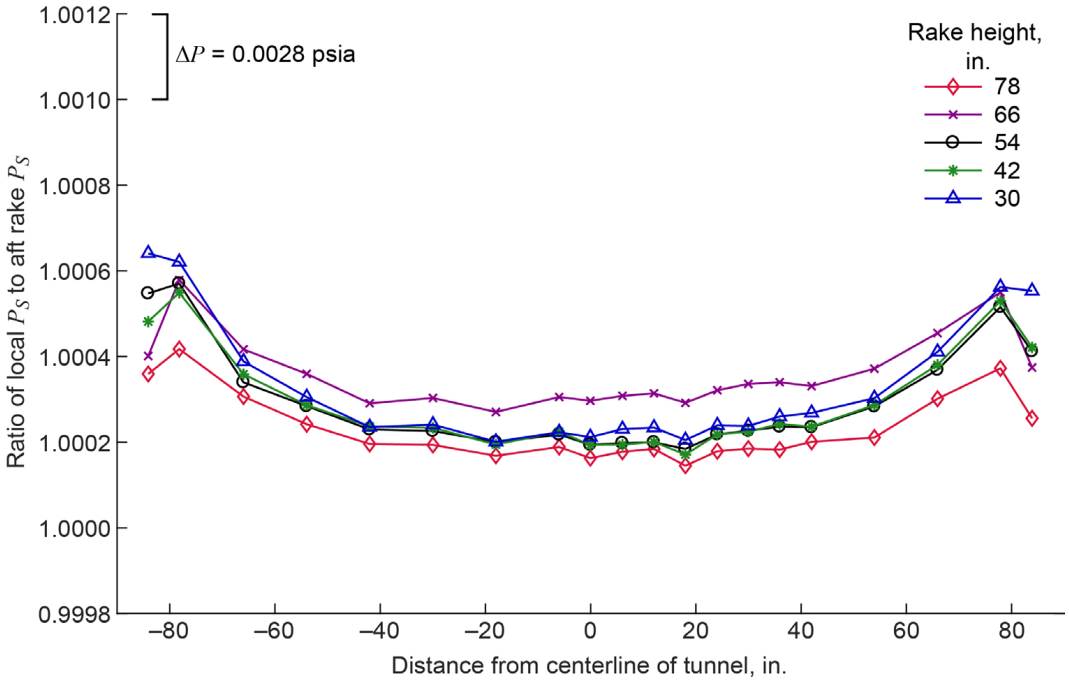

Figure 35.—Test section static pressure (P_S) distribution at test section station 198 during 2015/2016 flow quality survey in 9- by 15-Foot Low-Speed Wind Tunnel (upstream looking aft) at Mach 0.15 (one-motor operating mode).

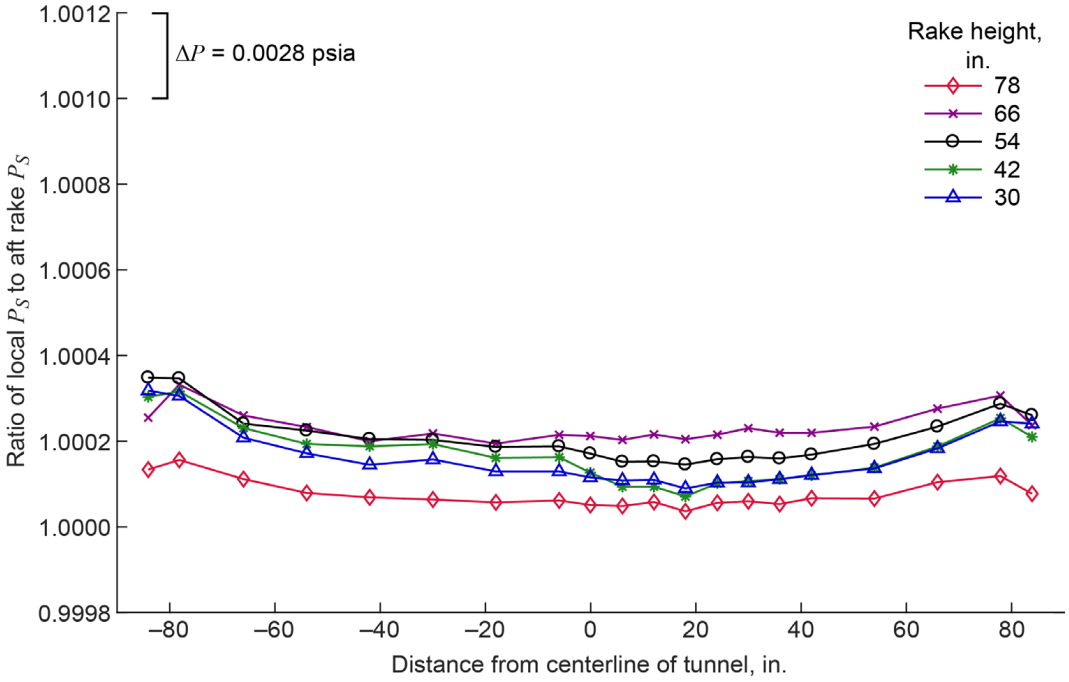

Figure 36.—Test section static pressure (P_S) distribution at test section station 198 during 2015/2016 flow quality survey in 9- by 15-Foot Low-Speed Wind Tunnel (upstream looking aft) at Mach 0.10 (one-motor operating mode).

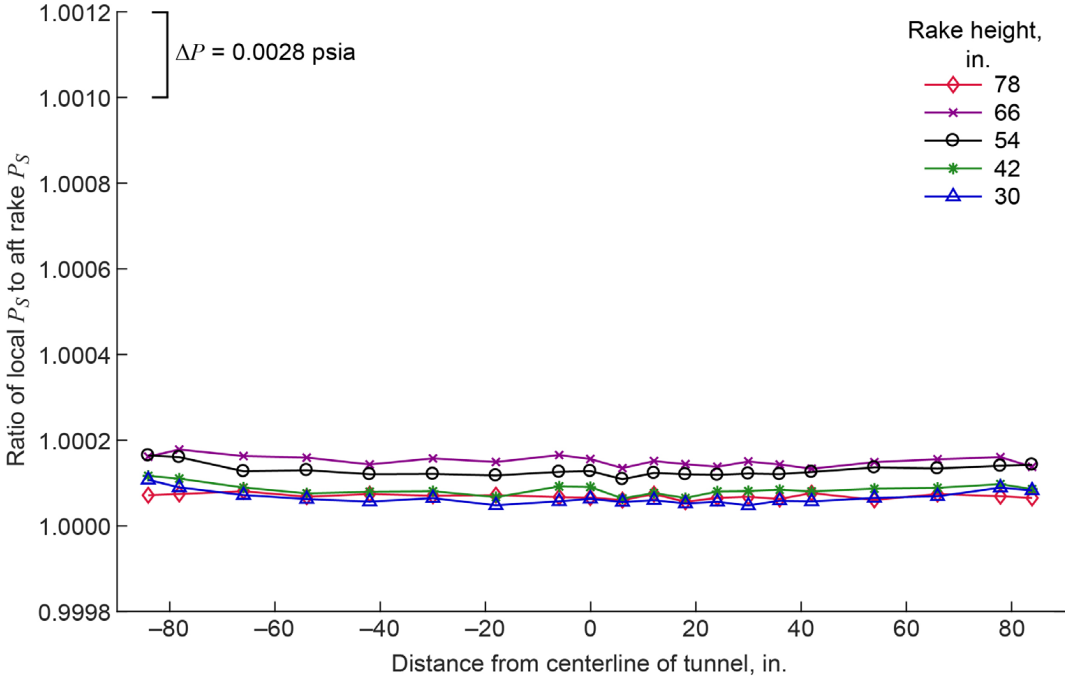

Figure 37.—Test section static pressure (P_S) distribution at test section station 198 during 2015/2016 flow quality survey in 9- by 15-Foot Low-Speed Wind Tunnel (upstream looking aft) at Mach 0.05 (one-motor operating mode).

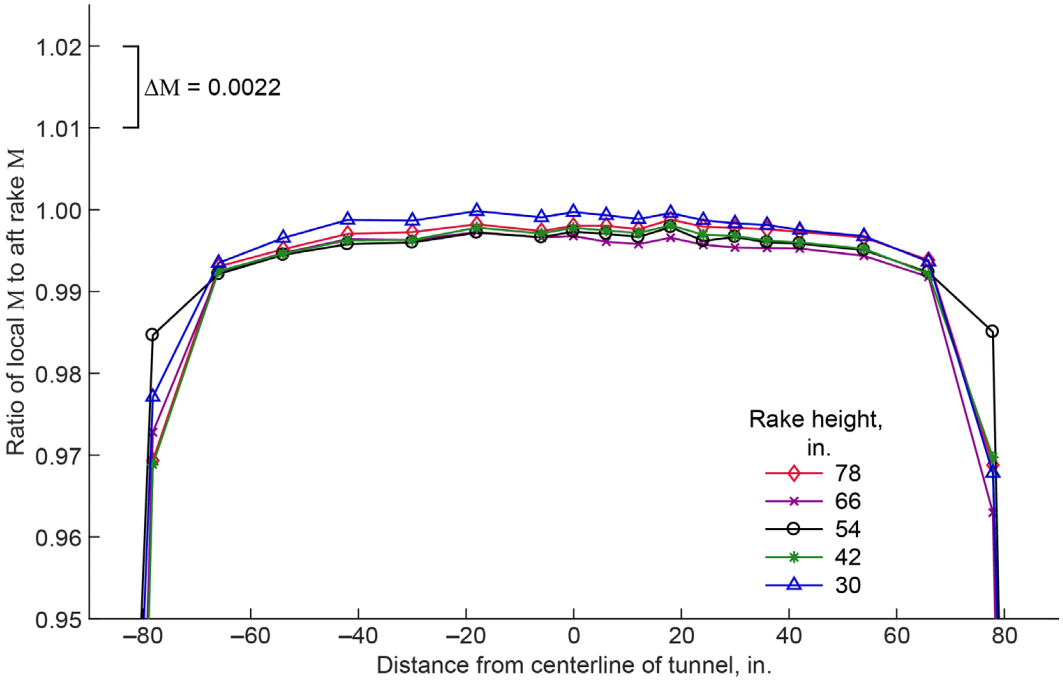

Figure 38.—Test section Mach number (M) distribution at test section station 198 during 2015/2016 flow quality survey in 9- by 15-Foot Low-Speed Wind Tunnel (upstream looking aft) at Mach 0.22 (three-motor operating mode).

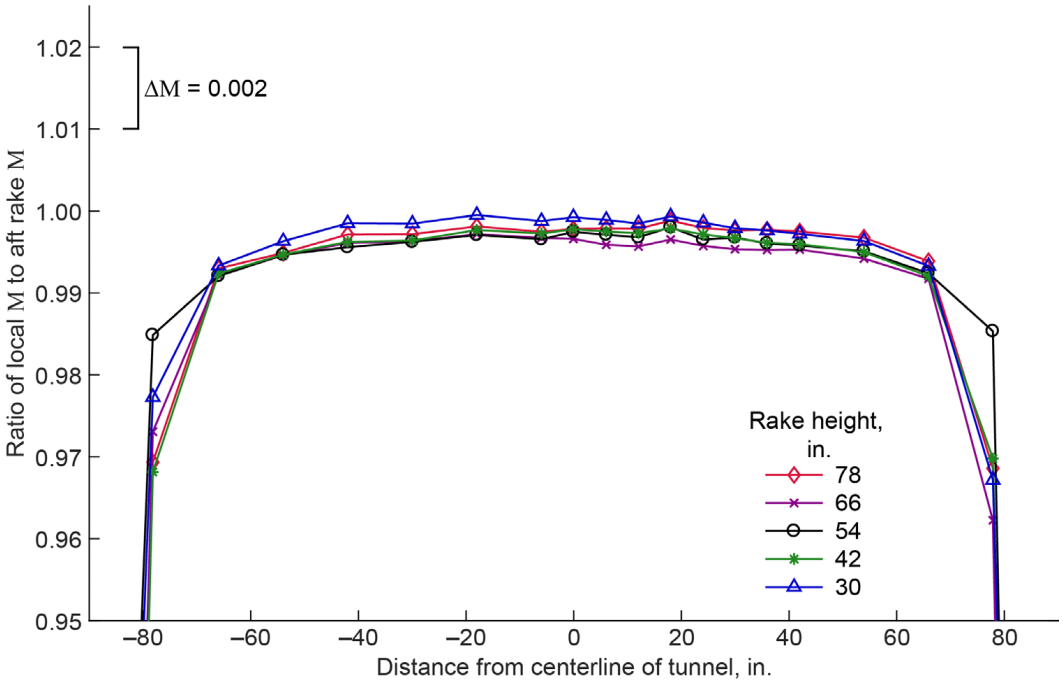

Figure 39.—Test section Mach number (M) distribution at test section station 198 during 2015/2016 flow quality survey in 9- by 15-Foot Low-Speed Wind Tunnel (upstream looking aft) at Mach 0.20 (three-motor operating mode).

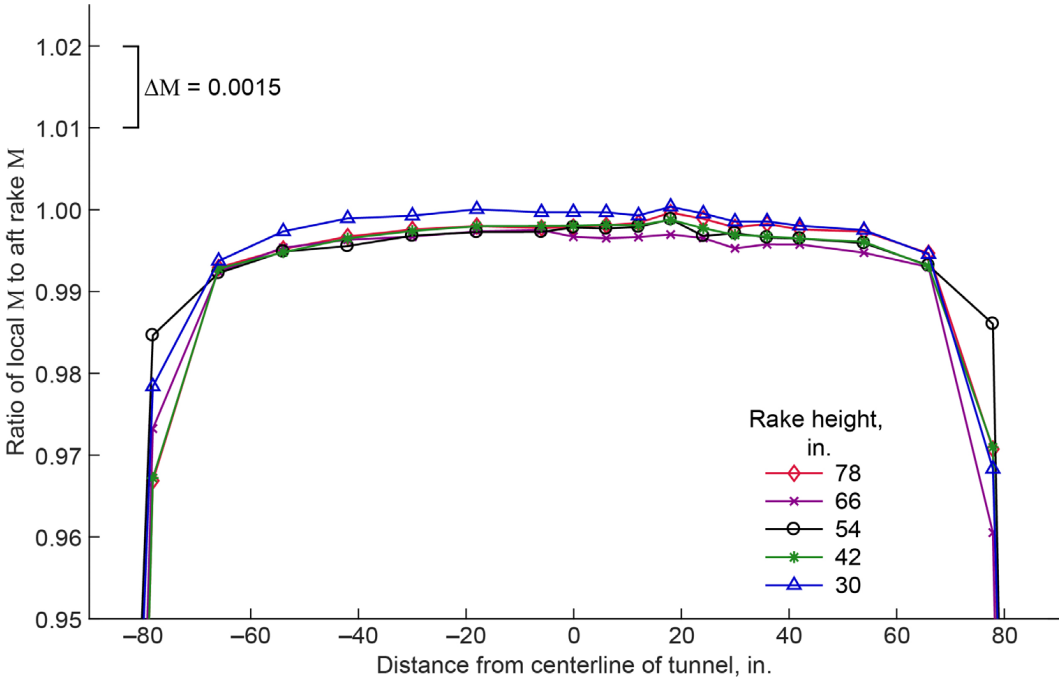

Figure 40.—Test section Mach number (M) distribution at test section station 198 during 2015/2016 flow quality survey in 9- by 15-Foot Low-Speed Wind Tunnel (upstream looking aft) at Mach 0.15 (three-motor operating mode).

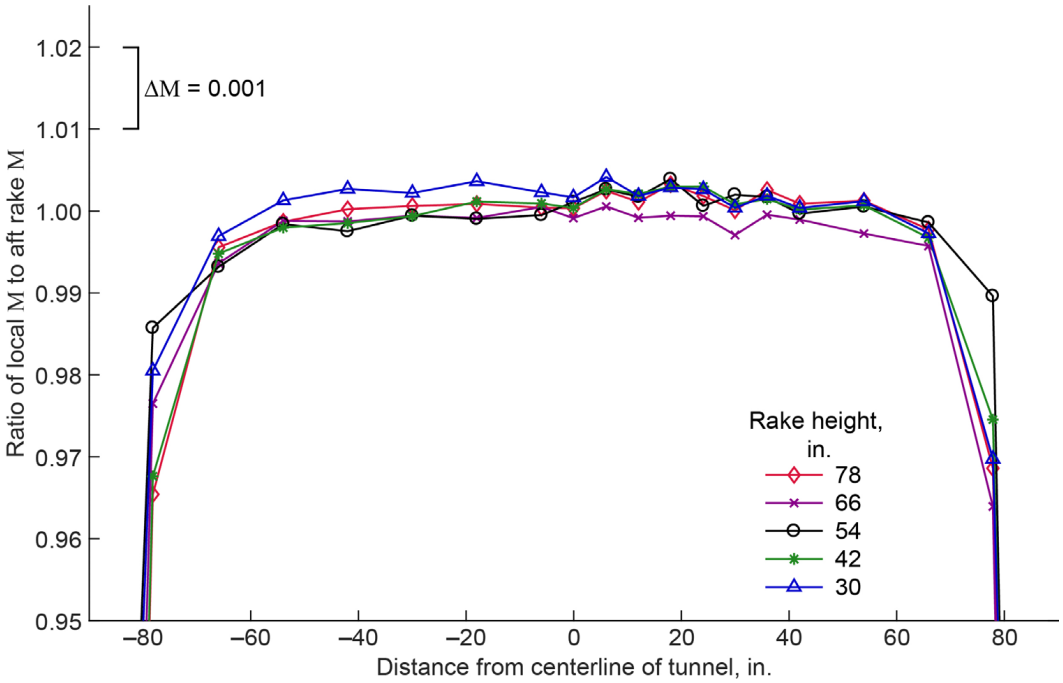

Figure 41.—Test section Mach number (M) distribution at test section station 198 during 2015/2016 flow quality survey in 9- by 15-Foot Low-Speed Wind Tunnel (upstream looking aft) at Mach 0.10 (three-motor operating mode).

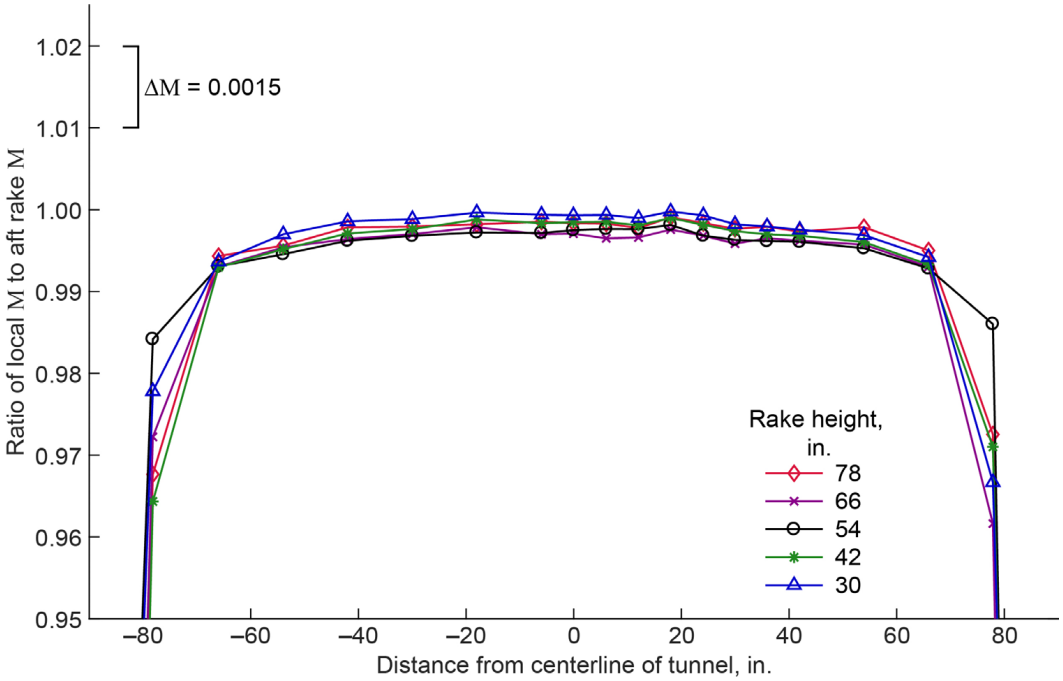

Figure 42.—Test section Mach number (M) distribution at test section station 198 during 2015/2016 flow quality survey in 9- by 15-Foot Low-Speed Wind Tunnel (upstream looking aft) at Mach 0.15 (one-motor operating mode).

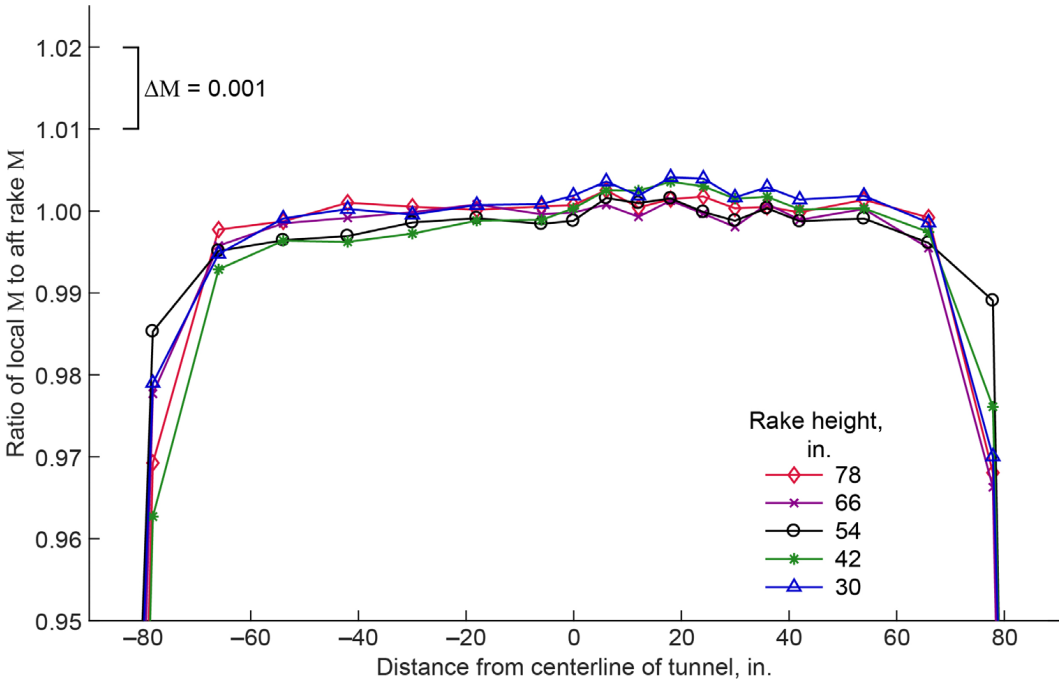

Figure 43.—Test section Mach number (M) distribution at test section station 198 during 2015/2016 flow quality survey in 9- by 15-Foot Low-Speed Wind Tunnel (upstream looking aft) at Mach 0.10 (one-motor operating mode).

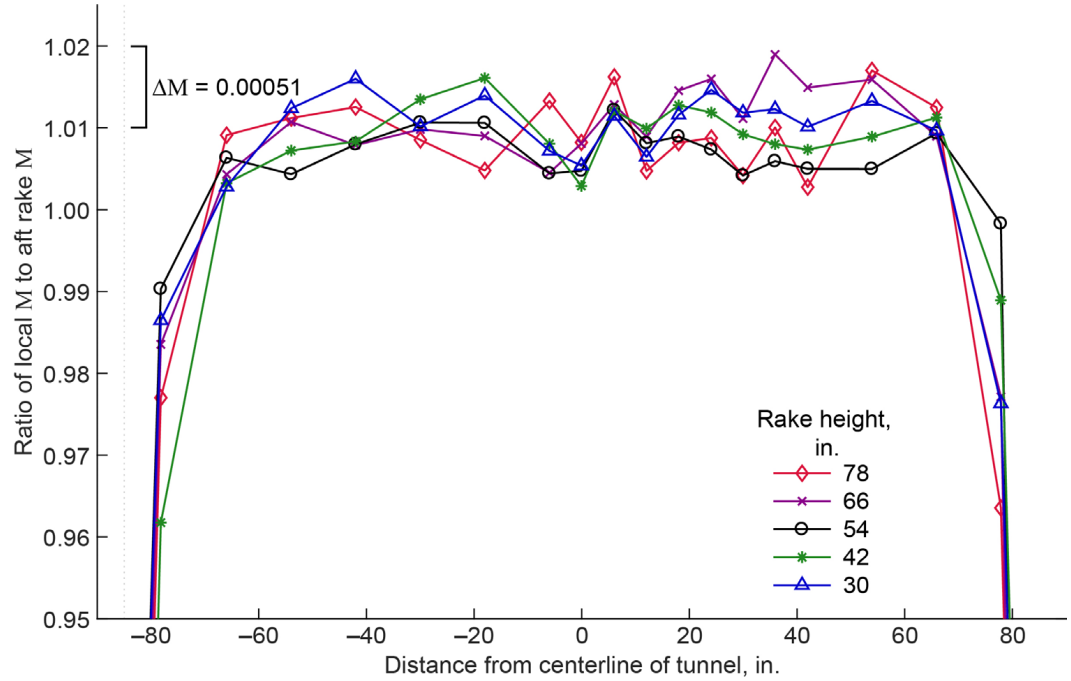

Figure 44.—Test section Mach number (M) distribution at test section station 198 during 2015/2016 flow quality survey in 9- by 15-Foot Low-Speed Wind Tunnel (upstream looking aft) at Mach 0.05 (one-motor operating mode).

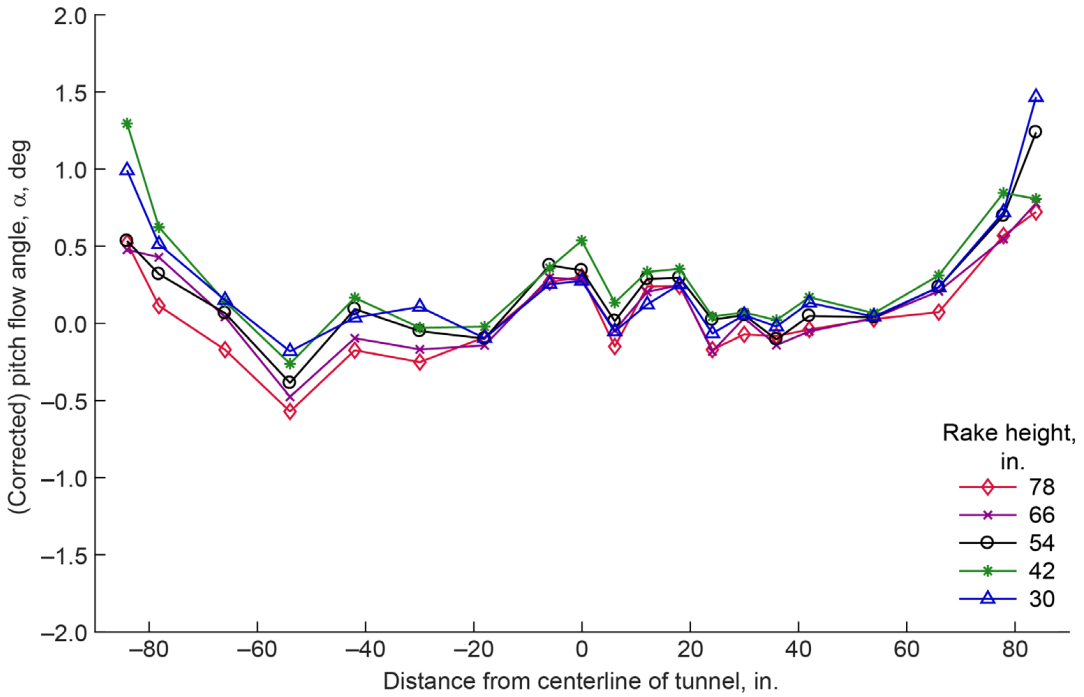

Figure 45.—Test section pitch flow-angle (α) distribution at test section station 198 during 2015/2016 flow quality survey in 9- by 15-Foot Low-Speed Wind Tunnel (upstream looking aft) at Mach 0.22 (three-motor operating mode).

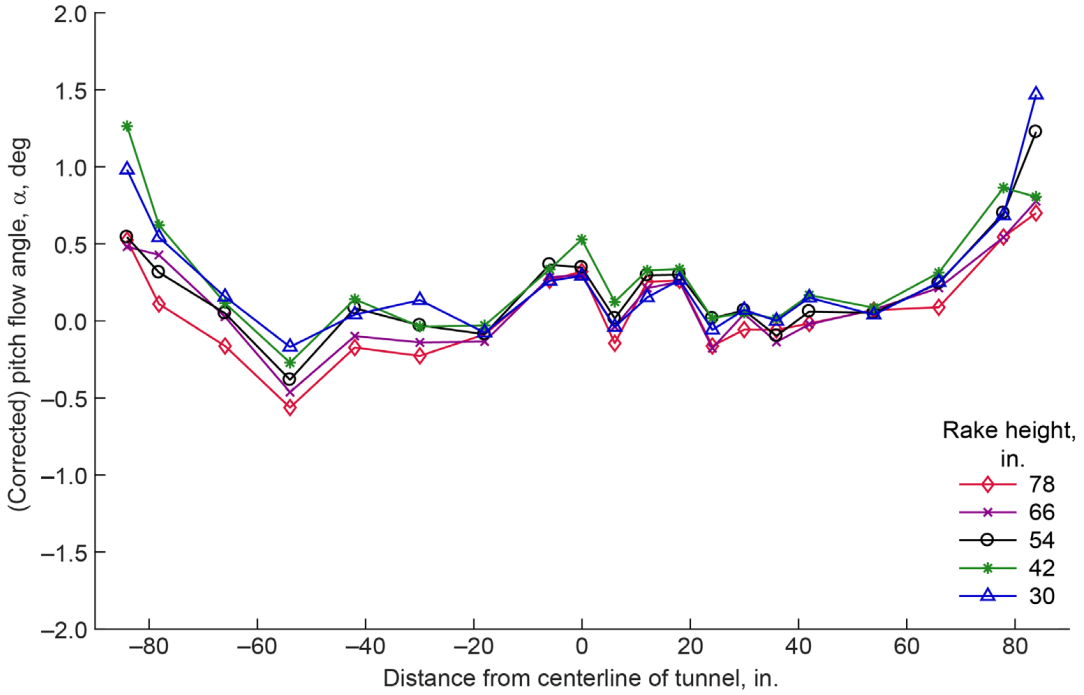

Figure 46.—Test section pitch flow-angle (α) distribution at test section station 198 during 2015/2016 flow quality survey in 9- by 15-Foot Low-Speed Wind Tunnel (upstream looking aft) at Mach 0.20 (three-motor operating mode).

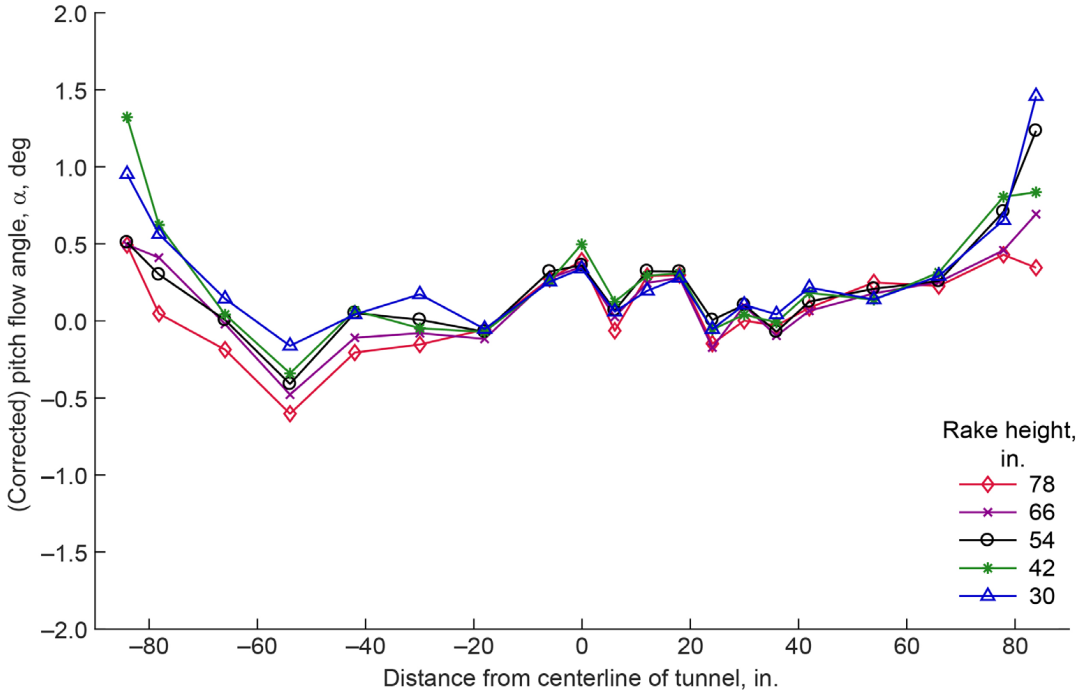

Figure 47.—Test section pitch flow-angle (α) distribution at test section station 198 during 2015/2016 flow quality survey in 9- by 15-Foot Low-Speed Wind Tunnel (upstream looking aft) at Mach 0.15 (three-motor operating mode).

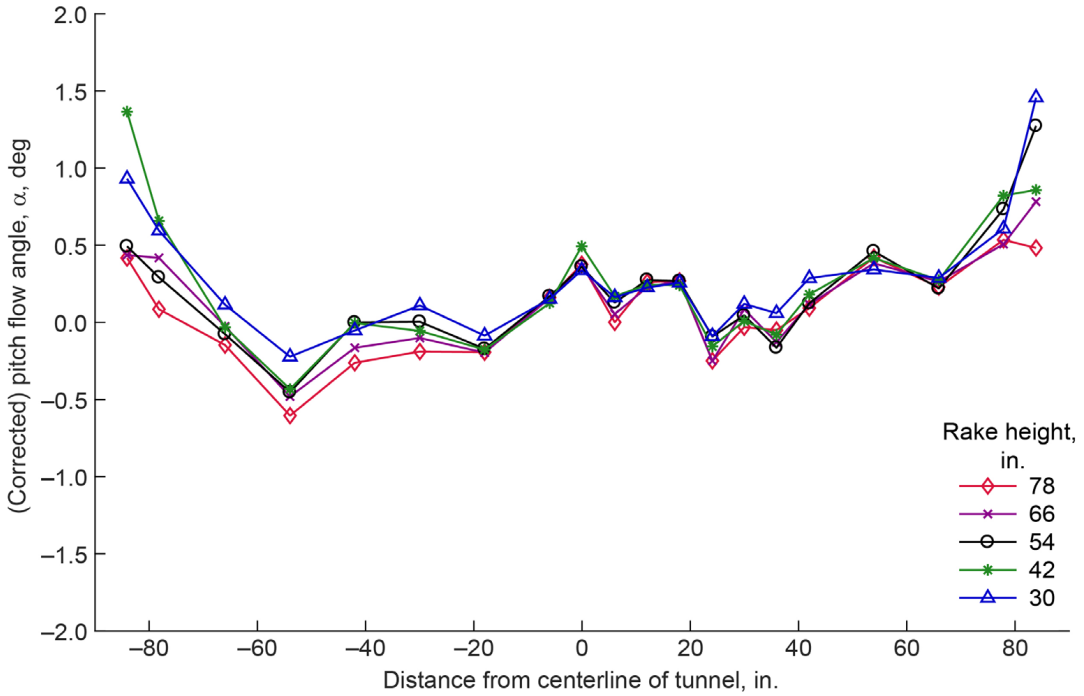

Figure 48.—Test section pitch flow-angle (α) distribution at test section station 198 during 2015/2016 flow quality survey in 9- by 15-Foot Low-Speed Wind Tunnel (upstream looking aft) at Mach 0.10 (three-motor operating mode).

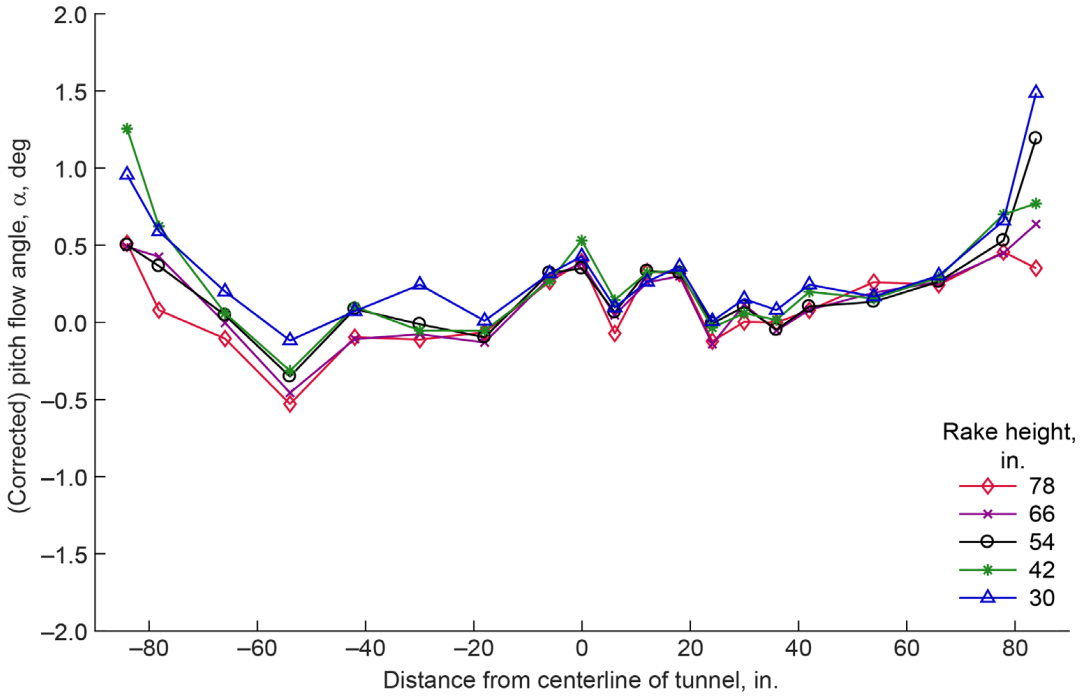

Figure 49.—Test section pitch flow-angle (α) distribution at test section station 198 during 2015/2016 flow quality survey in 9- by 15-Foot Low-Speed Wind Tunnel (upstream looking aft) at Mach 0.15 (one-motor operating mode).

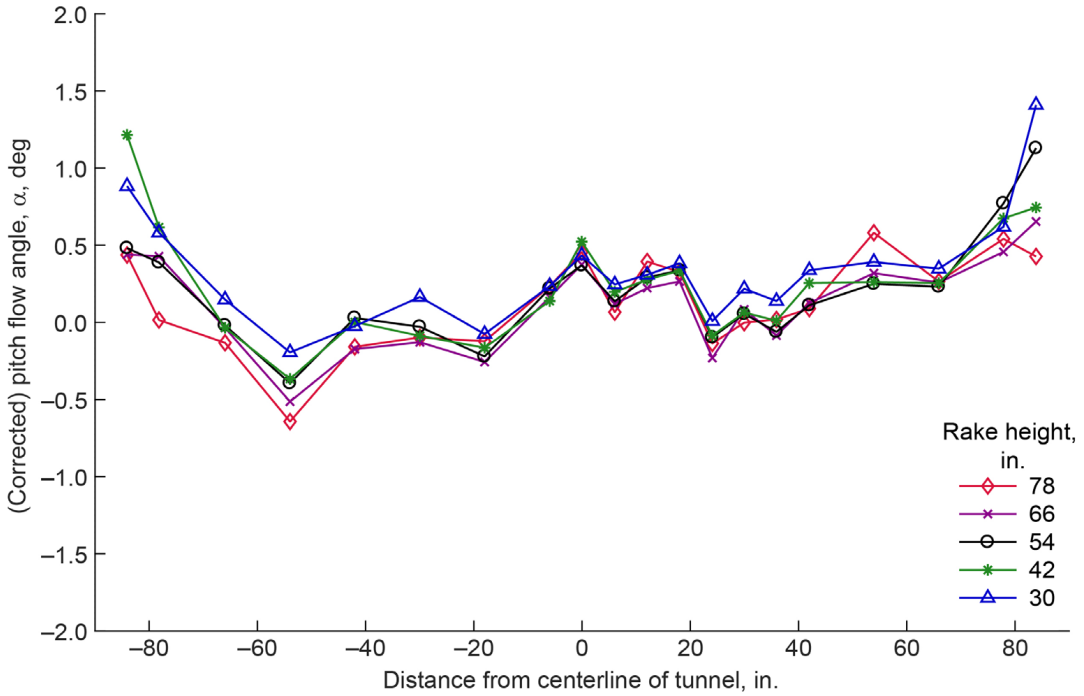

Figure 50.—Test section pitch flow-angle (α) distribution at test section station 198 during 2015/2016 flow quality survey in 9- by 15-Foot Low-Speed Wind Tunnel (upstream looking aft) at Mach 0.10 (one-motor operating mode).

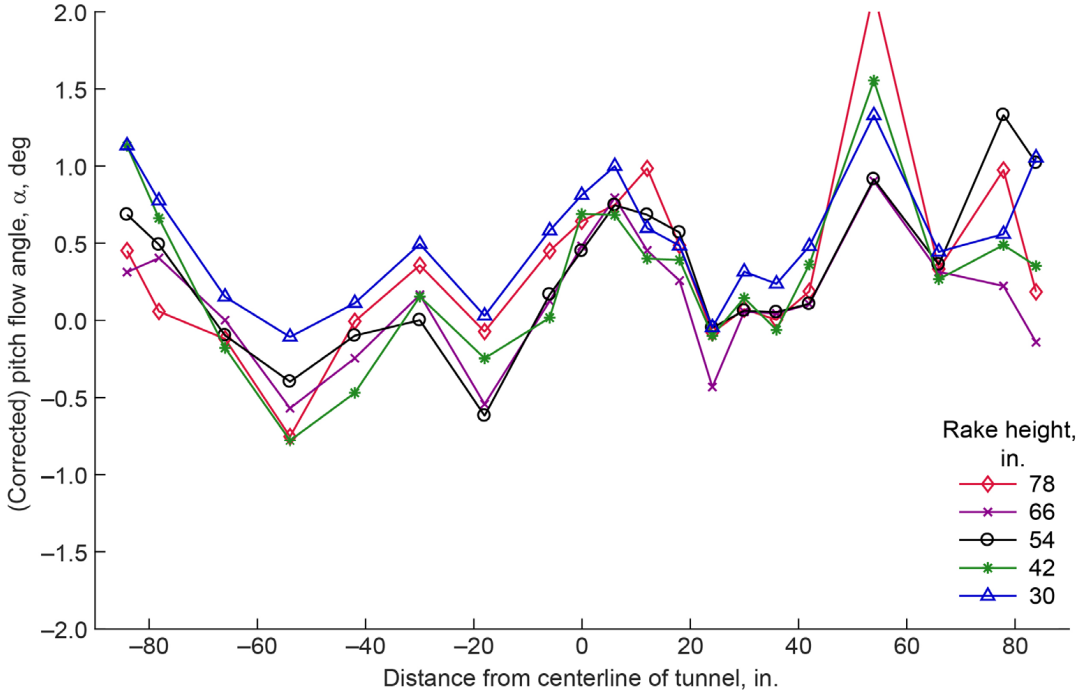

Figure 51.—Test section pitch flow-angle (α) distribution at test section station 198 during 2015/2016 flow quality survey in 9- by 15-Foot Low-Speed Wind Tunnel (upstream looking aft) at Mach 0.05 (one-motor operating mode).

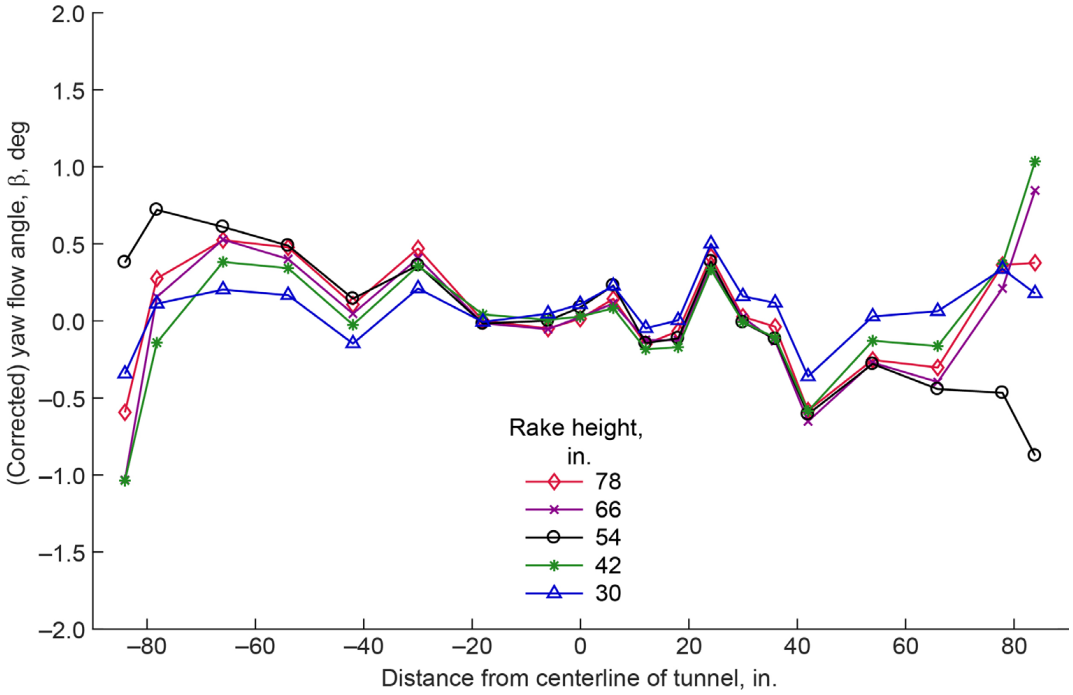

Figure 52.—Test section yaw flow-angle (β) distribution at test section station 198 during 2015/2016 flow quality survey in 9- by 15-Foot Low-Speed Wind Tunnel (upstream looking aft) at Mach 0.22 (three-motor operating mode).

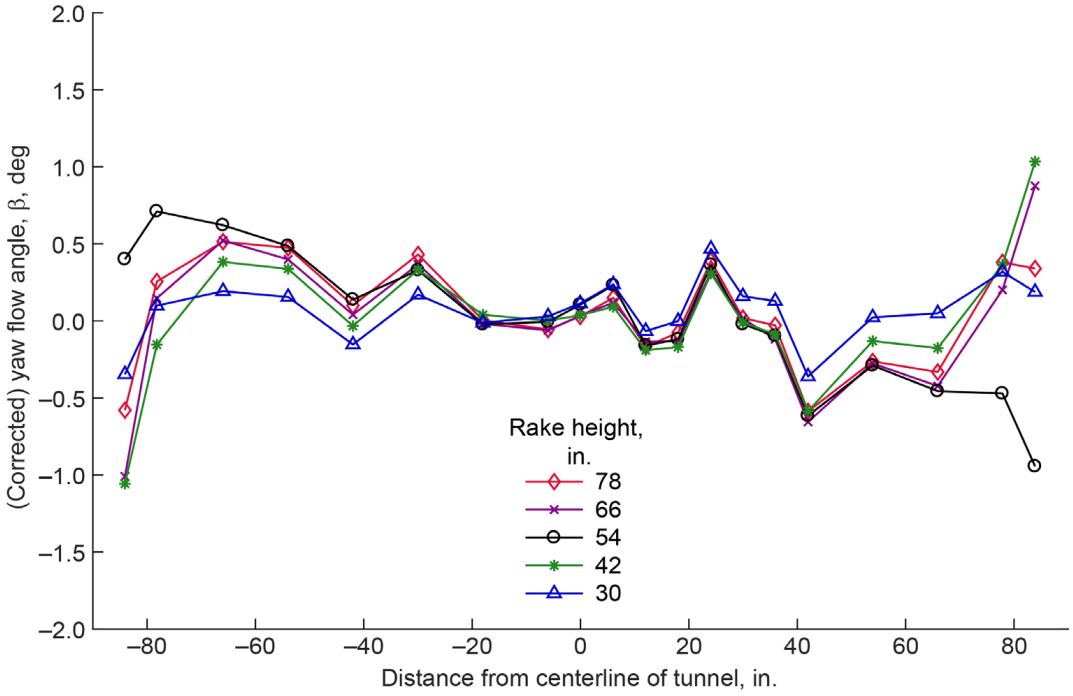

Figure 53.—Test section yaw flow-angle (β) distribution at test section station 198 during 2015/2016 flow quality survey in 9- by 15-Foot Low-Speed Wind Tunnel (upstream looking aft) at Mach 0.20 (three-motor operating mode).

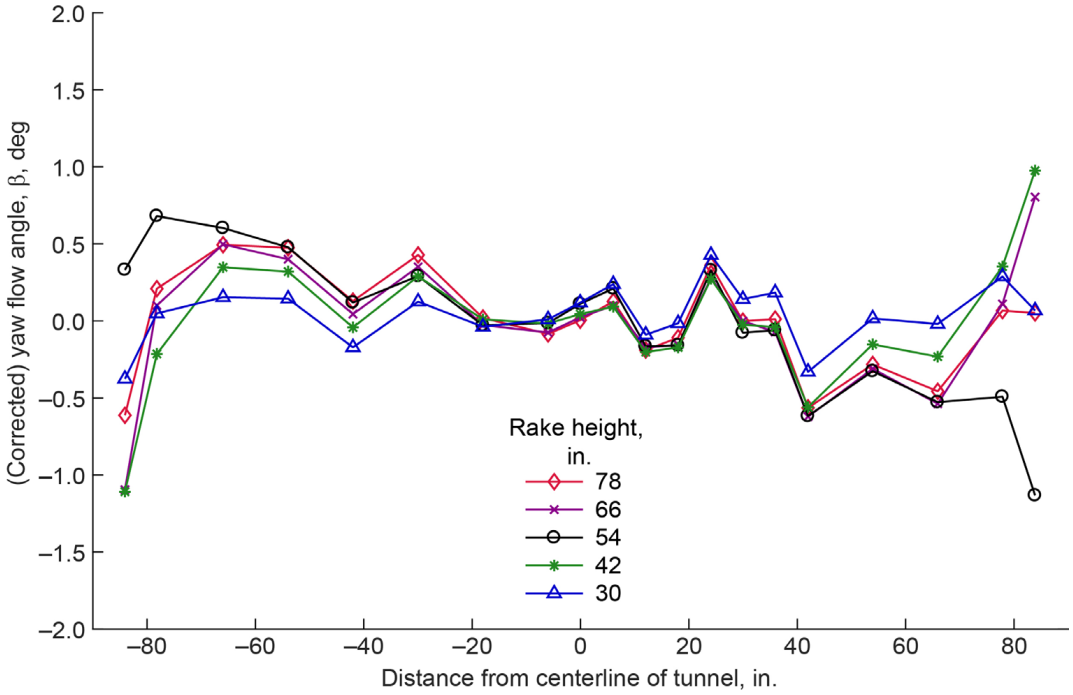

Figure 54.—Test section yaw flow-angle (β) distribution at test section station 198 during 2015/2016 flow quality survey in 9- by 15-Foot Low-Speed Wind Tunnel (upstream looking aft) at Mach 0.15 (three-motor operating mode).

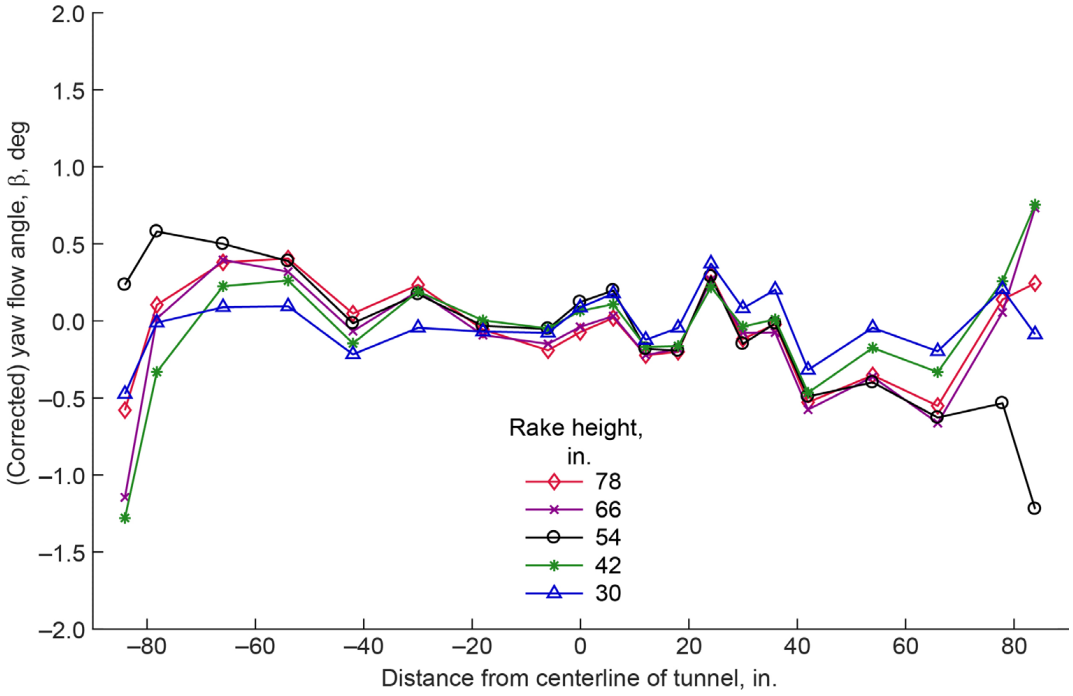

Figure 55.—Test section yaw flow-angle (β) distribution at test section station 198 during 2015/2016 flow quality survey in 9- by 15-Foot Low-Speed Wind Tunnel (upstream looking aft) at Mach 0.10 (three-motor operating mode).

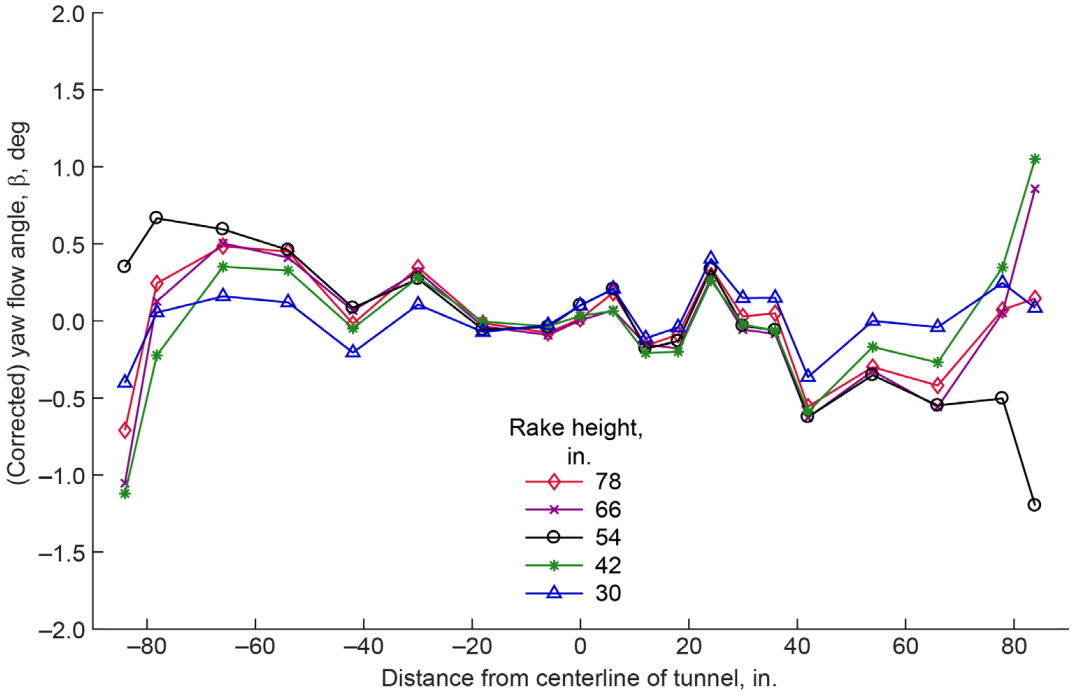

Figure 56.—Test section yaw flow-angle (β) distribution at test section station 198 during 2015/2016 flow quality survey in 9- by 15-Foot Low-Speed Wind Tunnel (upstream looking aft) at Mach 0.15 (one-motor operating mode).

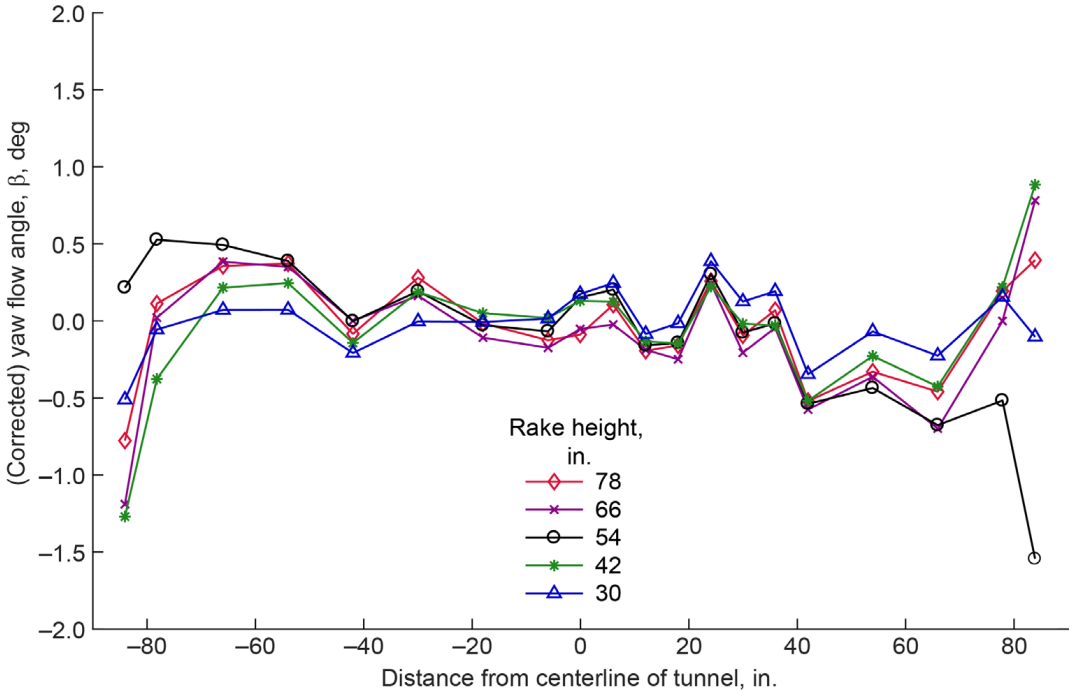

Figure 57.—Test section yaw flow-angle (β) distribution at test section station 198 during 2015/2016 flow quality survey in 9- by 15-Foot Low-Speed Wind Tunnel (upstream looking aft) at Mach 0.10 (one-motor operating mode).

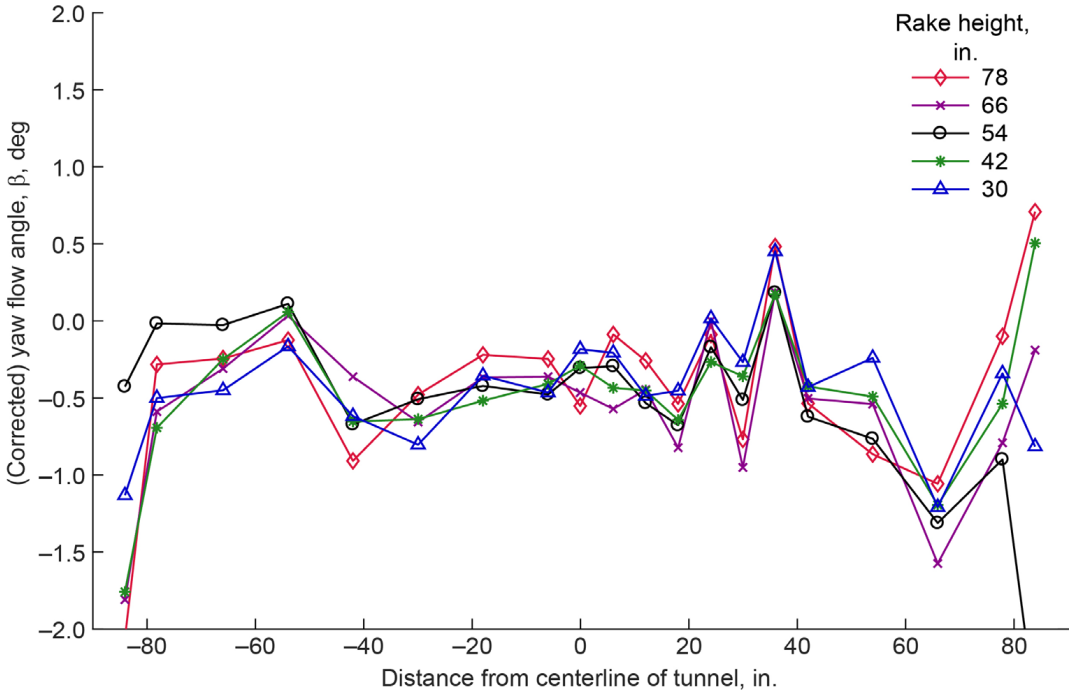

Figure 58.—Test section yaw flow-angle (β) distribution at test section station 198 during 2015/2016 flow quality survey in 9- by 15-Foot Low-Speed Wind Tunnel (upstream looking aft) at Mach 0.05 (one-motor operating mode).

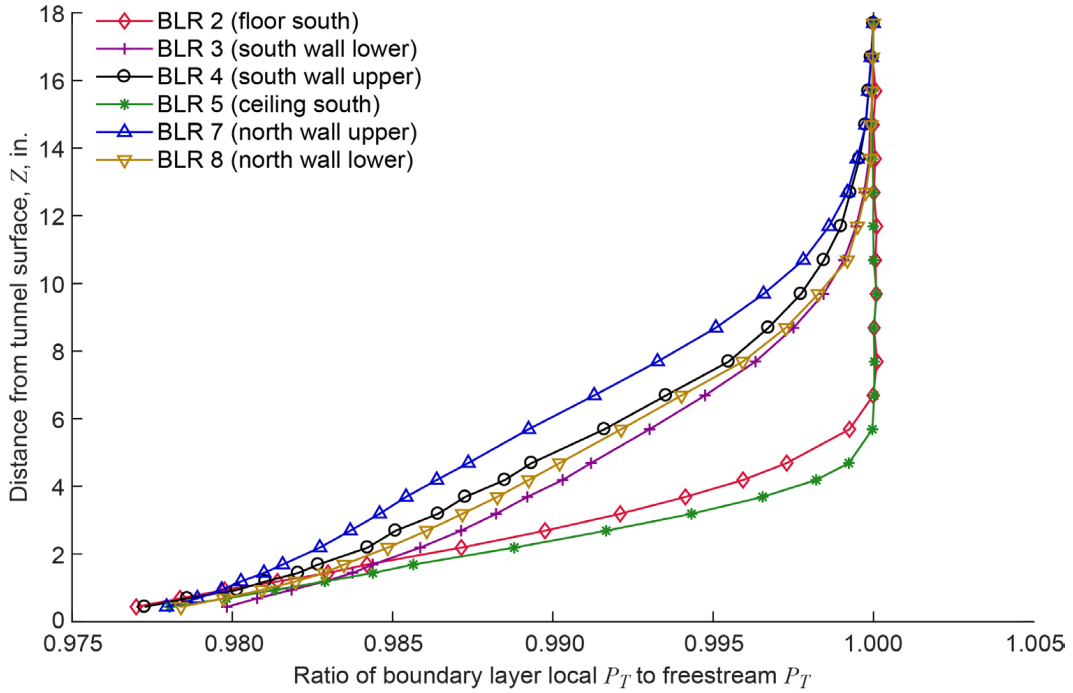

Figure 59.—Boundary layer total pressure (P_T) profile measured by boundary layer rakes (BLRs) at test section station 199 during 2015/2016 flow quality survey in 9- by 15-Foot Low-Speed Wind Tunnel at Mach 0.23 (three-motor operating mode).

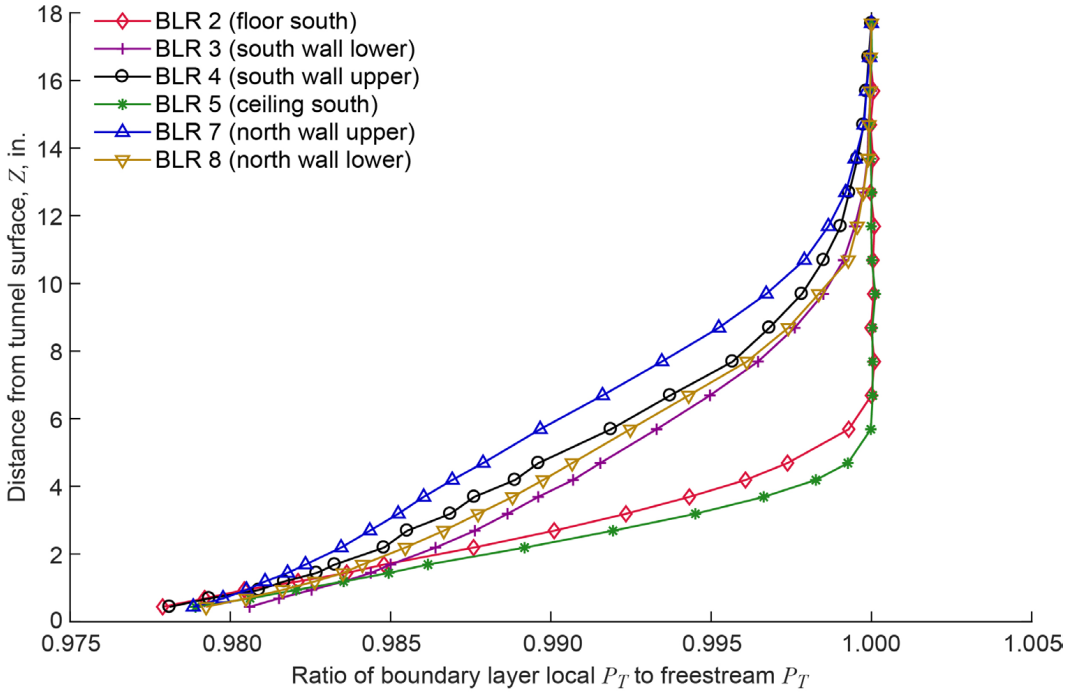

Figure 60.—Boundary layer total pressure (P_T) profile measured by boundary layer rakes (BLRs) at test section station 199 during 2015/2016 flow quality survey in 9- by 15-Foot Low-Speed Wind Tunnel at Mach 0.22 (three-motor operating mode).

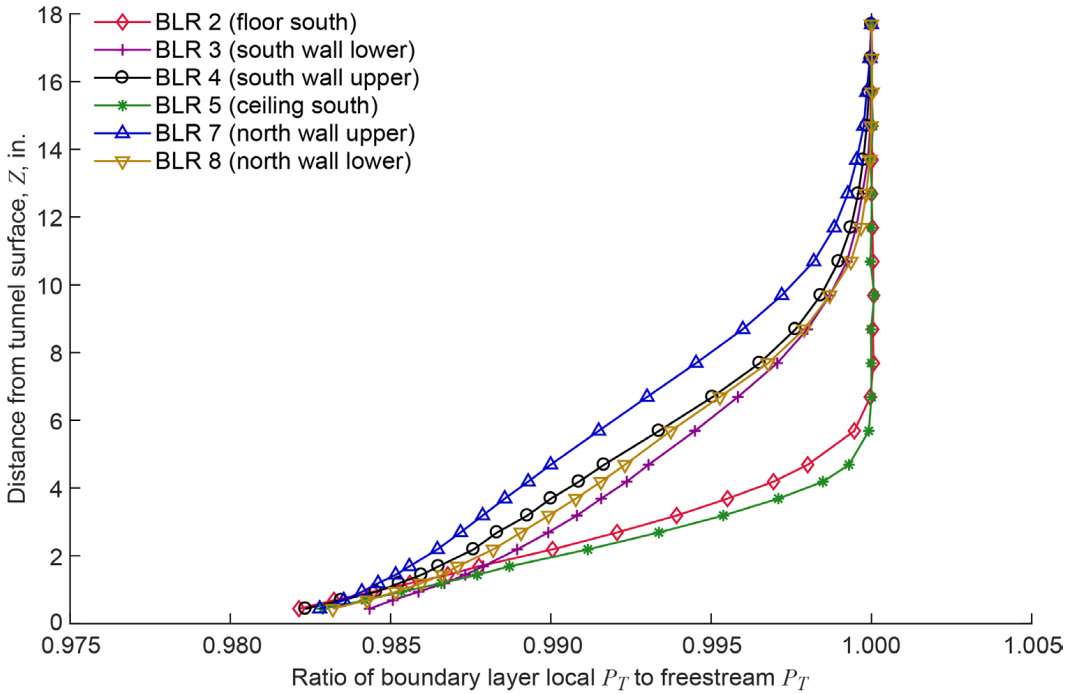

Figure 61.—Boundary layer total pressure (P_T) profile measured by boundary layer rakes (BLRs) at test section station 199 during 2015/2016 flow quality survey in 9- by 15-Foot Low-Speed Wind Tunnel at Mach 0.20 (three-motor operating mode).

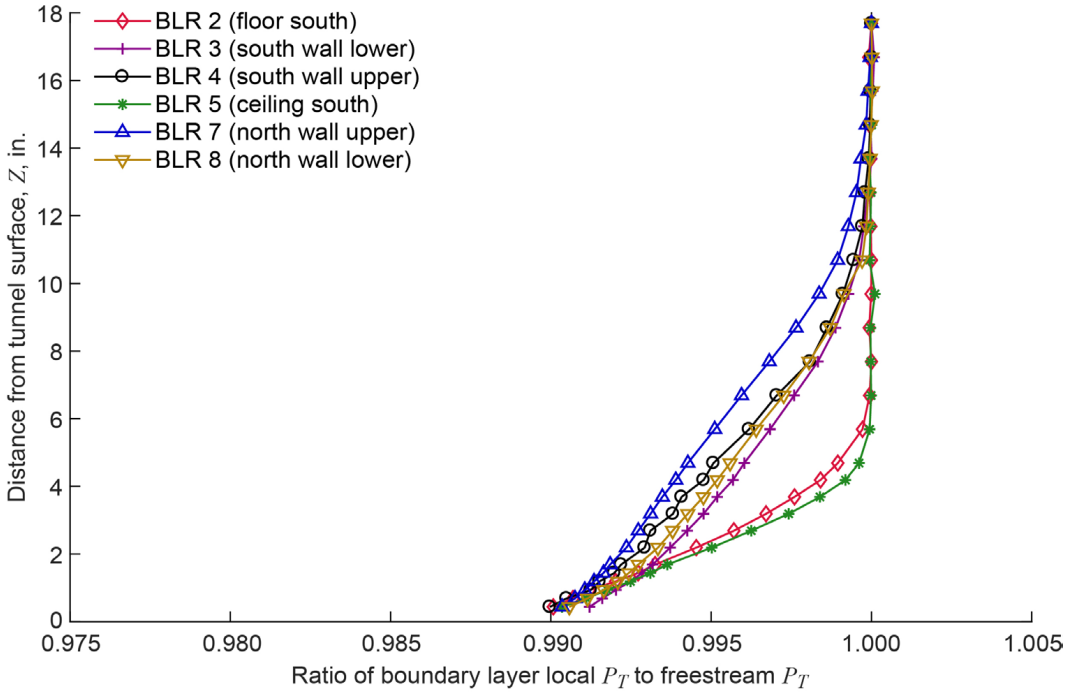

Figure 62.—Boundary layer total pressure (P_T) profile measured by boundary layer rakes (BLRs) at test section station 199 during 2015/2016 flow quality survey in 9- by 15-Foot Low-Speed Wind Tunnel at Mach 0.15 (three-motor operating mode).

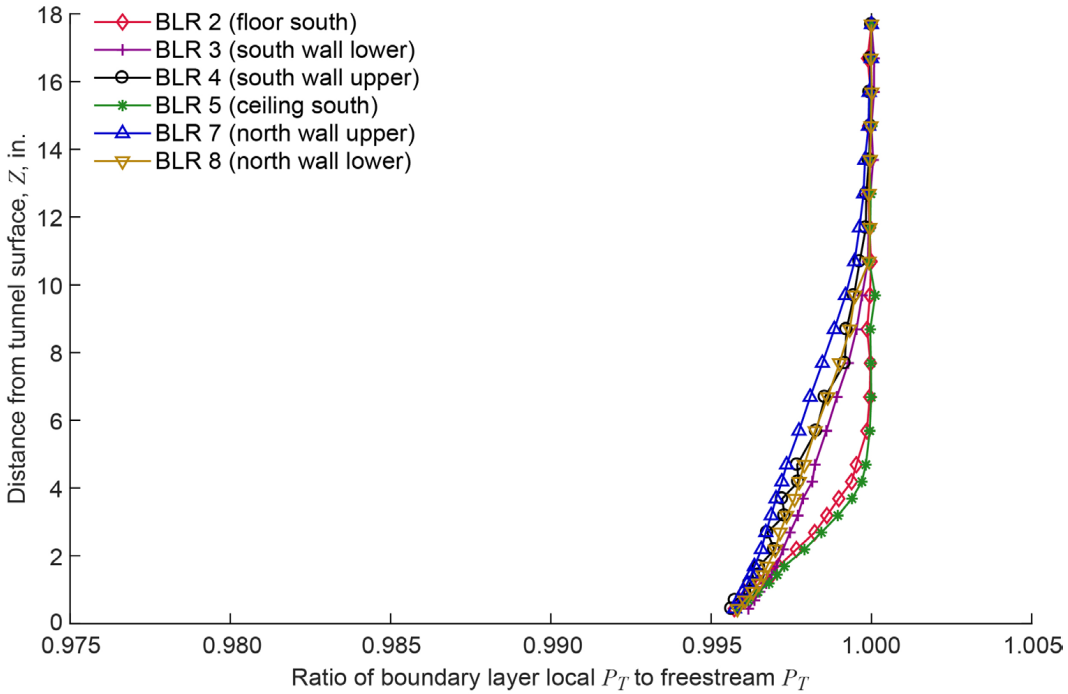

Figure 63.—Boundary layer total pressure (P_T) profile measured by boundary layer rakes (BLRs) at test section station 199 during 2015/2016 flow quality survey in 9- by 15-Foot Low-Speed Wind Tunnel at Mach 0.10 (three-motor operating mode).

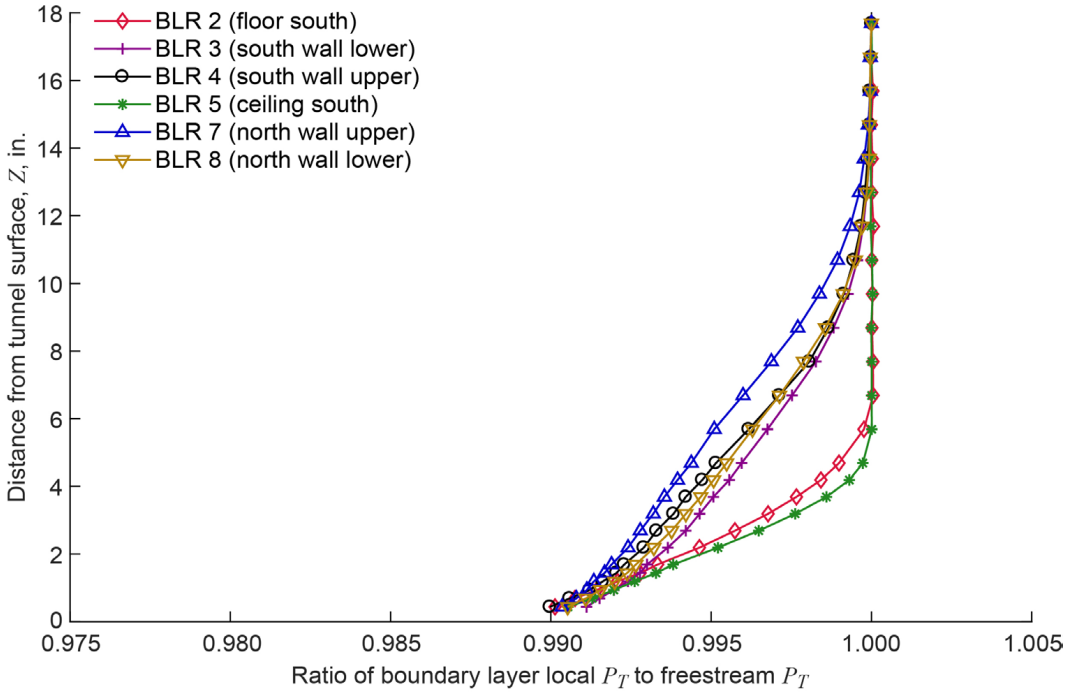

Figure 64.—Boundary layer total pressure (P_T) profile measured by boundary layer rakes (BLRs) at test section station 199 during 2015/2016 flow quality survey in 9- by 15-Foot Low-Speed Wind Tunnel at Mach 0.15 (one-motor operating mode).

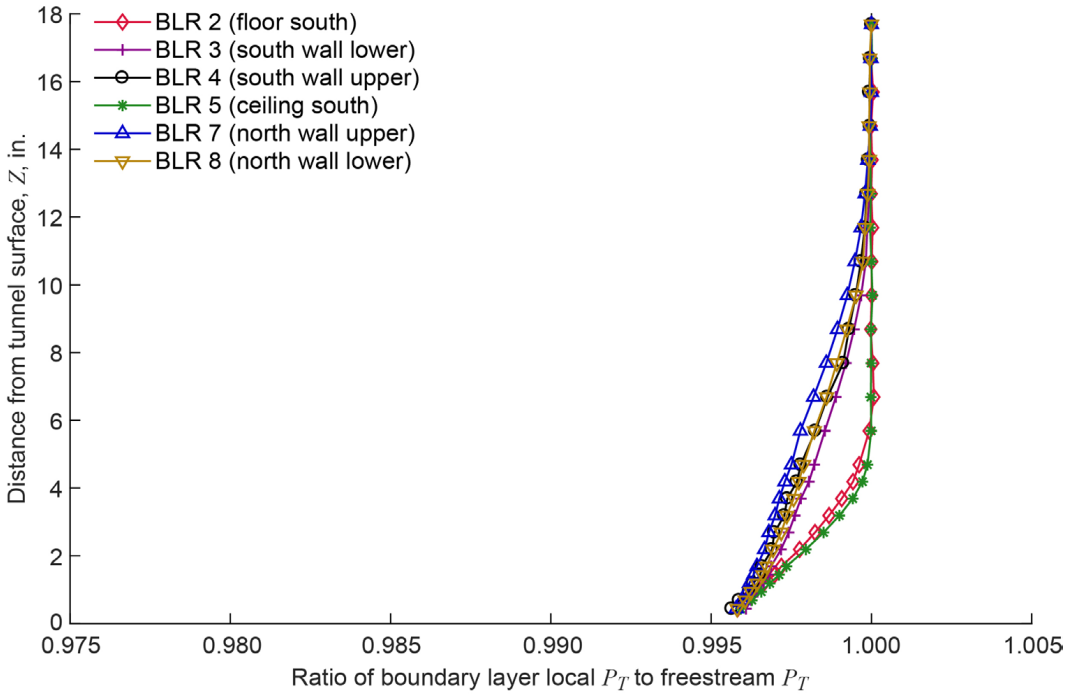

Figure 65.—Boundary layer total pressure (P_T) profile measured by boundary layer rakes (BLRs) at test section station 199 during 2015/2016 flow quality survey in 9- by 15-Foot Low-Speed Wind Tunnel at Mach 0.10 (one-motor operating mode).

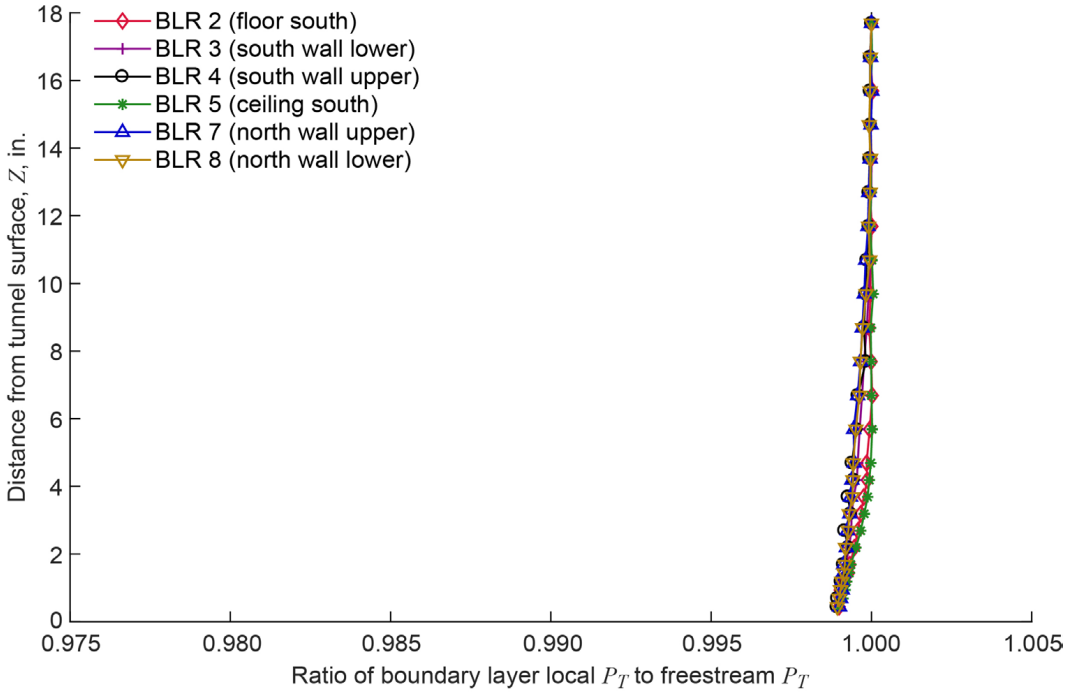

Figure 66.—Boundary layer total pressure (P_T) profile measured by boundary layer rakes (BLRs) at test section station 199 during 2015/2016 flow quality survey in 9- by 15-Foot Low-Speed Wind Tunnel at Mach 0.05 (one-motor operating mode).

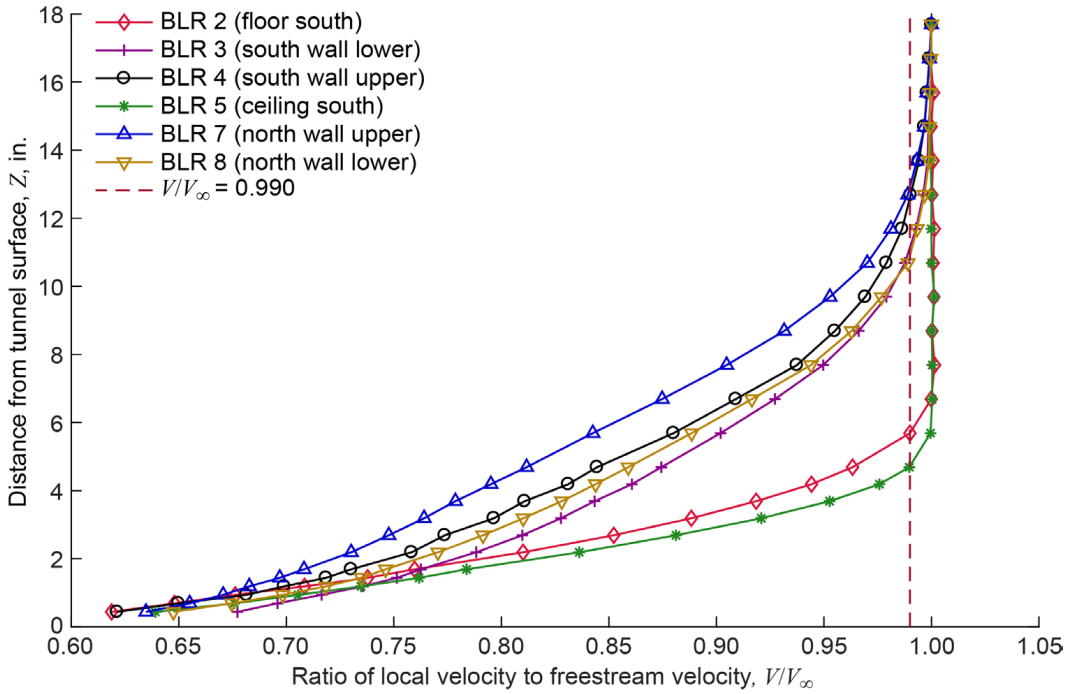

Figure 67.—Boundary layer velocity (V) profile measured by boundary layer rakes (BLRs) at test section station 199 during 2015/2016 flow quality survey in 9- by 15-Foot Low-Speed Wind Tunnel at Mach 0.23 (three-motor operating mode).

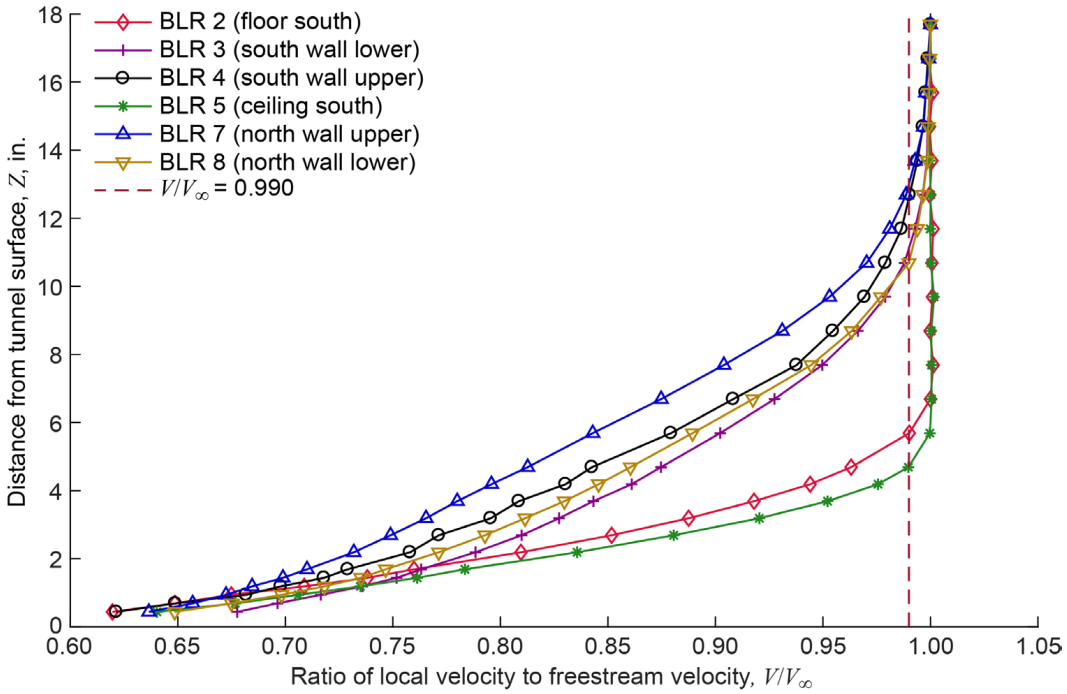

Figure 68.—Boundary layer velocity (V) profile measured by boundary layer rakes (BLRs) at test section station 199 during 2015/2016 flow quality survey in 9- by 15-Foot Low-Speed Wind Tunnel at Mach 0.22 (three-motor operating mode).

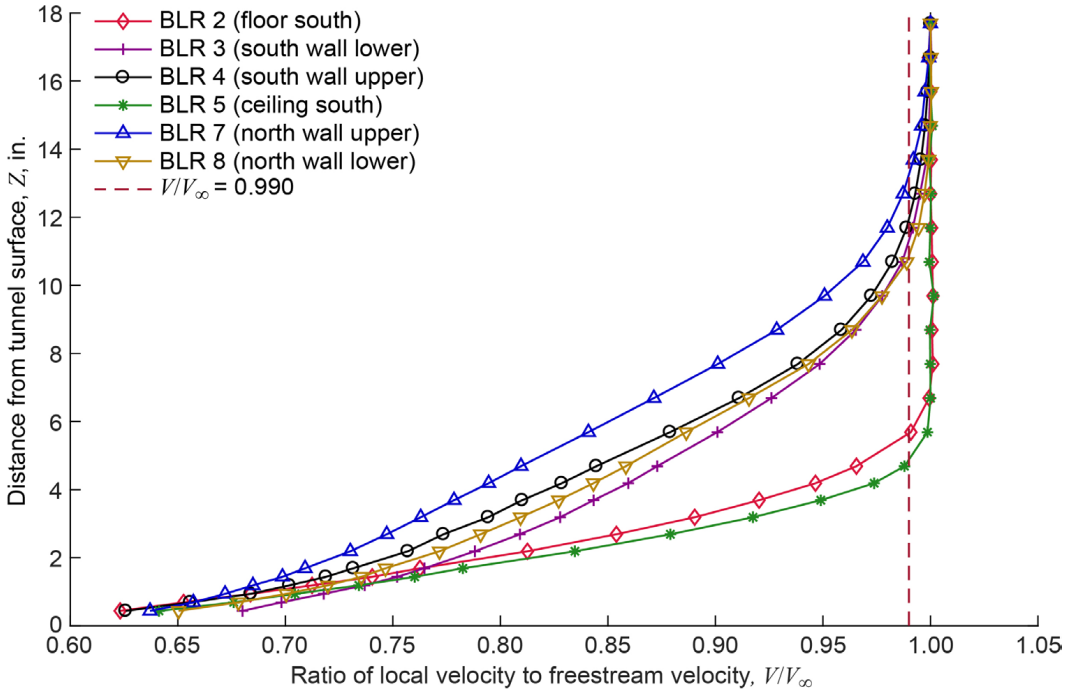

Figure 69.—Boundary layer velocity (V) profile measured by boundary layer rakes (BLRs) at test section station 199 during 2015/2016 flow quality survey in 9- by 15-Foot Low-Speed Wind Tunnel at Mach 0.20 (three-motor operating mode).

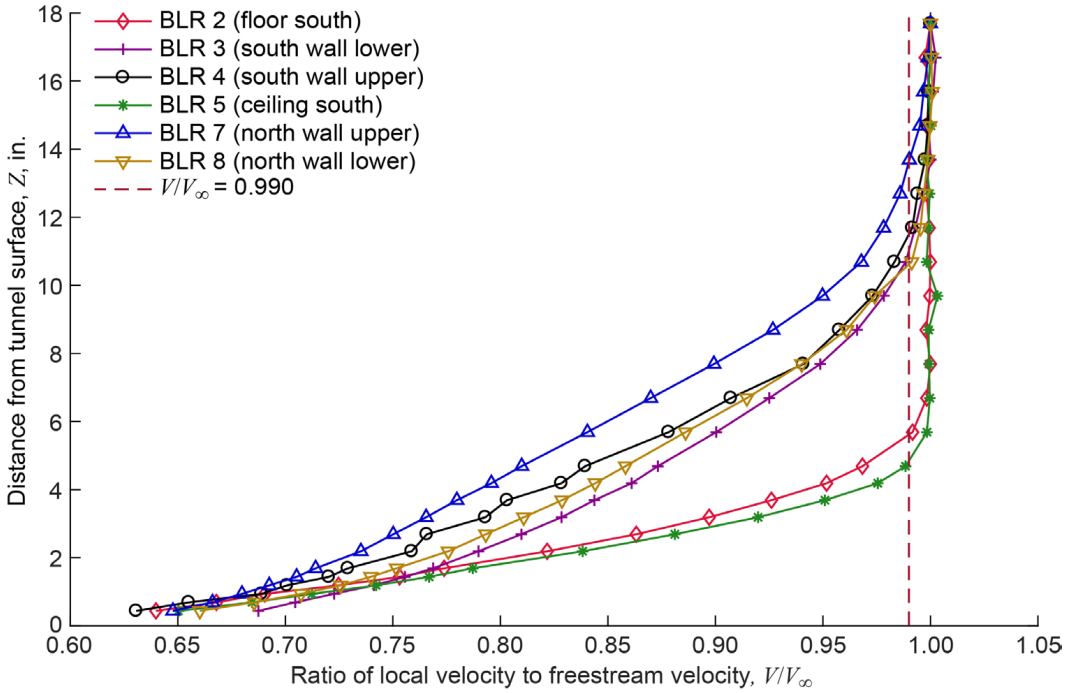

Figure 70.—Boundary layer velocity (V) profile measured by boundary layer rakes (BLRs) at test section station 199 during 2015/2016 flow quality survey in 9- by 15-Foot Low-Speed Wind Tunnel at Mach 0.15 (three-motor operating mode).

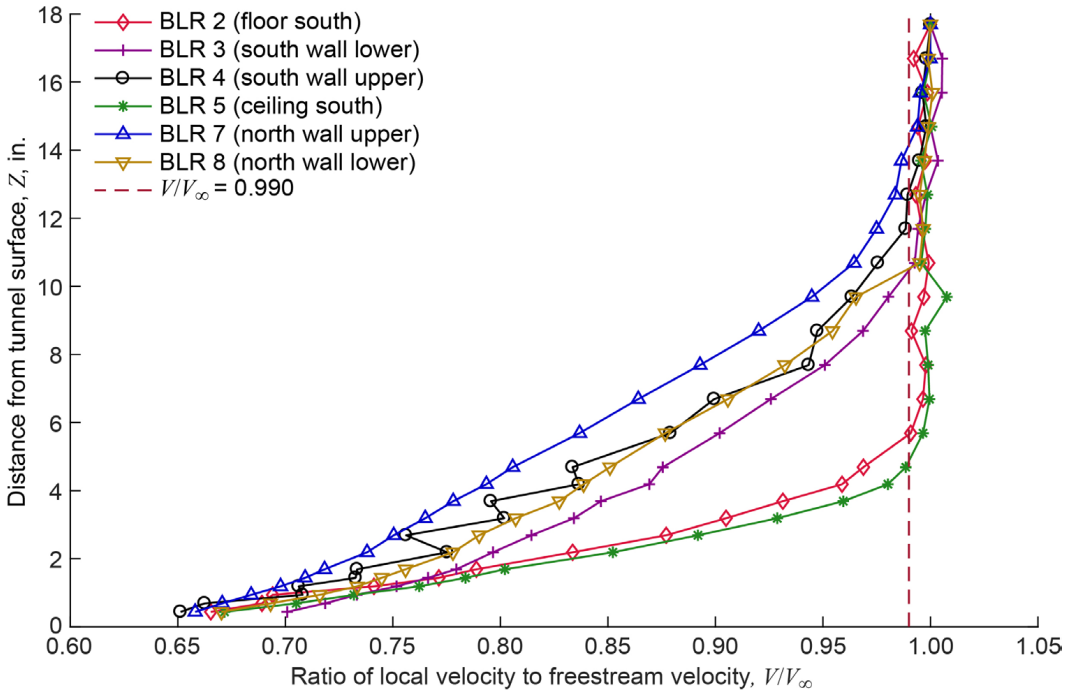

Figure 71.—Boundary layer velocity (V) profile measured by boundary layer rakes (BLRs) at test section station 199 during 2015/2016 flow quality survey in 9- by 15-Foot Low-Speed Wind Tunnel at Mach 0.10 (three-motor operating mode).

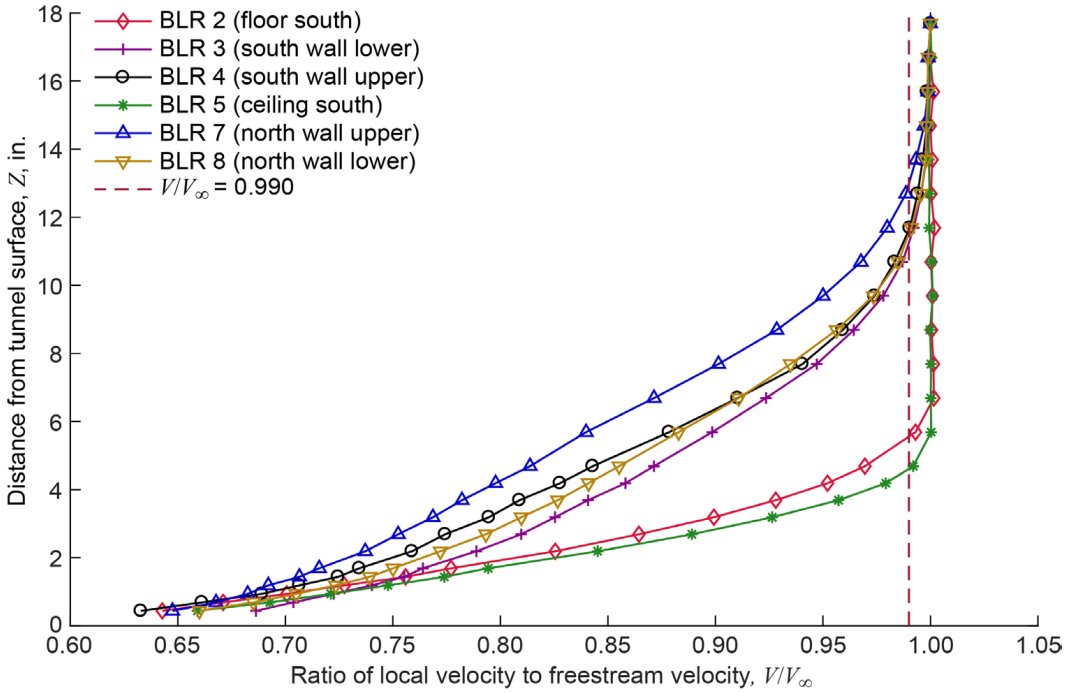

Figure 72.—Boundary layer velocity (V) profile measured by boundary layer rakes (BLRs) at test section station 199 during 2015/2016 flow quality survey in 9- by 15-Foot Low-Speed Wind Tunnel at Mach 0.15 (one-motor operating mode).

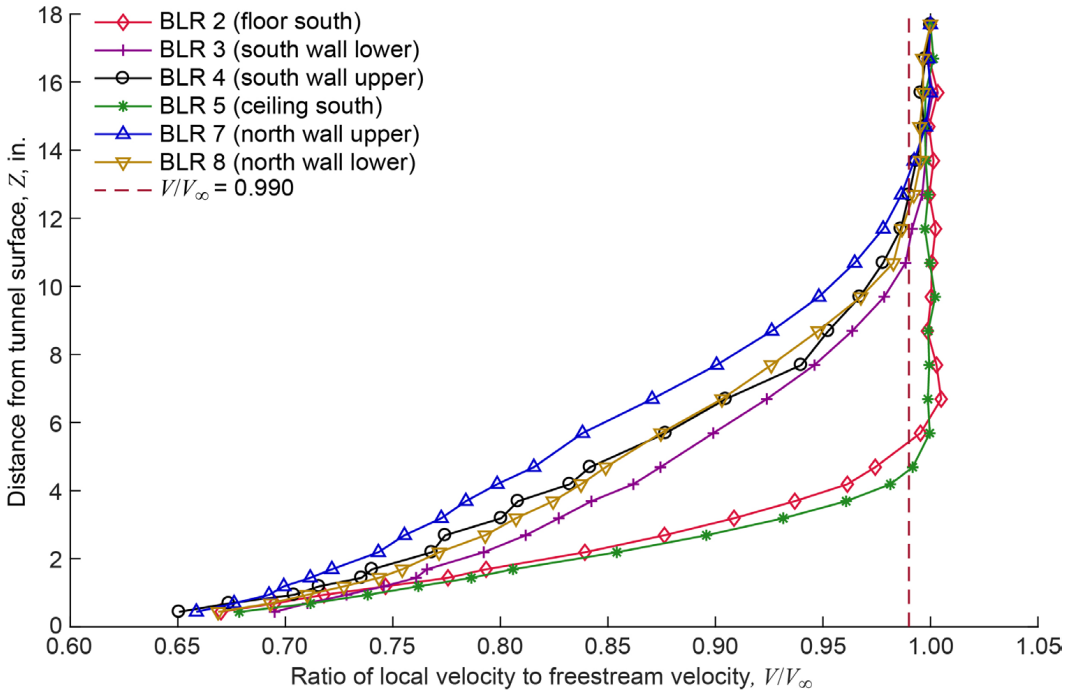

Figure 73.—Boundary layer velocity (V) profile measured by boundary layer rakes (BLRs) at test section station 199 during 2015/2016 flow quality survey in 9- by 15-Foot Low-Speed Wind Tunnel at Mach 0.10 (one-motor operating mode).

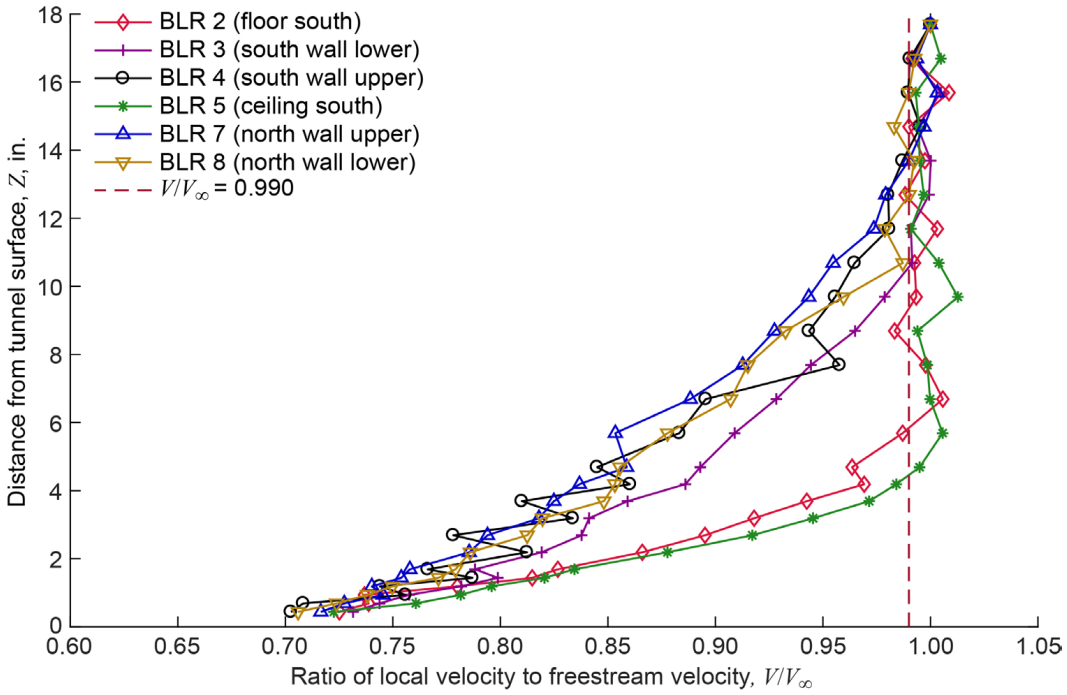

Figure 74.—Boundary layer velocity (V) profile measured by boundary layer rakes (BLRs) at test section station 199 during 2015/2016 flow quality survey in 9- by 15-Foot Low-Speed Wind Tunnel at Mach 0.05 (one-motor operating mode).

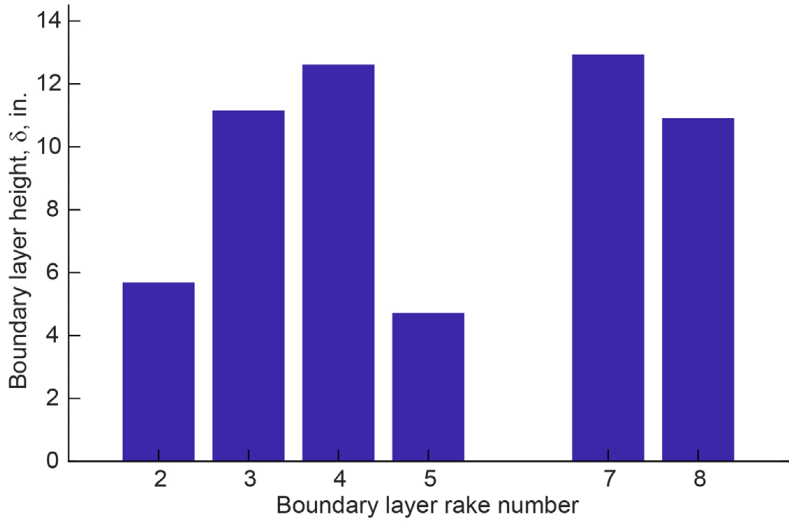

Figure 75.—Boundary layer height (δ) during 2015/2016 flow quality survey in 9- by 15-Foot Low-Speed Wind Tunnel at Mach 0.23 (three-motor operation).

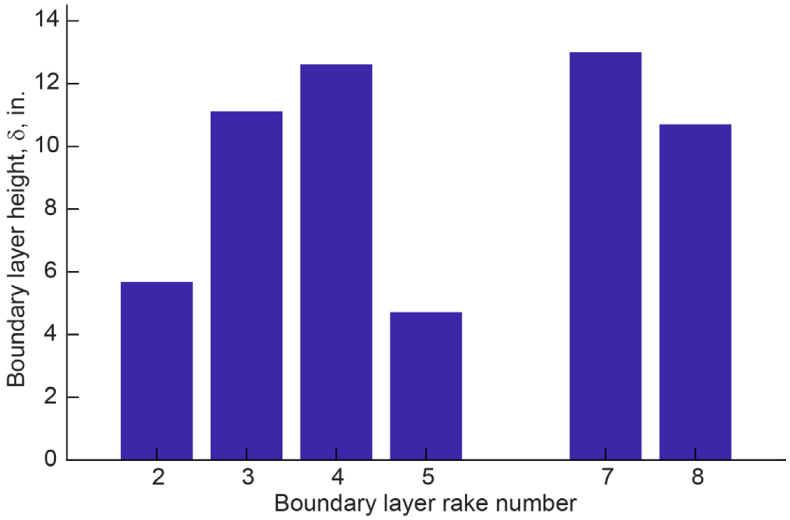

Figure 76.—Boundary layer height (δ) during 2015/2016 flow quality survey in 9- by 15-Foot Low-Speed Wind Tunnel at Mach 0.22 (three-motor operation).

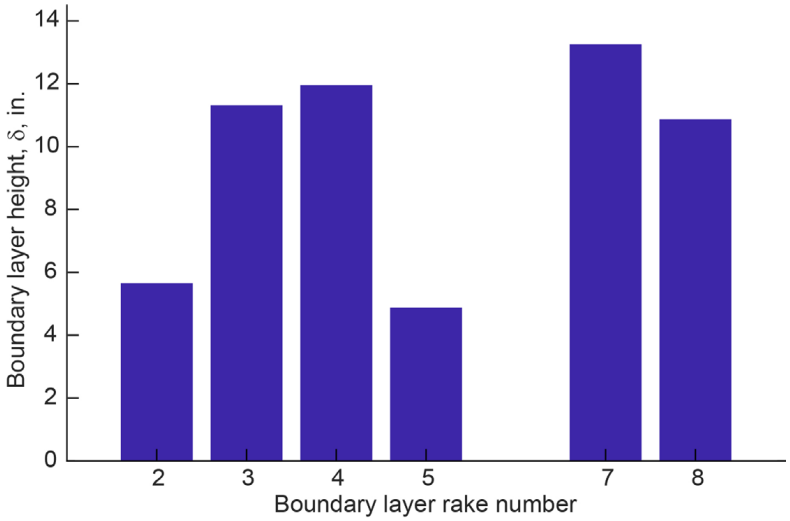

Figure 77.—Boundary layer height (δ) during 2015/2016 flow quality survey in 9- by 15-Foot Low-Speed Wind Tunnel at Mach 0.20 (three-motor operation).

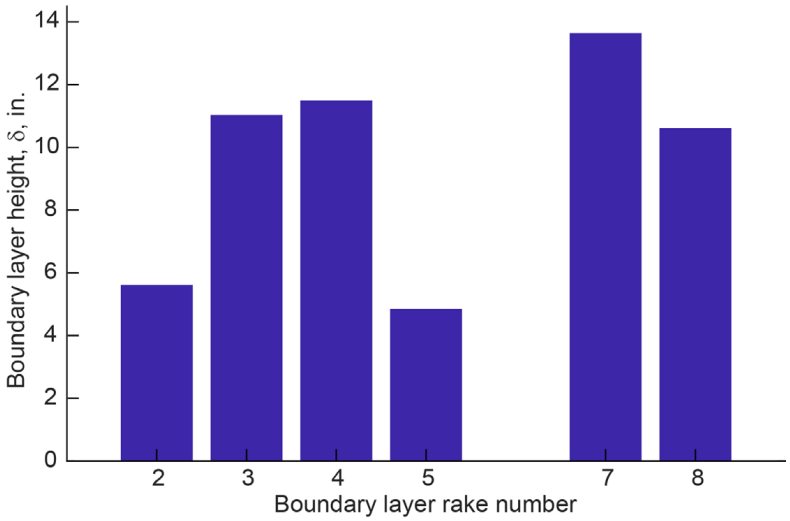

Figure 78.—Boundary layer height (δ) during 2015/2016 flow quality survey in 9- by 15-Foot Low-Speed Wind Tunnel at Mach 0.15 (three-motor operation).

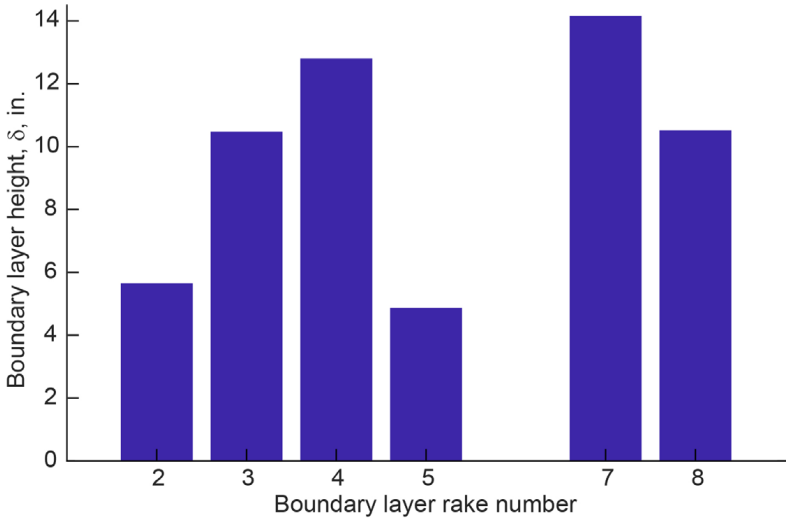

Figure 79.—Boundary layer height (δ) during 2015/2016 flow quality survey in 9- by 15-Foot Low-Speed Wind Tunnel at Mach 0.10 (three-motor operation).

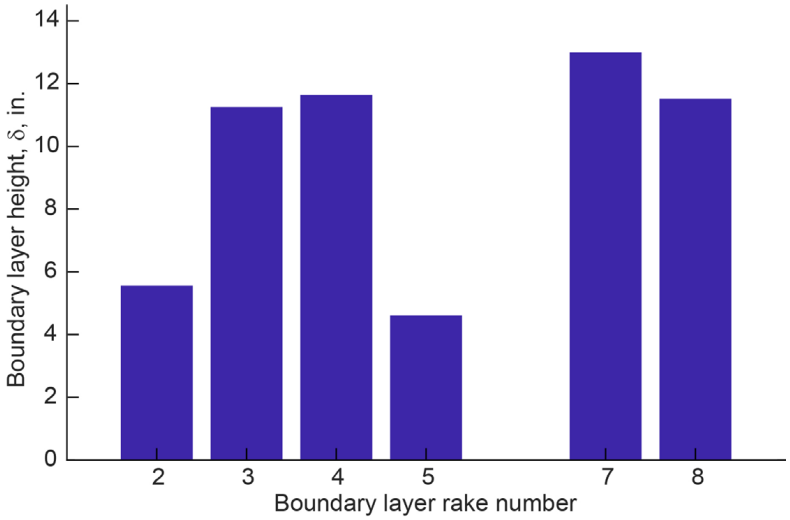

Figure 80.—Boundary layer height (δ) during 2015/2016 flow quality survey in 9- by 15-Foot Low-Speed Wind Tunnel at Mach 0.15 (one-motor operation).

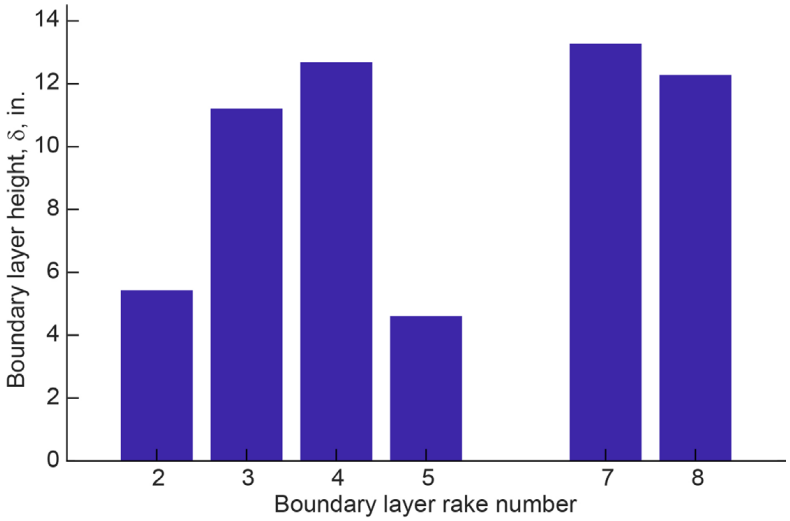

Figure 81.—Boundary layer height (δ) during 2015/2016 flow quality survey in 9- by 15-Foot Low-Speed Wind Tunnel at Mach 0.10 (one-motor operation).

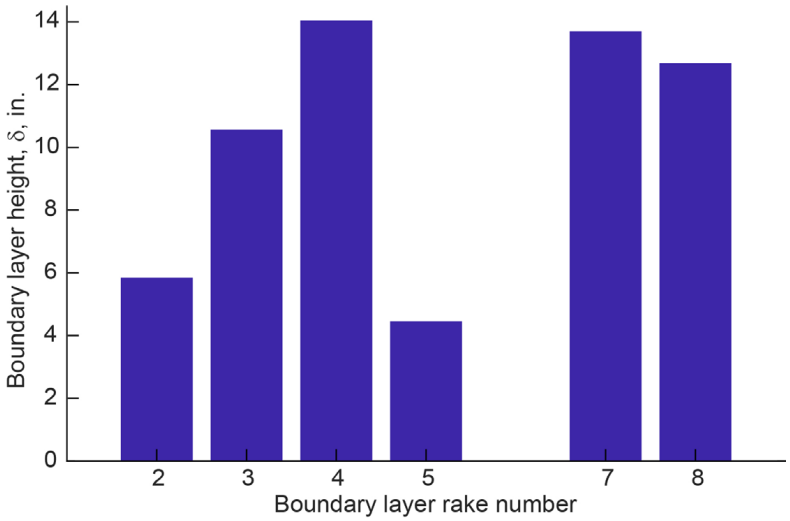

Figure 82.—Boundary layer height (δ) during 2015/2016 flow quality survey in 9- by 15-Foot Low-Speed Wind Tunnel at Mach 0.05 (one-motor operation).

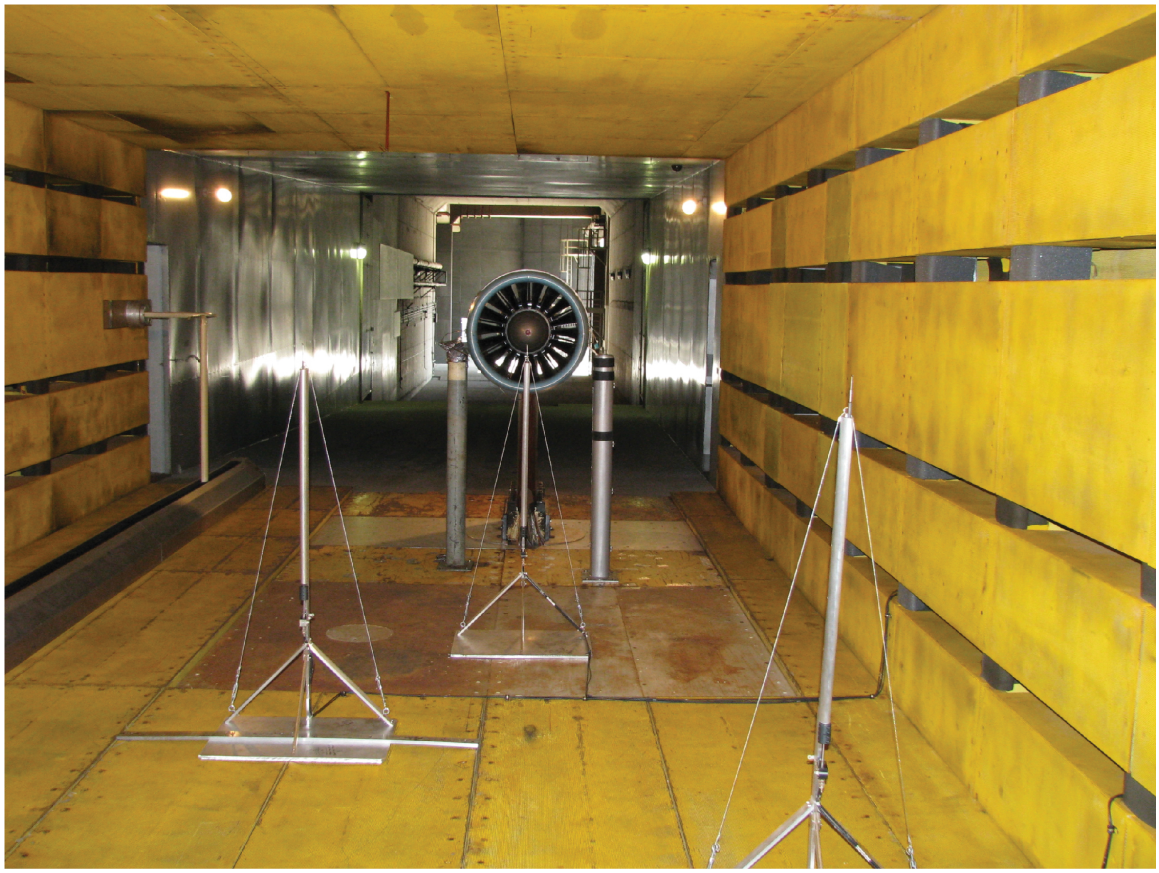

Figure 83.—Hot-wire stand arrangement as installed in 9- by 15-Foot Low-Speed Wind Tunnel test section during 2008 fan test entry.

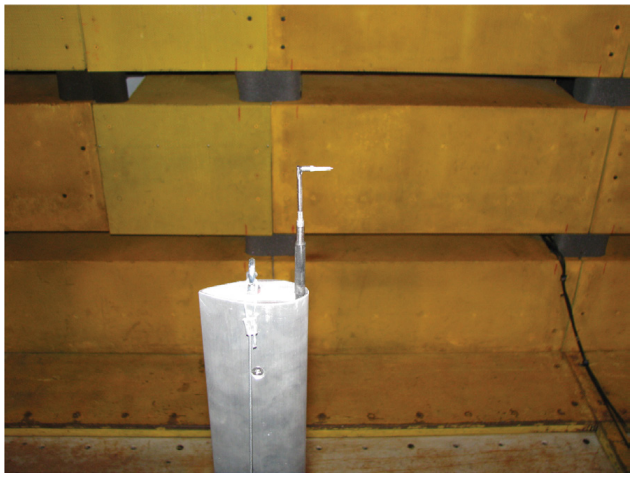

Figure 84.—Hot-wire stand profile view as installed in 9- by 15-Foot Low-Speed Wind Tunnel test section during 2008 fan test entry.